MINISTRY OF NATIONAL EDUCATION

THE ANNALS OF "DUNAREA DE JOS" UNIVERSITY OF GALATI

Fascicle IX
METALLURGY AND MATERIALS SCIENCE

YEAR XXXVI (XLI)
December 2018, no. 4

ISSN 2668-4748; e-ISSN 2668-4756

2018
GALATI UNIVERSITY PRESS

EDITORIAL BOARD

THE ANNALS OF "DUNAREA DE JOS" UNIVERSITY OF GALATI
FASCICLE IX. METALLURGY AND MATERIALS SCIENCE
Nº. 4 - 2018, ISSN 2668-4748; e-ISSN 2668-4756
Volume DOI: https://doi.org/10.35219/mms.2018.4

Table of Contents

THE ANNALS OF "DUNAREA DE JOS" UNIVERSITY OF GALATI
FASCICLE IX. METALLURGY AND MATERIALS SCIENCE
Nº. 4 - 2018, ISSN 2668-4748; e-ISSN 2668-4756
Volume DOI: https://doi.org/10.35219/mms.2018.4

THE ANNALS OF "DUNAREA DE JOS" UNIVERSITY OF GALATI
FASCICLE IX. METALLURGY AND MATERIALS SCIENCE
N°. 4 - 2018, ISSN 2668-4748; e-ISSN 2668-4756
Article DOI: https://doi.org/10.35219/mms.2018.4.01

EXPERIMENTAL RESEARCH ON THE VARIATION OF MECHANICAL PROPERTIES FOR AN ALUMINUM ALLOY SUBJECTED TO NATURAL AGEING

Marian-Iulian NEACȘU
"Dunarea de Jos" University of Galati, Romania
e-mail: uscaeni@yahoo.com

ABSTRACT

Aluminum alloys, due to their properties, have a very wide field in which they find application in the industry. Out of these, the alloys in the Al-Zn system are used predominantly in the aeronautical and machine building industries.

In this paper, we investigated the variation in mechanical properties of the Al-Zn alloy with a Zn content of 4.5%, subjected to a natural ageing treatment with various ageing times.

After conducting the research, we found that the mechanical properties studied vary with the natural ageing time and not all of them fit into the prescriptions imposed by the Euronorm in force. The only property whose values fall entirely within the required limits is elongation at breaking.

KEYWORDS: aluminum alloys, quitting, natural aging, homogenization

1. Introduction

There is a close link between the development of the aeronautical industry and the evolution of the materials used. It is well-known that this state-of-the-art field requires high performance materials with special physical-mechanical properties. Such materials require special elaboration and casting technologies as well as special further processing [1].

Aluminum alloys find their application in almost all branches of the contemporary industry, thus implicitly also in aeronautics due to special properties such as: high mechanical strength, low specific weight, chemical stability, good thermal conductivity, good to very good resistance to corrosion, etc. [2]. The close collaboration between aircraft manufacturers and metallurgical engineers has led to materials with special features and efficient equipment.

For a long time, the main materials used in aeronautics were high resistance duralumin (Al-Cu-Mg) alloys, but their range was reduced when special zicral-type aluminum alloys (Al-Zn-Mg-Cu) appeared [3].

In view of the choice of high strength aluminum alloys for the aeronautical industry, it must be taken into account that they must have high mechanical strength, satisfactory plasticity, corrosion resistance under load, and they also must have high fatigue strength and resistance to relatively high temperatures [4].

Due to their outstanding features, alloys in the Al-Zn-Mg-Cu system are used primarily in the aerospace and machine-building industries.

Al-Zn-Mg-Cu alloys are part of the deformable and hardening aluminum alloy category by applying thermal and (or) thermomechanical treatments [4].

The hardening phase after application of thermal treatments of natural or artificial ageing is represented by the precipitations formed, which the more numerous and more evenly distributed in the mass of the basic solid solution, the higher the mechanical resistance of the Al-Zn-Mg-Cu alloys. If ageing at higher temperatures and longer maintenance times continues, a decrease in mechanical properties is observed due to the increase in precipitate size by coagulation [5].

The alloys are put into service in the aeronautical industry at multidirectional stresses, therefore they must present an optimal combination of mechanical strength, plasticity, tenacity, fatigue strength, and good corrosion resistance.

In order to achieve this, it is necessary to replace the rough grain structure obtained from the alloy casting process as well as to modify the fibrous structure of the laminated semi-finished products, these being decisive factors in achieving optimal properties [6].

THE ANNALS OF "DUNAREA DE JOS" UNIVERSITY OF GALATI
FASCICLE IX. METALLURGY AND MATERIALS SCIENCE
Nº. 4 - 2018, ISSN 2668-4748; e-ISSN 2668-4756
Article DOI: https://doi.org/10.35219/mms.2018.4.01

In order to achieve this objective, the properties of these alloys of different chemical compositions have been varied as a result of applying experimental variants of thermic and thermomechanical treatment.

In this paper the experimental researches and their results are rendered following the application of a thermal treatment of natural ageing with the aim of obtaining semi-finished products with a structure that will give the material the desired properties.

2. Experimental research

Experiments were performed on samples from the alloy with the chemical composition given in Table 1. The mechanical properties of the alloys studied according to EN 485-2-2007 [180] are presented in Table 2.

Table 1. *Chemical composition of alloys under investigation*

Element / Alloy	Zn	Mg	Cu	Si	Fe	Cr	Mn	Al
AlZn4,5Mg1	**4.5**	**1.4**	**0.5**	**0.35**	**0.4**	**0.35**	**0.25**	**rest**

Table 2. *Alloy properties according to EN 485-2-2007* [7]

Mechanical property / Alloy	Rm, [MPa]	$Rp_{0,2}$ [MPa]	A_5 [%]	HB
AlZn4,5Mg1	**350**	**280**	**10**	**104**

These alloys were developed, cast into ingots and homogenized at S.C. ALRO S.A. Slatina. The test specimens for the mechanical tests were made according to the specifications given in SR EN 10 002 -1/1995 [8] for the traction tests.

The alloy subjected to the research is an aluminum alloy in which the main alloying element is zinc and, as shown in the Al-Zn equilibrium diagram in Figure 1, the zinc content of this alloy being 4.5% Zn, it belongs to the category of alloys deformable and hardening by heat treatment.

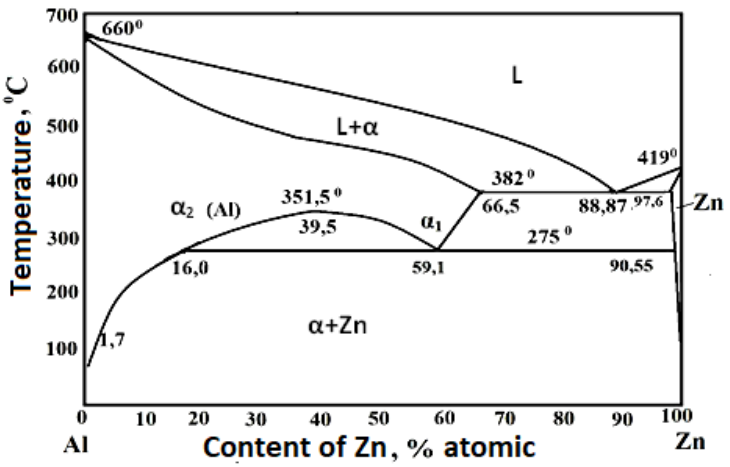

Fig. 1. *Al-Zn balance diagram* [9]

Based on the data presented in the literature on the thermal processing applied to the aluminum alloys, we have established the following technological variant of the alloy processing, which is illustrated schematically in Figure 2.

As a result of structural changes, homogenization improves the plasticity of alloys and uniformizes their final properties, reduces internal stresses and leads to changes in microstructure. In the first phase of homogenization, a part of $MgZn_2$ is converted to Al_2CuMg, and the other untransformed part is dissolved in the mass of the solid solution. The AlFeSi-containing phase is partially converted to Al_7Cu_2Fe.

The Mg_2Si compound undergoes small changes, and slow cooling from the homogenization temperature to ambient temperature leads to precipitation of $MgZn_2$ [3.9].

Hot lamination was achieved with only a 25% deformation because, due to the mechanical

THE ANNALS OF "DUNAREA DE JOS" UNIVERSITY OF GALATI
FASCICLE IX. METALLURGY AND MATERIALS SCIENCE
Nº. 4 - 2018, ISSN 2668-4748; e-ISSN 2668-4756
Article DOI: https://doi.org/10.35219/mms.2018.4.01

characteristics evaluated, the degree of deformation of 25% gave the most favorable combination between the hardness properties and the plasticity properties.

After hot rolling and cooling the material in air, the samples were heated in the oven at 500 °C and maintained at this temperature for 120 minutes in order to quench the solution.

Cooling from this temperature was done in water to affect the solution quenching in order to dissolve the alloying elements in aluminum, thus obtaining an over-saturated solid solution.

The higher the degree of deformation prior to the solution hardening process of the alloy, the finer the structure, and thus the secondary phases will dissolve at a higher rate at the quench temperature.

The range of quenching temperatures is very narrow for most aluminum alloys, but for the Al-Zn-Mg-Cu and Al-Zn-Mg alloys, the range of the solid solution is high and ranges between 400 °C and 580 °C [5, 9, 10-14].

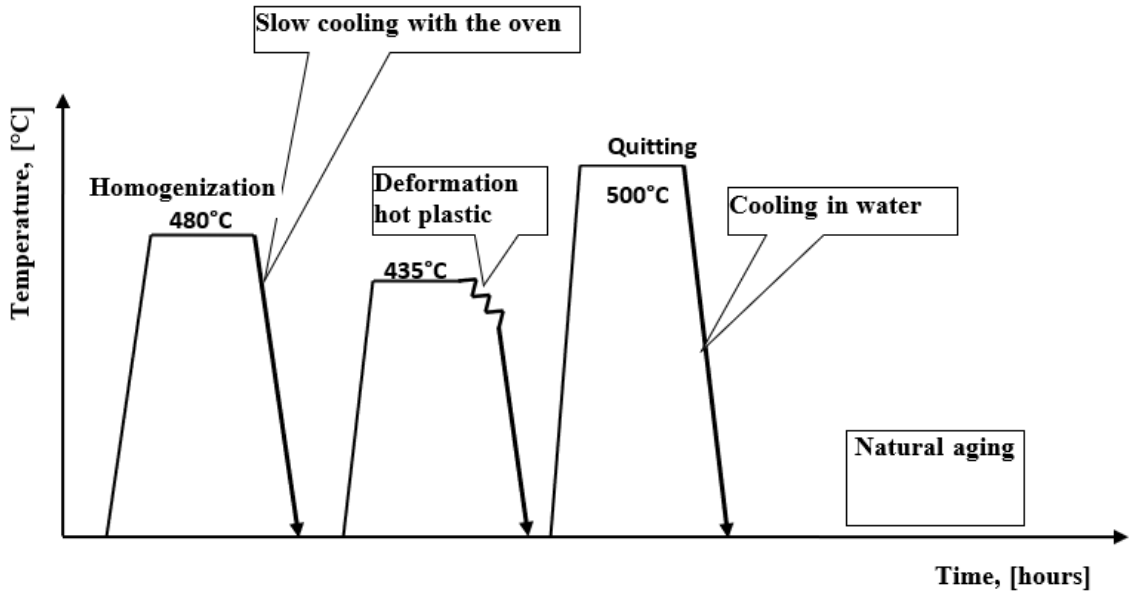

Fig. 2. *Representation of the thermal processing scheme*

The relationship between the solidus Ts temperature and the transformation curve temperature on the curve in C, Tmin is linear: Tmin = (0.7-0.9) • Ts, [K], [5, 9, 11-14].

The structural hardening by precipitation from the supersaturated solid solution was achieved by the natural ageing of the material which had been left at ambient temperature in the laboratory for 60 days.

Measurement of property values was made after several time intervals: 24 hours, 72 hours, 168 hours, 360 hours, 720 hours, 1080 hours and 1440 hours.

Table 3. *Properties of the alloy after natural ageing*

Aging time [hours]	Mechanical characteristics			
	HB	Rm MPa	$Rp_{0,2}$ MPa	A_5 %
24	47	150	116	22
72	56	179	138	19
168	80	256	197	18
360	111	355	273	17
720	127	400	308	16
1080	136	435	335	15
1440	140	421	323	16

THE ANNALS OF "DUNAREA DE JOS" UNIVERSITY OF GALATI
FASCICLE IX. METALLURGY AND MATERIALS SCIENCE
N°. 4 - 2018, ISSN 2668-4748; e-ISSN 2668-4756
Article DOI: https://doi.org/10.35219/mms.2018.4.01

Table 3 shows the values representing the arithmetic mean of 5 measurements after performing the tests for finding the values of the investigated properties. Mechanical strength properties increase as the natural aging time increases, with a peak for ageing time of 1,080 hours, and then decreases over 1440 hours.

The graphical representation of the mechanical properties variation with the natural ageing time of the samples that have undergone research on this topic is shown in Figures 3-6.

Ageing of the hardened alloys leads to the decomposition of the supersaturated solid solution with the appearance of the secondary phases in a controlled dispersion and the equilibrium approximation of the solid solution. The type, size, distribution and amount of precipitated particles in an alloy depend on temperature, ageing time and initial state of the microstructure.

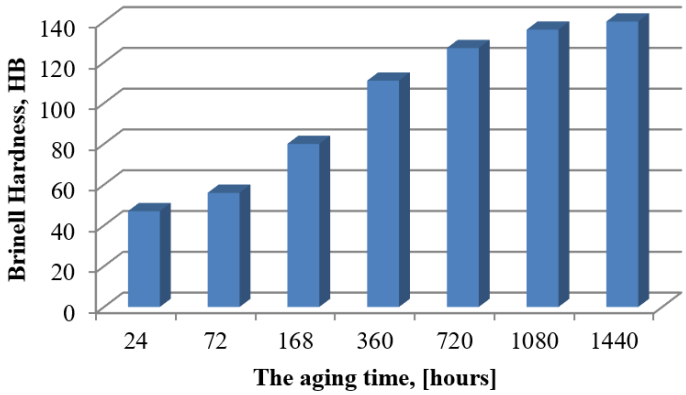

Fig. 3. *Variation of Brinell hardness with aging*

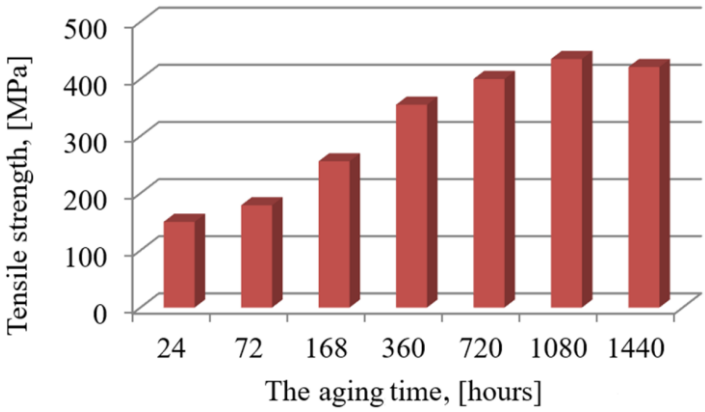

Fig. 4. *Variation of mechanical strength at breaking with aging*

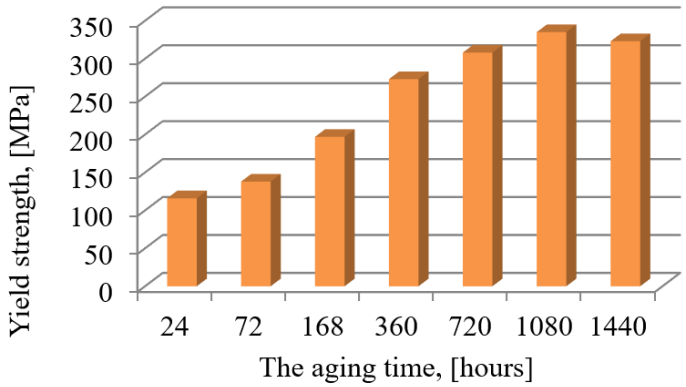

Fig. 5. *Variation of flow limit with the aging time*

THE ANNALS OF "DUNAREA DE JOS" UNIVERSITY OF GALATI
FASCICLE IX. METALLURGY AND MATERIALS SCIENCE
N°. 4 - 2018, ISSN 2668-4748; e-ISSN 2668-4756
Article DOI: https://doi.org/10.35219/mms.2018.4.01

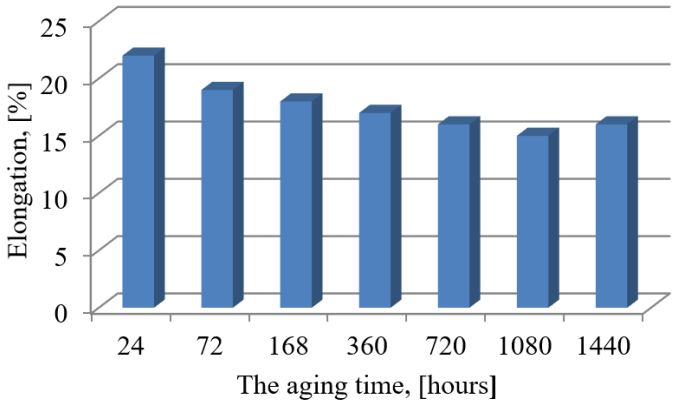

Fig. 6. *Variation of elongation at break with aging*

As it can be seen from the variation graphs of mechanical resistance, yield strength and Brinell hardness with ageing time, the two mechanical properties do not fall within the required norms for all these ageing times.

The decrease of the values of the mechanical resistance properties studied after natural ageing with the time of 1440 hours compared to those of the aging time of 1080 hours, is due to the occurrence of the coalescence phenomenon of the precipitates which has the effect of diminishing these values.

Elongation at break has the lowest value for samples left to naturally age for 1080 hours, after which, for naturally aged samples for 1440 hours, there is a slight increase but it is an increase in A5.

The increase of precipitations by the phenomenon of coalescence is responsible for this situation and in structural terms there is a decrease of the grain boundaries, which leads to the decrease of the mechanical properties of resistance, to the detriment of the plasticity.

5. Conclusions

After the research, the following conclusions can be drawn:

- for mechanical resistance, the values that fall within the limits prescribed by the Eeuronorm in force are those obtained when the ageing time was 360, 720, 1080, 1440 hours.
- for the flow limit, we obtained values that correspond to the Euronorm recommendations for the following natural ageing times: 720, 1080, 1440 hours.
- the values obtained for the Brinell hardness are above those prescribed by the Euronorm when natural aging lasts between 360 and 1440 hours.
- elongation at break decreases as the ageing time increases (Figure 3).

The graph in Figure 6 shows that the elongation records a minimum of 1080 hours, followed by a slight increase. For both resistance and elongation properties, this variation is explained by the fact that the precipitations formed during the natural ageing process have reached a critical value of their size, followed by their growth through coalescence. More precisely, there is the increase of the big ones on the account of the small ones and structurally, there is a decrease of the grain boundaries, which leads to the decrease of the mechanical properties of resistance, to the detriment of the plasticity properties.

References

[1]. Bane M., ş.a., *Analiza structurii materialelor metalice*, Editura Tehnică, Bucureşti, 1991.
[2]. Baker K. B., Rowe H. J., *Aluminium, vol. III, Fabrication and Finishing*, ASM, Ohio, 1994.
[3]. Cieśla M., *Aluminium supplier selection for the automotive parts manufacturer*, Metalurgija, 55, 2, p. 237-240, 2016.
[4]. Rometsch P. A., Zhang Y., Knight S., *Transactions of Nonferrous Metals Society of China*, 24, p. 2003-2017, 2014.
[5]. Bunea D., Şaban R., Vasile T., Gheorghe D., Brânzei M., *Alegerea şi tratamentele termice ale materialelor metalice*, Editura Didactică şi Pedagogică. Bucureşti, 1996.
[6]. Chira I., Mărginean Şt., *Metale şi aliaje neferoase turnate*, Editura "Fundaţia Metalurgia Română", Bucureşti, 2003.
[7]. ***, www.en-standard.eu/csn-en-573-3-2013aluminium.
[8]. ***, SR.EN. 10002-1/1995 – *Încercarea la tracţiune.*
[9]. Ienciu M., Moldovan P. *et al.*, *Elaborarea şi turnarea aliajelor neferoase speciale*, Ed. Didactică şi Pedagogică, Bucureşti, 1985.
[10]. Chira I., Cernat C., *Tehnologia elaborării şi turnării aliajelor neferoase*, Editura Litografia, Bucureşti, 1988.
[11]. Dumitrescu C., Şaban R., *Metalurgie fizică – Tratamente termice*, Editura. Fair Partners, Bucuresti, 2001.
[12]. Piątkowski J., *AlSi17Cu5Mg-Alloy as future material for castings of pistons for internal combustion engines*, METABK 54(3), p. 511-514, 2015.
[13]. Armăşoiu P., Dobrotă D., Petrescu V., *Analysis of metal lographic structure and hardness of aluminum alloy 3l59 from the structure of vulcanization equipment*, METABK 54(3), p. 547-550, 2015.
[14]. Essari A., Sariuglo F., Petrovic Z., Sedmak A., Samardžić I., *Effect of aging on mechanical properties of Al-8Si-8Fe-1.4V/SICP composites*, METABK 55(2), p. 189-192, 2016.

THE ANNALS OF "DUNAREA DE JOS" UNIVERSITY OF GALATI
FASCICLE IX. METALLURGY AND MATERIALS SCIENCE
N°. 4 - 2018, ISSN 2668-4748; e-ISSN 2668-4756
Article DOI: https://doi.org/10.35219/mms.2018.4.02

INFLUENCE OF ALLOYING ELEMENTS IN ZINC MELTS ON THE STRUCTURE OF LAYERS OBTAINED BY GALVANIZING

Tamara RADU, Florentina POTECAȘU
"Dunarea de Jos" University of Galati, Romania
e-mail: tradu@ugal.ro

ABSTRACT

Zinc melts has been alloyed, in various proportions and combinations, with Bi, Sn, Ni, Pb. Depending on the characteristics of the alloying elements, the alloying technology of the zinc bath was established. To determine the degree of homogenization of the melt, samples were taken for metallographic analyses and chemical composition. In zinc alloyed melts were coated steel strips with low carbon. The layers obtained were analyzed in cross-section to determine the influence of the alloying elements on the Zn-Fe alloys from the support/zinc interface and on the thickness and structure of the phase η (zinc). The chemical composition was determined by X-ray fluorescence and microstructure analysis by optical microscopy.

KEYWORDS: coating layer, optical microscopy, X-ray fluorescence, Zn-Sn-Pb-Bi-Ni alloy, galvanizing

1. Introduction

Hot dip galvanizing technology is widely applied for the corrosion protection of steel parts so that half of the world's zinc production is used for this purpose [1]. Classical hot dip galvanizing has seen many improvements over time. Most of them aimed at increasing the corrosion resistance of the layer, changes in the melt characteristics (fluidity, superficial tension, etc.) and reducing the amount of dross. In order to achieve these objectives, a modification of the composition of the zinc bath by alloying with various elements was applied in various combinations, namely: Al [2, 3], Sn [4], Mg [5], Bi [6, 7], Ni [8-10]. Aluminum is the most widely used and studied alloying element of zinc melt having favorable effects both on the characteristics of the layer and on the zinc melt [11]. At present, galvanizing in alloys Zn-Mg-Al is being investigated with significant improvements in technology and product [12-14].

Bismuth is an expensive metal but can replace lead in galvanizing baths with the same effect in increasing fluidity and reducing surface tension to much lower contents and is not toxic.

Tin increases corrosion resistance of zinc layers and nickel increases melt fluidity and corrosion resistance [4, 9]. The paper analyses the influence of some of these alloying elements on the structure of the obtained layers. Several types of zinc alloys and alloying elements Bi, Ni, Sn, Pb have been studied in various combinations and concentrations.

2. Experimental conditions

In the pure zinc melt (Table 1) alloys were introduced in different combinations, Bi, Sn, Ni and Pb. The chemical composition of the zinc coatings studied is presented in Table 2.

Table 1. *Chemical composition of zinc used in experiments, in %*

Zn	Pb	Cu	Fe	Sn	Al	Cd
99.996	0.0014	0.0004	0.0005	0.0005	0.0005	0.0004

The alloying elements were gradually introduced into the zinc bath taking account their physical characteristics (Table 3). As can be seen from Table 3, Bi, Sn and Pb have physical

THE ANNALS OF "DUNAREA DE JOS" UNIVERSITY OF GALATI
FASCICLE IX. METALLURGY AND MATERIALS SCIENCE
No. 4 - 2018, ISSN 2668-4748; e-ISSN 2668-4756
Article DOI: https://doi.org/10.35219/mms.2018.4.02

characteristics close to that of zinc and were introduced into the galvanizing bath at 450 °C in the form of a pure metal crushed and preheated at 200 °C. Nickel has a much higher melting temperature than zinc, and Zn-Ni pre-alloyed with 2% Ni, finely ground and preheated at 200 °C, was used to alloy the zinc bath. It was introduced into zinc bath at 600 °C. In all cases, mechanical homogenization was applied. After homogenization, samples were taken which were analyzed with an X-ray spectrometer type Invov-X System.

Table 2. *Chemical composition of alloys used in experiments*

Alloy	Alloying elements, [%]				
	Pb	Bi	Sn	Ni	Zn
Zn-Bi	0	0.36	0	0	rest
Zn-Bi-Sn	0	0.35	3.50	0	rest
Zn-Bi-Sn- Ni	0	0.41	3.49	0.17	rest
Zn-Pb- Bi-Sn-Ni	0.72	0.41	3.88	0.16	rest

Table 3. *Physical characteristics of zinc and alloying elements used*

Element	Physical characteristics			
	Density [kg/dm^{3}x10^{-3}] at 20 °C	Melting point °C	Boiling point °C	Latent heat [Cal/g]
Zn	7.13	419.5	907	27.3
Bi	9.8	271	1440	-
Sn	7.3	232	2590	13.96
Ni	8.9	1455	3000	73
Pb	11.34	327.4	1750	5.75

Table 4. *Chemical composition of strip steel (support) in [%]*

C	Si	Mn	P	S	Al	Cu	Ni	Cr
0.040	0.023	0.210	0.010	0.012	0.039	0.015	0.020	0.020

The chemical composition, of covered steel strip is shown in Table 4.

The galvanizing was done at a temperature of 450 °C with a 10 second immersion time. The obtained layers were analyzed in cross-section by optical microscopy on an Olympus-type microscope.

3. Results and discussions

The metallographic analysis of the microstructure of the coating layer, obtained in alloyed zinc, shows significant changes compared to the microstructure of pure zinc layers (Fig. 1).

The influence of the alloying elements is manifested both in the structure and size of the alloy layer, which is formed at the interface with the support steel, following the reactions between iron and zinc, as well as in the structure of the resulting zone by the entrainment of the bath melt and located over the Zn-Fe alloys layer.

The two areas are distinct both on attacked and un-attacked samples. On the attacked sample (Fig. 1), the layer of Zn-Fe alloys (formed of phases Γ, δ, ζ) appears darker than the zinc sheet in the layer surface (phase η). On non-attack samples the intermetallic compounds white bright are observed.

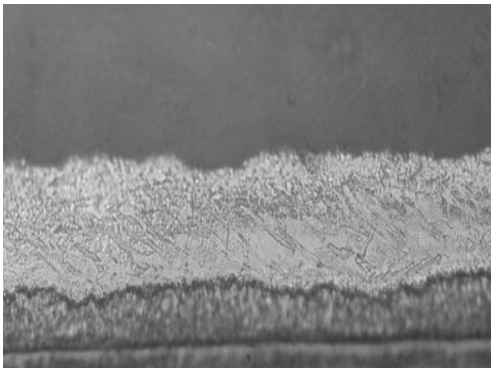

Fig. 1. *The layer microstructure obtained in pure zinc, x200*

THE ANNALS OF "DUNAREA DE JOS" UNIVERSITY OF GALATI
FASCICLE IX. METALLURGY AND MATERIALS SCIENCE
Nº. 4 - 2018, ISSN 2668-4748; e-ISSN 2668-4756
Article DOI: https://doi.org/10.35219/mms.2018.4.02

Alloying of the zinc with 0.36% Bi. Bismuth is added to the zinc bath to increase the melt fluidity and it can replace the lead, considered toxic to the environment. Microstructural analysis of the layer obtained in this alloy (Figures 2a and b) shows a decrease in the phase layer η due to the increase in melt fluidity. The Zn-Fe alloy layer does not change significantly from pure zinc coating. However, there is a diminution of this when bismuth particles mechanically block Zn-Fe layer growth (Fig. 3). Since bismuth and zinc are insoluble in the solid phase, separation of bismuth crystals is observed in the η phase (zinc) layer. On rapid cooling they are dispersed homogeneously (Fig. 2b) and during slow cooling they clump to the surface (Fig. 3).

Separation of bismuth crystals in the zinc matrix was also revealed in the microstructural analysis of samples taken from the bath with Zn-Bi alloy (Fig. 4).

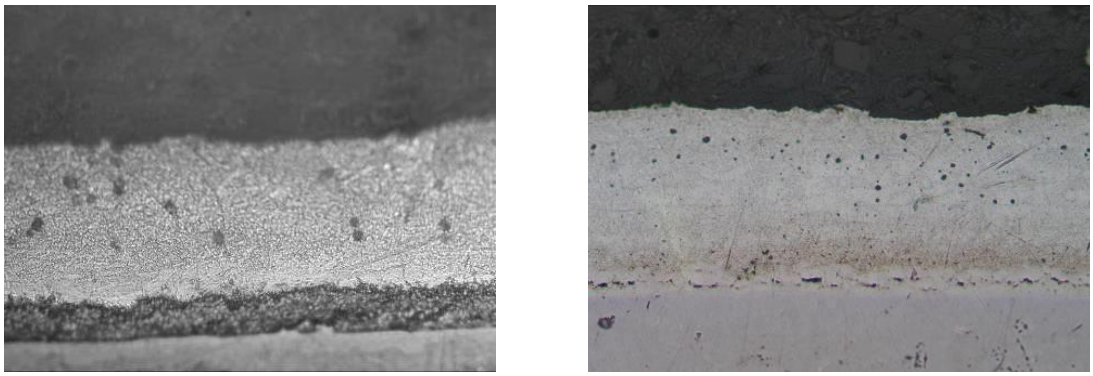

a) with attack b) non attack

x800

Fig. 2. *Microstructure of coating layer obtained by micro alloying with 0.36% Bi*

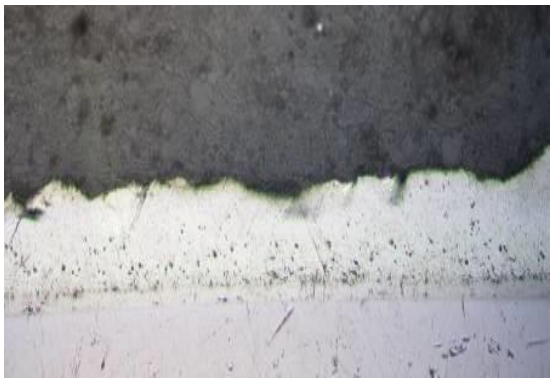

Fig. 3. *Agglomeration of the bismuth crystals at the growth front of Zn-Fe phase, x400, non-attack*

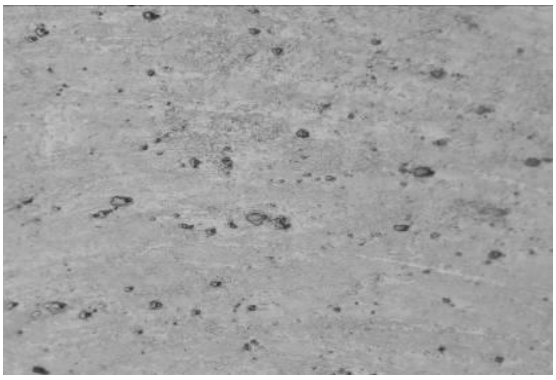

Fig. 4. *Microstructure of Zn-Bi alloy, x400*

THE ANNALS OF "DUNAREA DE JOS" UNIVERSITY OF GALATI
FASCICLE IX. METALLURGY AND MATERIALS SCIENCE
Nº. 4 - 2018, ISSN 2668-4748; e-ISSN 2668-4756
Article DOI: https://doi.org/10.35219/mms.2018.4.02

Microstructure of Zn-Sn-Bi layers. The Tin is added to the zinc bath in order to increase the corrosion resistance of the layer. Alloying with tin increases the corrosion resistance of the coating but, at the same time, leads to an increase in layer thickness (Fig. 5 a and b). For this reason, tin is not added alone to the zinc bath and it is accompanied by a melt fluidity enhancing element such as lead or bismuth. Tin, in a concentration of over 2.5%, acts on the layer of Zn-Fe alloys to reduce it by forming a mechanical barrier between the intermetallic and zinc phase (Fig. 5b).

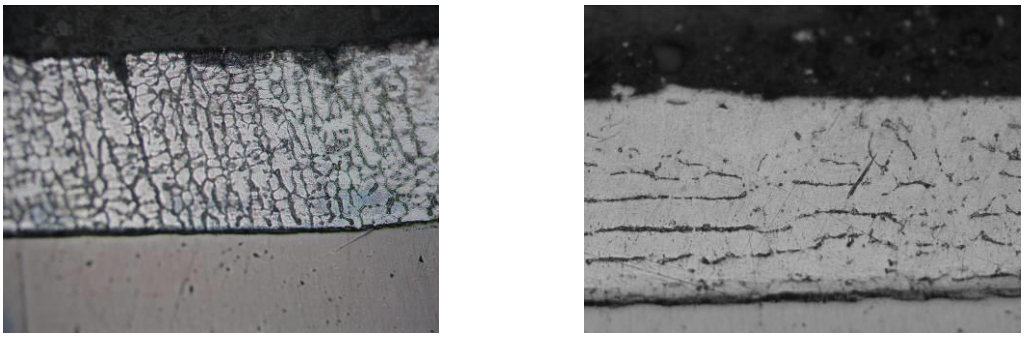

a) with attack b) non attack

x400

Fig. 5. *The microstructure of the coating layer obtained in Zn-Bi-Sn alloy*

Fig. 6 shows the microscopic appearance of the Zn-Sn-Bi alloy. Tin and bismuth are elements insoluble in zinc and they separate as crystals in the zinc mass or at grain boundary.

Melt alloying with Ni. Nickel increases the fluidity of the zinc melt and increases the corrosion resistance of the coating. In the structure of the protective layers obtained in alloyed baths simultaneously with nickel-tin-bismuth (Fig. 7), it is observed the effect on the iron-zinc alloy layer, which is drastically reduced. The effect is cumulative of nickel and tin, the bismuth acting on the thickness of the layer, in the sense of reducing it, by increasing the melt fluidity and decreasing the superficial tension.

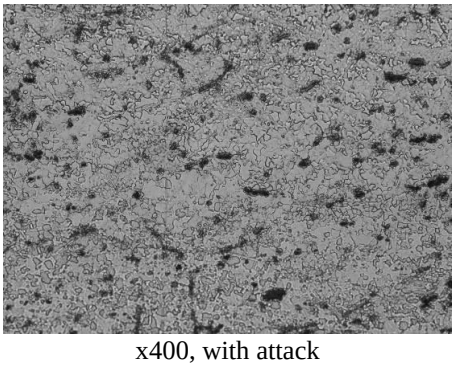

x400, with attack

Fig. 6. *Microstructure of the Zn-Sn-Bi alloy*

The formation of many compounds between nickel and zinc and between nickel and the other micro alloying elements (Sn and Bi) leads to the obtaining of a composite structure for Zn-Ni-Sn-Bi alloy with intermetallic compounds dispersed in the zinc matrix (Fig. 8).

x400, with attack

Fig. 7. *The microstructure of the coating layer obtained in Zn-Sn-Bi-Ni alloy*

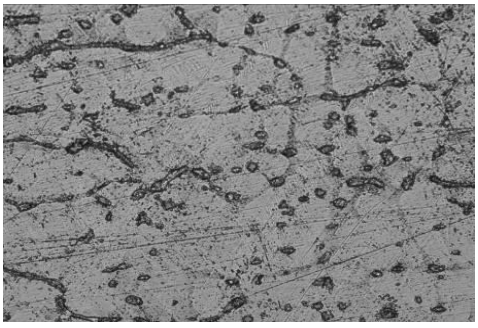

Fig. 8. *Microstructure of the Zn-Sn-Bi-Ni alloy, x400, with attack*

At the simultaneous alloying with lead and bismuth we obtain finer and uniform layers with the same aspect of the microstructure (Fig. 9 a and b) as the layer obtained in Zn-Sn-Bi-Ni alloy. The presence near bismuth of an important percentage of lead

THE ANNALS OF "DUNAREA DE JOS" UNIVERSITY OF GALATI
FASCICLE IX. METALLURGY AND MATERIALS SCIENCE
N°. 4 - 2018, ISSN 2668-4748; e-ISSN 2668-4756
Article DOI: https://doi.org/10.35219/mms.2018.4.02

increases significantly the fluidity of the melt, and the amount of zinc (phase ɳ) entrained on the sheet is smaller. Thus, a large amount of precipitates is formed in the zinc matrix and coalescing phenomena are manifested.

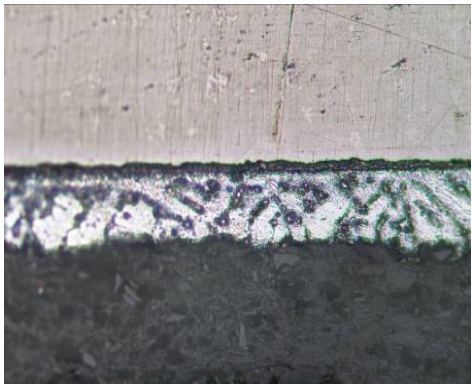

a) x400 with attack

b) x400, non-attack

Fig. 9. *The microstructure of the coating layer obtained in Zn-Sn-Pb-Bi-Ni alloy (intermetallic compounds and lead crystals in dendrite zinc matrix)*

4. Conclusions

Microstructural analysis of the layer obtained in Zn-Bi alloy, with 0.36% Bi, shows a decrease in the phase layer ɳ due to the increase in melt fluidity in presence of Bi. The Zn-Fe alloy layer does not change significantly from pure zinc coating.

Tin leads to an increase in layer thickness of the coating and for this reason, tin is not added alone to the zinc bath and it is accompanied by a melt fluidity enhancing element such as lead or bismuth. In a concentration of over 2.5% tin acts on the layer of Zn-Fe alloys to reduce it by forming a mechanical barrier between the intermetallic and zinc phase

In the structure of the protective layers obtained in Zn-Sn-Bi-Ni alloy is observed the effect on the iron-zinc alloy layer, which is drastically reduced. The effect is cumulative of nickel and tin, the bismuth acting on the thickness of the layer, in the sense of reducing it.

At the simultaneous alloying with lead and bismuth we obtain finer and uniform layers with the same aspect of the microstructure (Fig. 9 a and b) as the layer obtained in Zn-Sn-Bi-Ni alloy but the amount of zinc (phase ɳ) entrained on the sheet is smaller because the presence simultaneous of bismuth and lead increases significantly the fluidity of the melt.

References

[1]. ***, http://www.vmzinc-us.com.
[2]. Ball J., Poos A., *Hot-dip galvanized product for the automotive industries*, Revue de Metallurgy, no. 6, p. 570, 2002.
[3]. Radu T., Balint L., Balint S., *The alloys Zn-Al used for protection of sheet steel*, Analele Universităţii "Dunărea de Jos" din Galaţi, Fascicula IX, Metalurgie şi Ştiinţa Materialelor, p. 54-60, ISSN 1453-083 X, 2003.
[4]. ***, https://www.researchgate.net/publication/222157292.
[5]. Shukla S. K., Deepa M., Santos h Kumar, *Effect of Mg Addition (in Zinc Bath) on Galvanized Sheet quality*, International Journal of Materials Engineering, 2(6), p. 105-111, DOI: 10.5923/j.ijme.20120206.05, 2012.
[6]. Tamara Radu, Florentina Potecasu, Maria Vlad, *Research on obtaining and characterization of zinc micro-alloyed with bismuth coatings*, Metalurgia International no. 1, ISSN 1582-2214, p. 44-48, 2011.
[7]. Pistofidis N., Vourlias G., Pavlidou E., Stergioudis G., *Effect of Ti, Ni and Bi addition to the corrosion resistance of Zn hot-dip galvanized coatings*, Journal of optoelectronics and advanced materials, vol. 9, no. 6, p. 1653, 2007.
[8]. Reumont G., Perrot P., Foct J., *Thermodynamic study of the galvanizing process in a Zn – 0,1 % Ni bath*, Journal of Materials Science 33, p. 4759-4768, 1998.
[9]. Lewis G. P., Pederson J., *Optimizing the Ni-Zn process for hot dip galvanizing*, Cominco LTD., 1998.
[10]. Alonso C., Sanchez J., Fullea J., Andrade C., Tierra P., Bernal M., *The addition of nickel to improve the corrosion resistance of galvanized reinforcement*, 1995.
[11]. ***, https://galvanizeit.org/uploads/publications.
[12]. Caizhen Yao, See Leng Tay, Ji Hyun Yang, Tianping Zhu, Wei Gao, *Hot Dipped Zn-Al-Mg-Cu Coating with Improved Mechanical and Anticorrosion Properties*, Int. J. Electrochem. Sci., 9, p. 7083-7096, 2014.
[13]. Min-Suk Oh, Sang-Heon Kim, Su-Young Kim, Tae-Chul Kim and Jong-Sang Kim, *Effect of coating composition on microstructural properties and corrosion resistance of Zn-Mg-Al alloy coated steel sheets*, METAL 2014, May 21st-23rd, Brno, Czech Republic, EU, 2014.
[14]. Commenda C., Pühringer J., *Microstructural characterization and quantification of Zn–Al–Mg surface coatings*, Materials Characterization, vol. 61, issue 10, p. 943-951, 2010.

THE ANNALS OF "DUNAREA DE JOS" UNIVERSITY OF GALATI
FASCICLE IX. METALLURGY AND MATERIALS SCIENCE
Nº. 4 - 2018, ISSN 2668-4748; e-ISSN 2668-4756
Article DOI: https://doi.org/10.35219/mms.2018.4.03

POLYMERIC BLENDS: A SHORT REVIEW

Mihaela Claudia GOROVEI, Marina BUNEA, Adrian CÎRCIUMARU, Iulian Gabriel BÎRSAN
"Dunarea de Jos" University of Galati, Romania
e-mail: adrian.circiumaru@ugal.ro

ABSTRACT

At present, the use of polymeric materials is so intense in our society, that we could consider ourselves to be living in the „polymer age". Due to their versatility, polymers are present in every step of our whole „infrastructure". It is a growing research field due to the need of extending the application horizon of polymers with the purpose of replacing other materials (e.g. metallic) that are predominantly used in certain industries. This article is a review that discusses both the classification of polymer materials and state-of-the-art research of other authors with respect to polymer blends.

KEYWORDS: polymeric blends, nanoparticles, synthesis, classification

1. Introduction

It is known that the materials composed of polymers have been part of our civilization since prehistoric times. Polymers are abundant in nature, found in all living systems and materials such as wood, paper, leather, natural fibers, which are used extensively. While natural polymers retain their intrinsic importance, nowadays the synthetic materials are mostly used [1–4].

The term "polymer" is derived from the Greek words *poly* ("many") and *meros* ("part"). Quite literally, a polymer consists of "many units". Polymers are formed from a large number of identical small molecules, called monomers [5].

There are six main areas of polymer application: plastics, rubbers or elastomers, fibers, surface finishes, floor protection by coatings, and adhesives (Fig. 1) [6–9].

Polymers are macromolecules constructed by linking together a large number of much smaller molecules resulting from the chaining of a large number of small monomer molecules linked by covalent bonds. Polymers are obtained from polymerization reactions [10-15].

Fig. 1. *Examples of polymer applications* [16]

THE ANNALS OF "DUNAREA DE JOS" UNIVERSITY OF GALATI
FASCICLE IX. METALLURGY AND MATERIALS SCIENCE
Nº. 4 - 2018, ISSN 2668-4748; e-ISSN 2668-4756
Article DOI: https://doi.org/10.35219/mms.2018.4.03

Polymer technology is considered a mature technology and relatively easy to achieve through complex forms of most materials in a cost-effective mean. Since most polymers are low-density materials, they have specific service advantages in transport and metal replacement, thus becoming important. Polymeric materials dominate packaging applications and environmental pressures will ensure that recycling and reuse of this type of waste will continue to be an important development area [8, 17, 18]. Also, a number of new applications are emerging as a result of major advances in the domain of molecular and cellular biology.

Polymers were initially classified by Carothers (1929) in condensation and addition polymers based on the compositional difference between the polymers and the monomers from which they were synthesized [10, 19-21].

2. Polymer classification

Polymers can be classified according to several criteria (Table 1). The most obvious classification is based on the origin of polymer, i.e., natural or synthetic. Of course, polymer classifications can be more elaborate, from polymer structures, mechanisms of polymerization, preparation methods, up to thermal behaviour, monomer chemical nature, growth mechanisms of polymer chains, among more others.

Table 1. *Types of polymers* [20, 22-28]

Nomenclature	
BIS-GMA - bisphenol A glycidyl methacrylate	PET - polyethylene terephthalate
C – carbon	PGA - poly (glycolic acid)
CF – carbon fibres	PHB - polyhydroxybutirate
GF – glass fibers	PHEMA - poly (HEMA) or poly (2-hydroxyethyl)
HA - hydroxyapatite / hydroxylapatite methacrylate	PLA - poly (lactic acid)
HDPE - high density polyethylene	PLDLA - poly (L-DL-lactic acid)
KF – Kevlar fiber	PLLA - poli (acid L-lactic)
LCP - liquid crystal polymers	PMA - polymethylacrylate
LDPE - low density polyethylene	PMMA - polymethylmethacrylate
MMA - methyl methacrylate	POLIGLACTIN - PLA and PGA copolymer
PA – polyamide	POM - polyoxymethylene - polyacetal
PBT - polybutylene terephthalate	PP - polypropylene
PC - polycarbonate	PS - polysulfone
PCL - polycaprolactone	PTFE - polytetrafluoroethylene
PE - polyethylene	PU - polyurethane
PEA - polyethylacrylate	PVC - polyvinyl chloride
PEEK – polyetheretherketone	SR - silicone rubber
PEG - polyethylene glycol	THFM - tetrahydrofurfuryl methacrylate

Polymers can be either natural or synthetic. All the conversion processes that occur in our body (e.g. energy generation from food intake) is due to the presence of enzymes. Polymers of biological origins are enzymes, proteins and nucleic acids, as well. There are a large number of synthetic (artificial) polymers that are composed of different groups: fibers, elastomers, plastics, adhesives, etc. Each group itself has subgroups [29-31].

2.1. Classification based on polymer structure

Linear, Branched or Reticular, Ladder vs. Functionality:

Linear Structure

If a polymer is made of highly difunctional monomers, the result is a linear polymer chain.

The term linear may be somewhat misleading, however, because molecules do not necessarily require a linear geometric conformation as shown in Figure 2(a).

Branched structure

If several molecular reactions with three (or higher) functionalities (either intentionally or by side reactions) are introduced, the resulting polymer will have a branched structure.

One such example is the grafting of the branches made from the repeating unit "B" to a linear backbone

THE ANNALS OF "DUNAREA DE JOS" UNIVERSITY OF GALATI
FASCICLE IX. METALLURGY AND MATERIALS SCIENCE
N°. 4 - 2018, ISSN 2668-4748; e-ISSN 2668-4756
Article DOI: https://doi.org/10.35219/mms.2018.4.03

of the repeating units. Here it is said that B is grafted on A (Figure 2(b)).

Reticular structure

As the length and frequency of branches on polymer chains increases, the probability that the branches eventually reach from one backbone chain to another increases. When backbone is connected in this way, the molecular structure becomes a network, with all chains linked by covalent bonds (Figure 2(c)) [7, 19, 32].

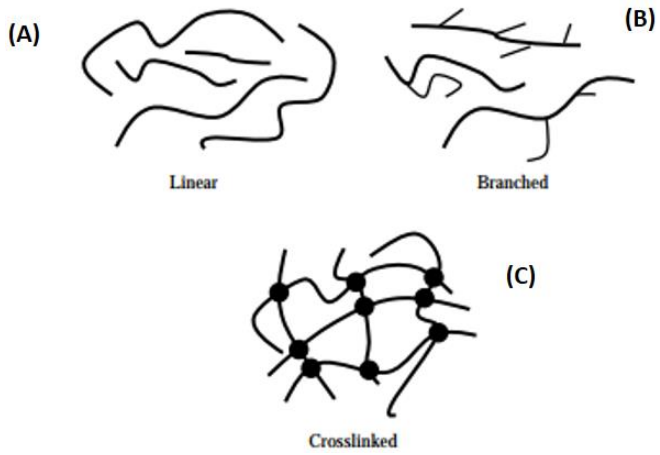

Fig. 2. *Schematic representation of polymer structures* [6]

Amorphous or crystalline state

Depending on structural state, the solid-state polymers can be considered amorphous, crystalline or, in some cases, semi-crystalline. In the cooling step of the molten-state polymer, molecules usually are attracted together leading to a relatively strong aggregation which forms a solid of low potential energy.

Homo/Co-polymers

When discussing composition, polymers can be copolymers or homopolymers. Polymers composed of a single repeat unit in the polymer molecule are known as homopolymers. In any case, chemistry researchers have developed techniques to build polymer chains that contain more than one repeated unit. Polymers composed of two different repeating units in the polymer molecule are defined as copolymers [7, 19].

Polymer classification based on the degree of stereoisomerism relative to the configurations of units in a chain:

- Geometrical isomerism - is understood as different configurations of substituents on a carbon-carbon double bond or a cyclic structure.
- Optical isomerism - comes from different configurations of substituents on a saturated carbon atom.

Classification of polymers based on the results of the polymer chain growth mechanism:

- Stable growth polymers (polycondensation)
- Chain polymerization (e.g., free radicals, anionic and cationic radicals).

3. Polymerization

Polymerization by chain or addition: Polymer chains increase by repeated addition of monomer molecules to an active chain centre, contrary to stepping polymerization. The polymerized chain can be made by free radicals and ionic moieties [33, 34].

Radical free polymerization: In free radical polymerization, three basic reactions occur during polymerization. These are initiation, propagation and termination reactions. In the initiation reactions there is continuous generation of free radicals.

Ionic polymerization: Ionic polymerization is a chain process that is used on an industrial scale to produce thermoplastic polymeric materials.

Anionic polymerization: Anionic polymerizations are industrially used for the production of thermoplastics, especially formaldehyde and e-caprolactam and block copolymers (e.g., styrene-butadiene-styrene type thermoplastic elastomers) [35-37].

Cationic polymerization: Cationic polymerization is defined as a polymerization reaction of adhesion mediated by a propagating carbocyte.

Stage growth or condensation polymerization: Forms the lifespan of the growing polymer chain until the functional group reaches its end [38].

THE ANNALS OF "DUNAREA DE JOS" UNIVERSITY OF GALATI
FASCICLE IX. METALLURGY AND MATERIALS SCIENCE
Nº. 4 - 2018, ISSN 2668-4748; e-ISSN 2668-4756
Article DOI: https://doi.org/10.35219/mms.2018.4.03

4. Nanoparticles and their role in polymer composites

Nanoparticles (NP) are a wide class of materials that include substances in the form of particles that are at least one size less than 100 nm. Depending on the global form, these materials can be 0D, 1D, 2D or 3D.

For the preparation of nanoparticles, most methods are performed in the emulsified system, involving two steps: preparing an emulsified system and forming nanoparticles by precipitating/gelling a polymer or polymerizing the monomers. Other methods of nanoparticle manufacturing are possible that do not involve their preparation from an emulsion, one example is the microfabrication process that produces nanoparticles from solid templates. In addition, nanoparticles can be manufactured by an inter/intramolecular crosslinking process. However, emulsification pathways and polymerization emulsion remain the most commonly used methods of preparing polymeric nanoparticles. [39-63].

5. Short review regarding synthesis of polymer blends

Aziz Babapoor and his collaborators have manufactured and characterized the nanoparticle-nanoparticle composites with electrophoretic/electrospinning phase change materials. The following conclusions can be drawn from the experimental results:

(a) The diameter of the fiber is strongly dependent on the electrical conductivity of solutions; for example, the fiber diameter is reduced to a higher electrical conductivity value. The smallest average fiber diameter of 59 nm for Fe^{-4} was found;

(b) FTIR results indicate that the addition of Al_2O_3 nanoparticles has a significant impact on PEG crystallization structure, and there is a strong interaction between Al_2O_3 and PEG;

(c) Of all the tested composites, the initial SiO_2 composite temperature was the highest, while the Al^{-2} composition provided the maximum temperature [64].

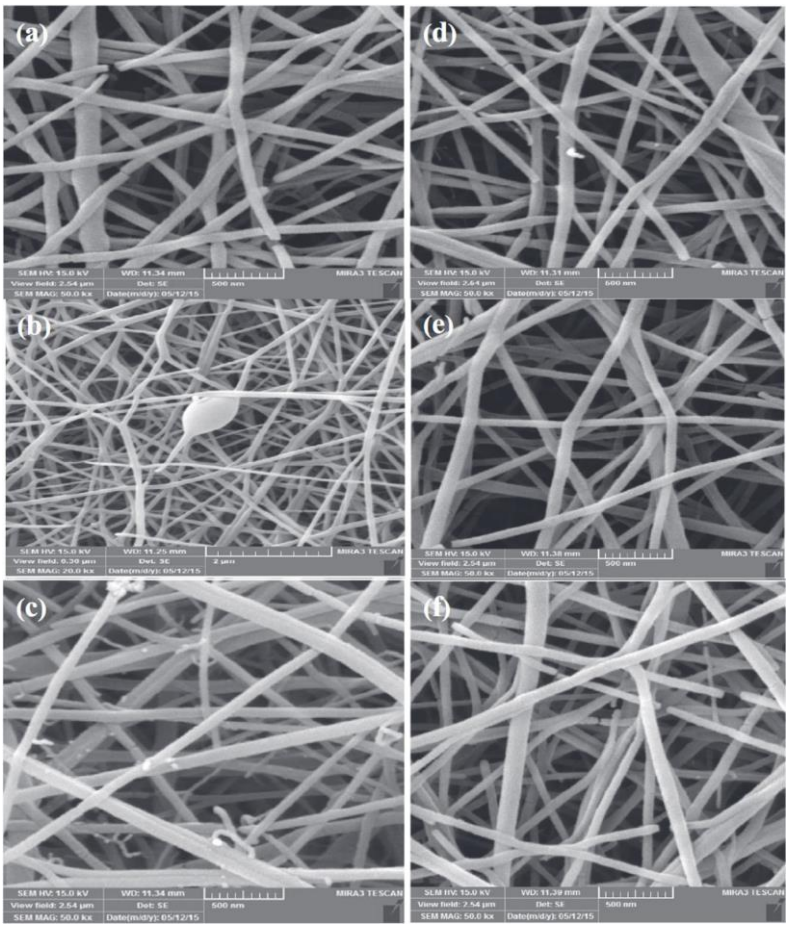

Fig. 3. *SEM images of nanofibers (a) Al^{-2}, (b) Zn^{-4}, (C) Si^{-2} and (d) Fe^{-1}* [64]

THE ANNALS OF "DUNAREA DE JOS" UNIVERSITY OF GALATI
FASCICLE IX. METALLURGY AND MATERIALS SCIENCE
Nº. 4 - 2018, ISSN 2668-4748; e-ISSN 2668-4756
Article DOI: https://doi.org/10.35219/mms.2018.4.03

S. E. Jasim and his collaborators have manufactured superconducting nanoparticles YBCO (Yttrium, Barium, Copper Oxide) by electrochemical electrospinning method. The sample was prepared by dissolving 4 g of Y-Ba-Cu acetate and 3 g of PVP powder in 25 mL of a mixture of propionic acid, acetic acid and methanol [65].

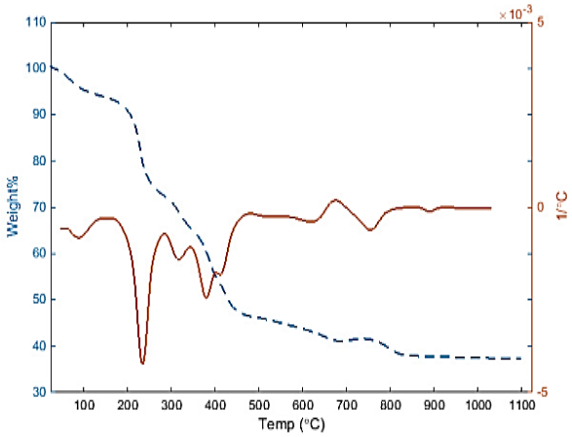

Fig. 4. *Thermogravimetric Analysis (TGA) and Differential Scanning Calorimetry (DSC) of YBCO electroplated nanoparticle samples* [65]

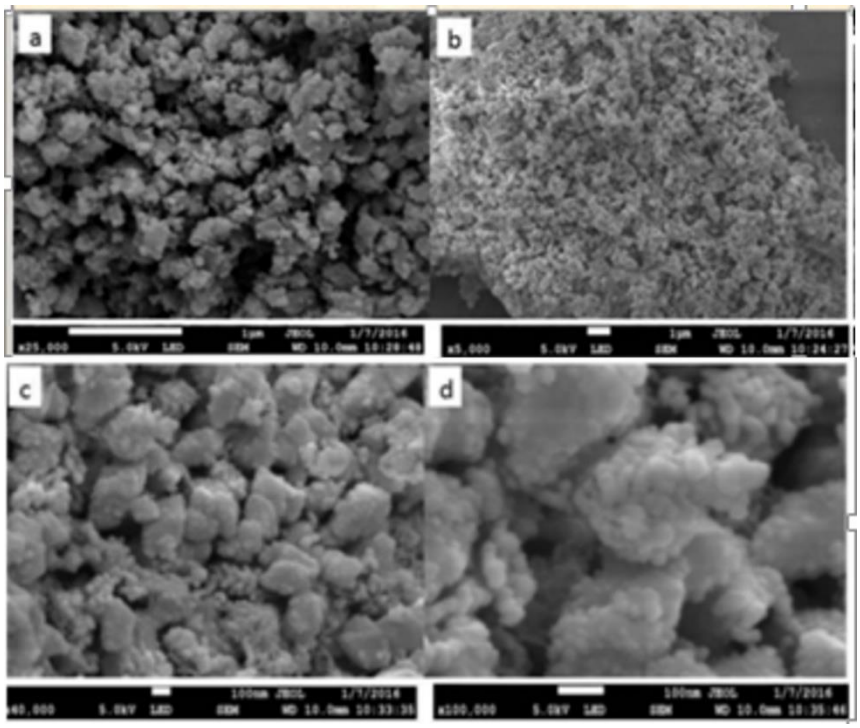

Fig. 5. *FESEM images of YBCO HTS nanoparticles (a), (b) after first heat treatment and (c), (d) after second heat treatment* [65]

The YBCO nanoparticle thin film temperature transition showed a zero resistance at 78 K with a semi-sharpened transverse width of 13 K. While the blank samples showed zero resistance at 85 K and a sharp transition width of 6 K. A typical nanoparticle diameter between 20 and 50 nm was obtained and agglomerated nanoparticles of about 388 nm were obtained. The measured area of the YBCO nanoparticle was higher than that for the semi-finished product and was not influenced by the calcination temperature [65].

THE ANNALS OF "DUNAREA DE JOS" UNIVERSITY OF GALATI
FASCICLE IX. METALLURGY AND MATERIALS SCIENCE
N°. 4 - 2018, ISSN 2668-4748; e-ISSN 2668-4756
Article DOI: https://doi.org/10.35219/mms.2018.4.03

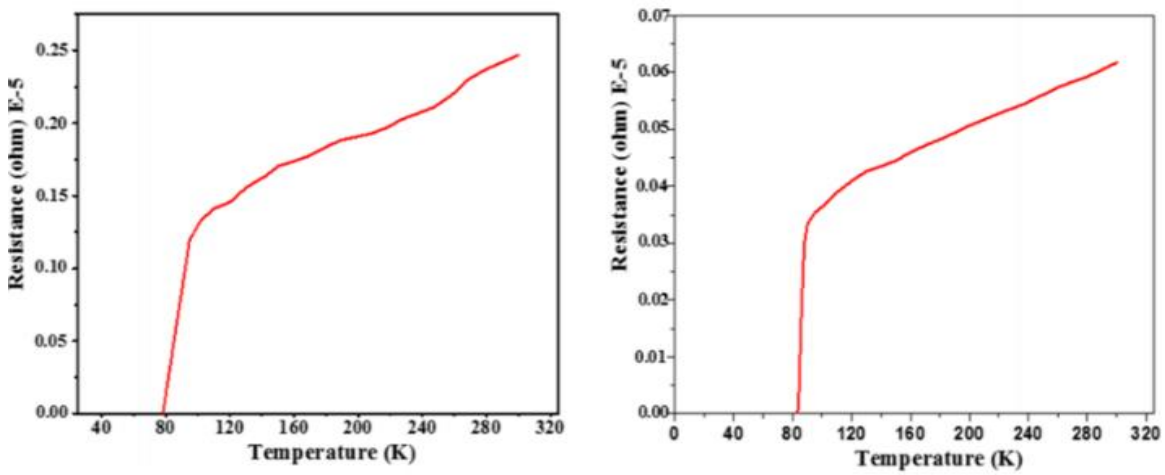

Fig. 6. *Tc measurements of YBCO HTS, (a) thin film nanoparticles Tc = 78K, (b) block sample Tc = 85K* [65]

Yun Wei *et al.* have manufactured TiN/carbon nanotubes by the electrospinning method. They synthesized TiN / carbon nanofibers by electrospinning of a polyvinylpyrrolidone (PVP, Mw = 1,300,000) and tetrabutyl titanate ($Ti(OC_4H_9)_4$), followed by two-stage heat treatment processes for nitration. $Ti(OC_4H_9)_4$ was dissolved in 10 mL ethanol (PVP was added to the mixture to control the viscosity of the solution).

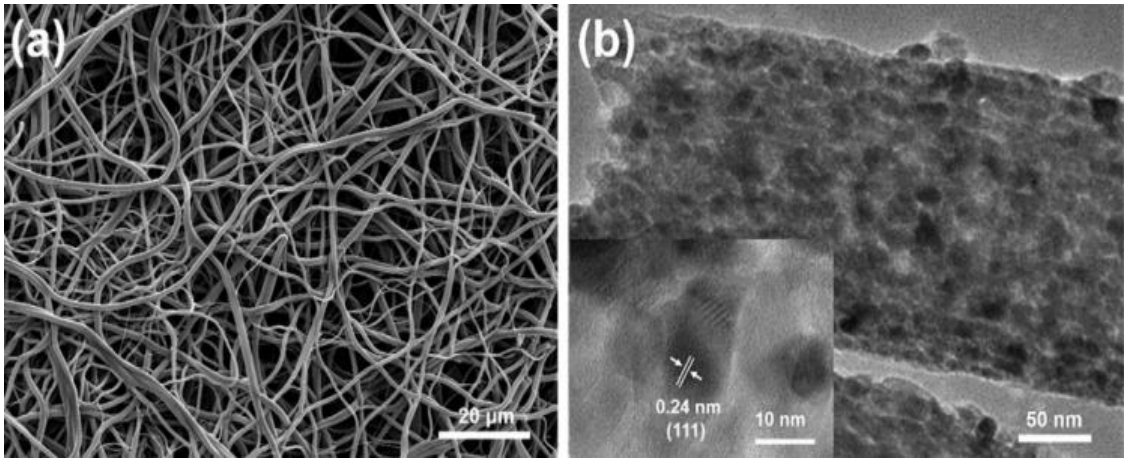

Fig. 7. *SEM (a) and TEM (b) images of TiN/carbon nanofibers under the insertion* [66]

Ti-containing polymer nanofibers were collected on the substrate by application of a high voltage of 11 kV. Polymeric nanofibers were calcined at 280 °C in air for 2 hours to obtain precursor nanofibers. Next, the synthesized precursor nanofibers were calcined in an oven under an ammonia atmosphere at 900 °C for 4 hours.

Finally, after the sample was cooled to room temperature under ammonia, the TiN/carbon counterparts were obtained.

The nanofiber morphology was examined with an electronic scanning microscope and an electronic TEM transmission microscope, at a 200 kV accelerating voltage [66].

Lu *et al.* have prepared PVP/Ag_2S nanoparticles in ethanol solution by Qian's method.

In a typical procedure:

- 0.1 g of $AgNO_3$ was dissolved in 3.45 g of ethanol with vigorous stirring, then various amounts of PVP (0.15, 0.31 and 0.48 g) were added and stirred for about 10 minutes to obtain different concentrations of PVP (4, 8 and 12 %v/v).

- an excess amount of CS2 was then introduced into the three solutions and stirred in the absence of light to allow sulfurization reaction for 24 hours to obtain different PVP/Ag_2S ratios (5.2:1 for 4%PVP, 10.6:1 for 8% PVP and 16.6:1 for 12% PVP).

THE ANNALS OF "DUNAREA DE JOS" UNIVERSITY OF GALATI
FASCICLE IX. METALLURGY AND MATERIALS SCIENCE
Nº. 4 - 2018, ISSN 2668-4748; e-ISSN 2668-4756
Article DOI: https://doi.org/10.35219/mms.2018.4.03

The black viscous solution obtained was loaded into a plastic syringe equipped with a 14 cm platinum needle. The needle was connected to a high voltage source (15 kV) which was applied to the electro-spin.

A piece of flat aluminum foil was placed 20 cm from the tip of the needle to collect the nanofibers. Electrospinning was performed in air.

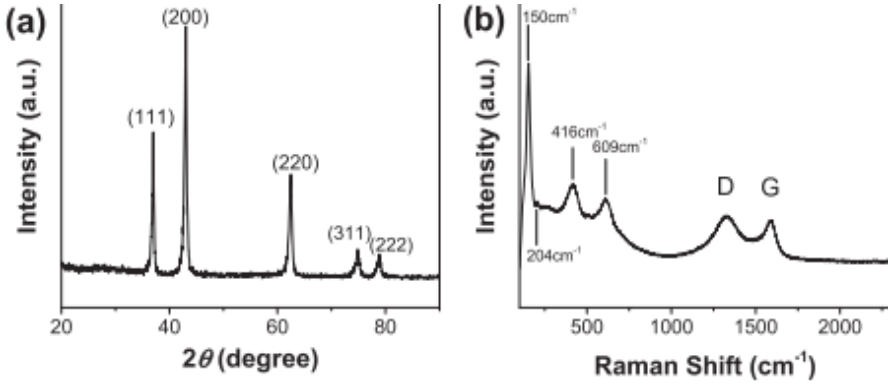

Fig. 8. *XRD (a) and Raman (b) spectra of prepared TiN/carbon fibers* [66]

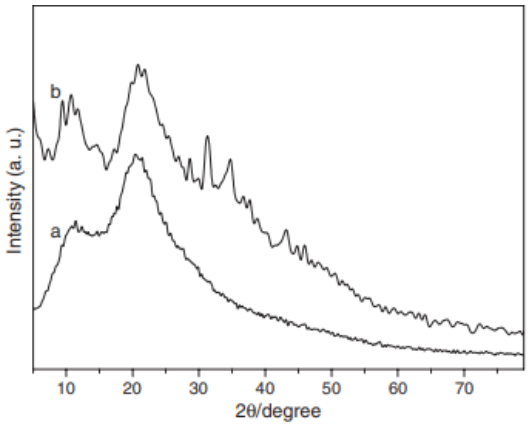

Fig. 9. *XRD patterns of (a) PVP and (b) PVP/Ag2S electro-spin composite fiber film* [67]

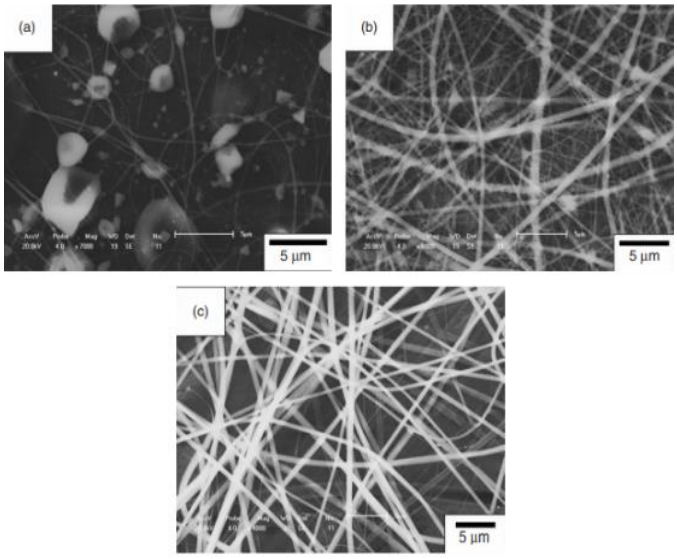

Fig. 10. *SEM images of PVP/Ag_2S composite fibers with different PVP concentrations. (a) [PVP] = 4% by mass; (b) [PVP] = 8% by mass; (c) [PVP] = 12% by mass* [67]

THE ANNALS OF "DUNAREA DE JOS" UNIVERSITY OF GALATI
FASCICLE IX. METALLURGY AND MATERIALS SCIENCE
Nº. 4 - 2018, ISSN 2668-4748; e-ISSN 2668-4756
Article DOI: https://doi.org/10.35219/mms.2018.4.03

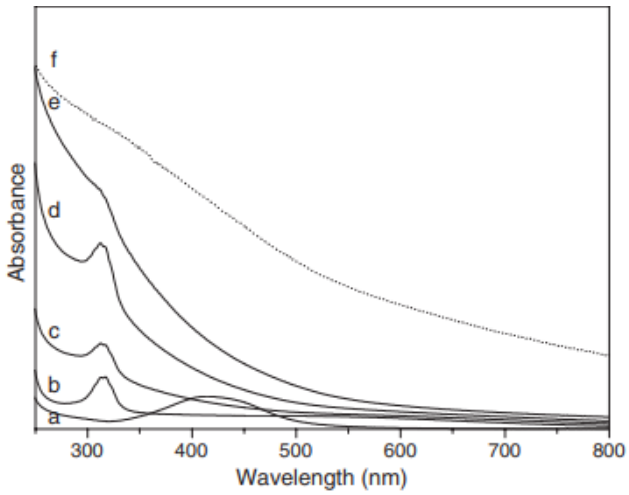

Fig. 11. *UV-vis spectra of PVP-$AgNO_3$ ethanol solutions with or without CS_2 at different reaction times and electro-spin PVP / Ag_2S composite fiber film: (a) PVP-$AgNO_3$ ethanol solution after agitation for 10 minutes; (b) - (e)) PVP / Ag_2S ethanol solution with a reaction time of 5 minutes, 2 hours, 6 hours and 24 hours; (f) PVP / Ag_2S glass fiber electroplating* [67]

Figure 12 shows TEM images of PVP/Ag_2S fibers which were electro-spinned from a solution containing 8% by weight PVP [67].

Vyacheslav V. *et al.* fabricated composite fibers by the intermediate electrospinning method containing $ZrOCl_2$ and $Al(NO_3)_3$ as ZrO_2 and Al_2O_3 precursors with PVP as additive. Figure 14 (A) discloses the microstructure of $ZrOCI_2/Al(NO_3)_3$/PVP for the manufacture of fibers. The average filament diameter is 284±69 nm. Data obtained by EDS indicate that the fibers prepared as an electrospinning solution contain the precursors of the polymer, ZrO_2 and Al_2O_3 (Zr, Cl, Al, N) [68].

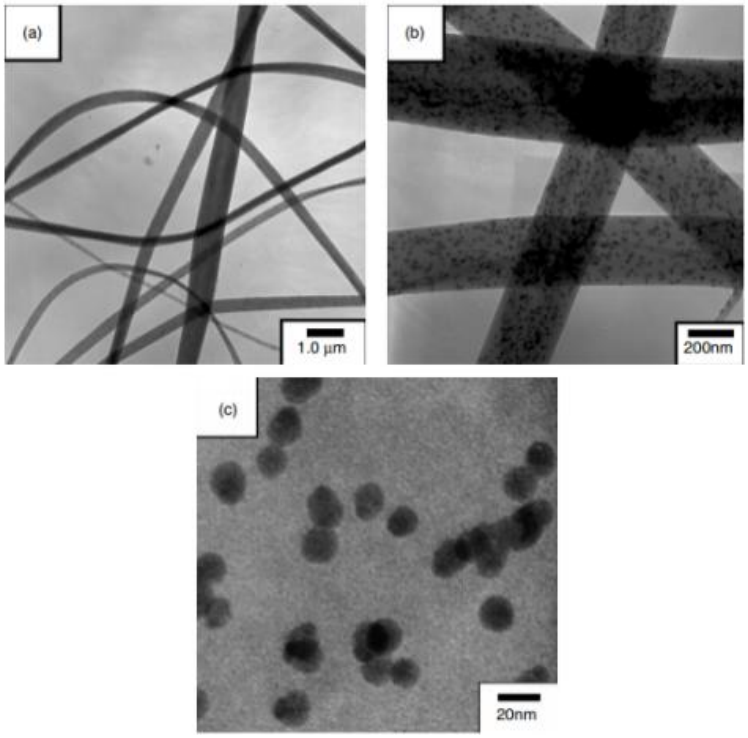

Fig. 12. *TEM images of PVP/Ag_2S composite fiber: [PVP] = 8% by mass* [67]

THE ANNALS OF "DUNAREA DE JOS" UNIVERSITY OF GALATI
FASCICLE IX. METALLURGY AND MATERIALS SCIENCE
Nº. 4 - 2018, ISSN 2668-4748; e-ISSN 2668-4756
Article DOI: https://doi.org/10.35219/mms.2018.4.03

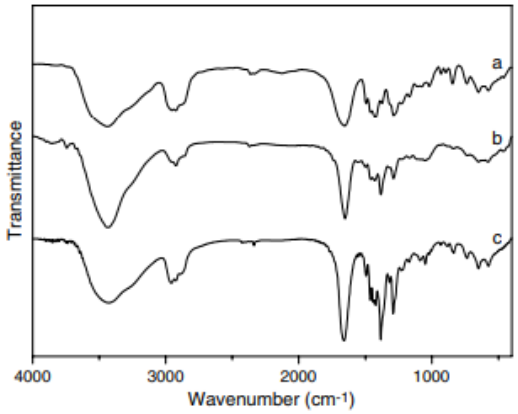

Fig. 13. *FTIR spectrum of (a) PVP, (b) PVP/silver nitrate fibers, (c) PVP/Ag_2S fibers* [67]

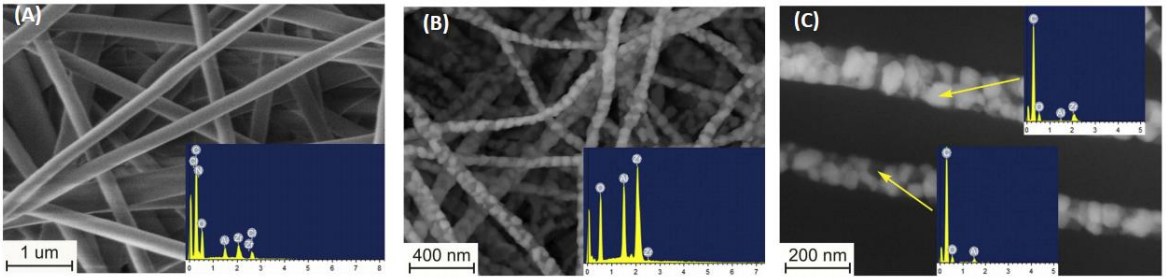

Fig. 14. *(A) SEM image of $ZrOCl_2/Al(NO_3)_3$/PVP fibers before calcination. The insert presents the EDS spectrum; (B) SEM image of $ZrOCl_2/Al(NO_3)_3$/PVP fibers is calcined at 1200 °C. The EDS spectrum is inserted; (C) SEM image of individual ceramic nanofibers. The inserts present the results of the local EDS analysis* [68]

The presence of the two distinct phases can be clearly seen in Fig. 14(C): ZrO_2 (brighter phase) and Al_2O_3 (dark phase). It should be noted that Al_2O_3 is partially dissolved in ZrO_2 (upper insert in Fig. 14(C). The carbon peak comes from the conductive tape used to fix samples for SEM visualization.

The formation and evolution of the crystalline structure of the composite fibers with the increase of calcination temperature is shown in Fig. 15. It can be seen that the $ZrOCl_2/Al(NO_3)_3$/PVP fibers before the thermal treatment are amorphous. The complete decomposition of the bonded polymer, zirconium and aluminum salts at 500 °C has no effect on the main crystal reflections at 20 = 30.2°, 35.2°, 50.2° and 60.2° [68].

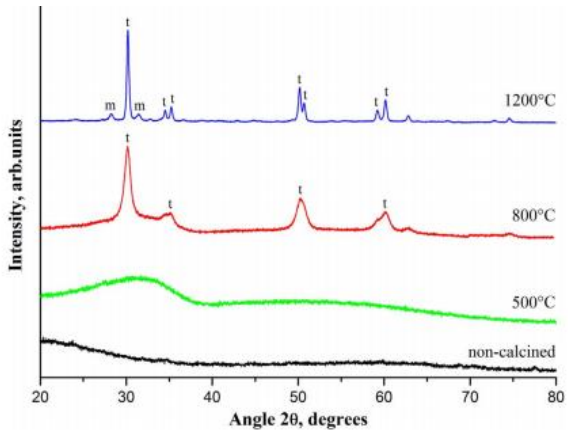

Fig. 15. *XRD formats of calcined $ZrOCl_2/Al(NO_3)_3$/PVP fibers at different temperatures; m - the monoclinic phase of ZrO_2, t - the tetragonal phase of ZrO_2* [68]

THE ANNALS OF "DUNAREA DE JOS" UNIVERSITY OF GALATI
FASCICLE IX. METALLURGY AND MATERIALS SCIENCE
Nº. 4 - 2018, ISSN 2668-4748; e-ISSN 2668-4756
Article DOI: https://doi.org/10.35219/mms.2018.4.03

Guo-Xun Sun *et al.* have manufactured zirconium nanofibers. Zirconium carbonate ($CH_2O_7Zr_2$), acetic acid (CH_3COOH), Nitrogen nitrate hexahydrate ($Y(NO_3)_3 \cdot 6H_2O$) were added to the experiment. Under stirring at 30 °C-40 °C, the appropriate amount of PVP (molar ratio Zr (atoms): PVP = 1:0.001-0.0012) mixture is added to the solution.

Gel fibers were obtained using electrospinning method. The effect of the process parameters (voltage, collection distance and flow) on fiber morphology and diameters have been studied. The processes were synthesized under the following electrospinning conditions: the voltage was in the range 18-20 kV, the collection distance in the range of 10-12 cm and the flow rate in the range of 0.7-1.0 mL/h.

Zirconium nanofibres were obtained after sintering at 1200 °C (holding time, 2 hours) under an air atmosphere. The gel fibers were sintered from room temperature to 300 °C with a temperature rise rate of 0.5 °C/min, 1 °C/min from 300 °C to 800 °C, with time-keeping time one hour and 5 °C/min from 800 °C to 1200 °C.

SEM image (Figure 16(a)) indicates that the fibers have diameters of 400-600 nm. The fibers showed moderate flexibility. Observation of a single fiber (Figure 16(b) and (c)) indicates that the fiber is made from 20-40 nm granules and does not contain cracks, having a smooth surface. The SEM image from Figure 16(d) has a dense and smooth cross-section of the fiber.

Figure 16. shows the XPS survey spectrum and the high resolution of the detailed spectra of calcined ZrO_2 fibers at 1200 °C, the sample contains only Zr, Y, O, and a small amount of carbon. The existence of the C 1s peak is mainly caused by CO_2, which is absorbed by the surface of the sample. The XPS spectrum of the sample exhibits peak Zr $3d_{5/2}$ peak energy of 181.4 eV, Y $3d_{5/2}$ peak of 156.7 eV [69].

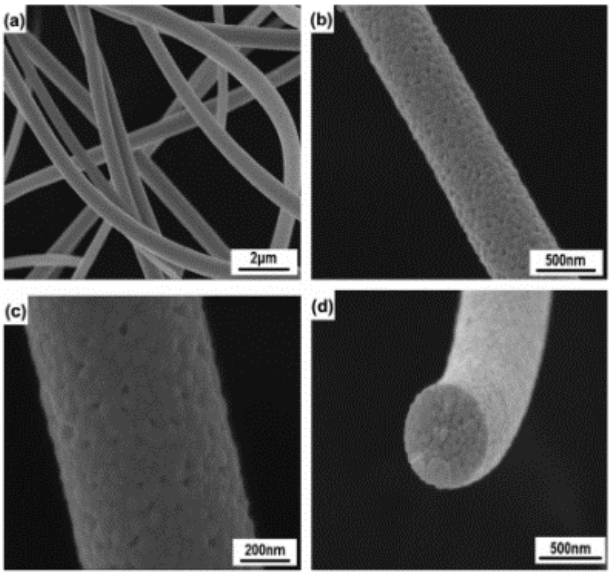

Fig. 16. *SEM images of fibers after calcination at 1200 °C* [69]

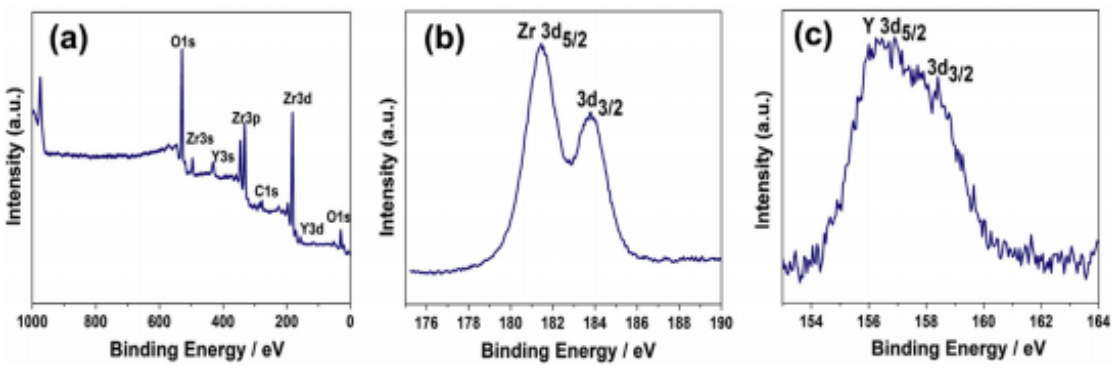

Fig. 17. *XPS spectra of (a) survey scan, (b) Zr 3d double, and (c) doublet of 3D in ZrO2 fibers calcined at 1200 °C* [69]

THE ANNALS OF "DUNAREA DE JOS" UNIVERSITY OF GALATI
FASCICLE IX. METALLURGY AND MATERIALS SCIENCE
N°. 4 - 2018, ISSN 2668-4748; e-ISSN 2668-4756
Article DOI: https://doi.org/10.35219/mms.2018.4.03

The absorption maximum at 1628 cm^{-1} is attributed to the bending vibration of H_2O. Absorption peaks (1556, 1456, 1352, 1032, 954 and 647 cm^{-1}) are attributed to bending vibrations of CH_3COOH functional groups, which can prove CH_3COO and Zr^{4+} binding. The broad absorption velocity at 470 cm^{-1} is the common contribution of the polymer in the Zr-O-Zr chain. From the data above, the minimalist structural formula of the zirconium acetate can be speculated as $ZrO(OH)(CH_3COO)\cdot H_2O$.

The process of idealized spinned soil in the experiment is shown in Figure 17. The transition in the soil solution is the first stage. At this stage, the possible structure of the poly-zirconia acetate (PZA) and the idealized formation of the PZA were speculated. In the second step, polyvinylpyrrolidone (PVP) was added and mixed with soil particles. Then, during the spinning process, there was a transition of sol-gel (gelation). The soil particles were dried, crosslinked and finally assembled into the gel with a coherent mesh.

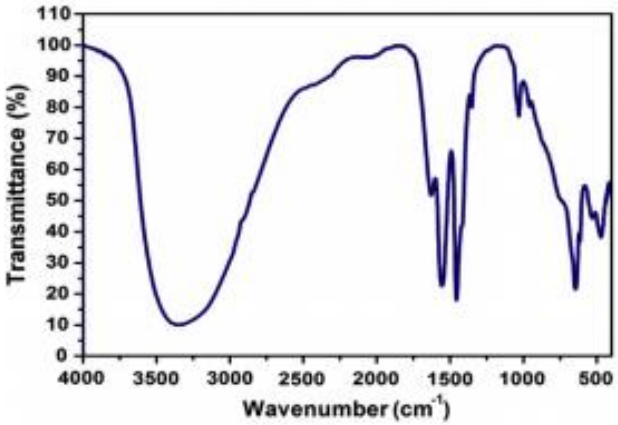

Fig. 18. *Infrared Fourier Transform Spectroscopy (FT-IR) of PZA* [69]

From the TG-DTA curves of the gel fibers, which is shown in Figure 19 it can be seen that the fibers have undergone three weight loss stages from room temperature to 800 °C, with a total loss of approx. 48.3%. The 24% weight loss below 240 °C was due to the loss of solvents including water and acetic acid.

From 240 to 450 °C, weight loss was approximately 19% corresponding to the decomposition and carbonization of PVP and acetic acid, which accompany the removal of solvent molecules in the gel network.

The weight loss of 5% between 450 °C and 700 °C corresponds to the expulsion of water molecules formed by the dehydroxylation of the materials together with the removal of the residual carbon by oxidation.

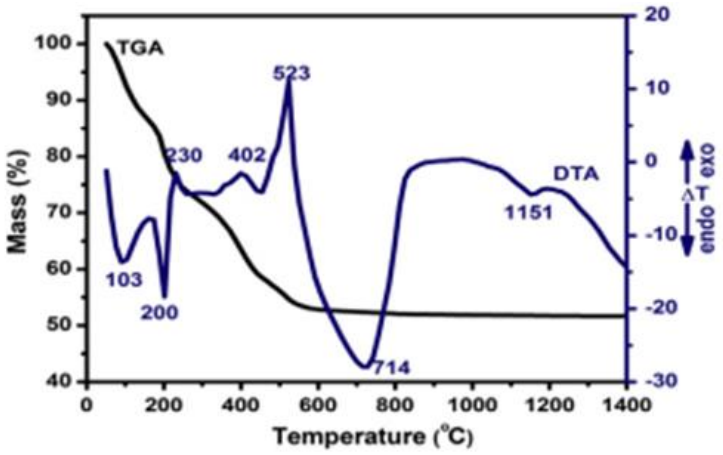

Fig. 19. *TG-DTA curves of gel fibers* [69]

THE ANNALS OF "DUNAREA DE JOS" UNIVERSITY OF GALATI
FASCICLE IX. METALLURGY AND MATERIALS SCIENCE
N°. 4 - 2018, ISSN 2668-4748; e-ISSN 2668-4756
Article DOI: https://doi.org/10.35219/mms.2018.4.03

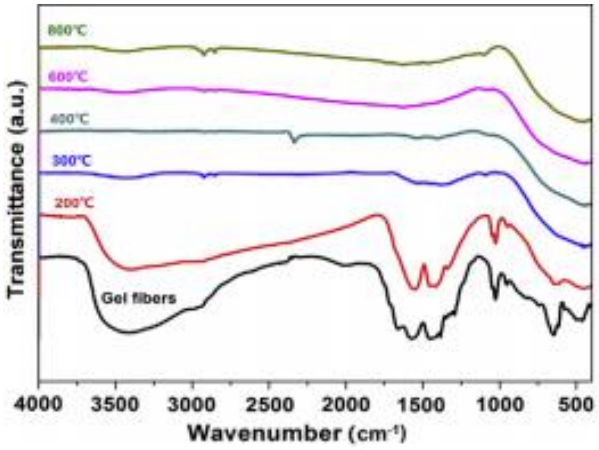

Fig. 20. *FT-IR spectra of gel fibers and calcined fibers at different temperatures* [47]

In the DTA curve, the rise of endothermic peaks at 103 °C and 200 °C may be due to the removal of adsorbent water, bound water and some organics in gel fibers.

Both weak, the exothermic foot at 230 °C and the exothermic peak at 402 °C corresponded to the decomposition and carbonization of acetates and PVP.

The carbon combustion and initiation of crystallization was indicated by the exothermic peak at 523 °C, which was confirmed by XRD results.

The endothermic peak at 714 °C was attributed to the growth of ZrO_2 granules. The low endothermic peak at 1151 °C was mainly attributed to the further increase of ZrO_2 grains [47].

5. Conclusions

Internal properties of materials such as solubility, interactions between polymer and payload, polymer chain flexibility, surface loading, stereochemistry, surface chemistry, molecular weight and crystallization capability, etc. should be taken into account in choosing the right method of preparation and appropriate processing.

Design of polymer blends is an interesting alternative for obtaining micro and nanostructured surfaces.

The cost is reasonable and does not contain time-consuming procedures.

Despite the crucial role of superhydrophylic and superhydrophobic surfaces play in the final application of the material, so far, most studies on polymer blends have been linked to control of physical and chemical properties, their barrier properties or electrical conductivity.

From the current review, it appears that control of polymer nanostructure and addition of nanoparticles has led to improvements in structural and functional properties in a number of polymer systems as a response to continuous requirements in advanced industrial sectors.

The availability of new nanoparticles with extraordinary properties (i.e. carbon nanotubes, graphites, but also nanoclays, nanocellulose, metals and ceramics) leads to new and interesting possibilities for a continued expansion of the polymer markets.

Acknowledgements

This work has been funded by the European Social Fund through the Sectoral Operational Programme Human Capital 2014-2020, through the Financial Agreement with the title „Burse pentru educaţia antreprenorială în rândul doctoranzilor şi cercetătorilor postdoctorat (Be Antreprenor!)", Contract no. 51680/09.07.2019 - SMIS code: 124539.

References

[1]. Thomas S., Mathew A. P., V. P. M., *Advances in natural polymers: composites and nanocomposites*, Heidelberg, New York, Springer, 2013.

[2]. Pearce E. M., Howell B. A., Pethrick R. A., Zaikov G. E., *Physical chemistry research for engineering and applied sciences*, Oakville, ON, Canada, Waretown, NJ, USA, Apple Academic Press, 2015.

[3]. Briscoe B. J., Sinha S. K., *Tribological applications of polymers and their composites – past, present and future prospects*, Tribology of Polymeric Nanocomposites, Elsevier, p. 1-22, 2013.

[4]. Guo H. C., Ye E., Li Z., Han M.-Y., Loh X. J., *Recent progress of atomic layer deposition on polymeric materials*, Materials Science and Engineering: C, vol. 70, p. 1182-1191, 2017.

[5]. McKeen L., *Introduction to Plastics and Polymers*, The Effect of Sterilization Methods on Plastics and Elastomers, Elsevier, p. 41-61, 2018.

[6]. Brazel C. S., Rosen S. L., Rosen S. L., *Fundamental principles of polymeric materials*, Third edition. Hoboken, New Jersey, Wiley, 2012.

[7]. Fried J. R., *Polymer science and technology, Third edition*, Upper Saddle River, NJ, Prentice Hall, 2014.

THE ANNALS OF "DUNAREA DE JOS" UNIVERSITY OF GALATI
FASCICLE IX. METALLURGY AND MATERIALS SCIENCE
N°. 4 - 2018, ISSN 2668-4748; e-ISSN 2668-4756
Article DOI: https://doi.org/10.35219/mms.2018.4.03

[8]. Buggy, *Polymeric Materials*, Reference Module in Materials Science and Materials Engineering, Elsevier, 2016.
[9]. Young R. J., Lovell P. A., *Introduction to polymers*, Boca Raton, CRC Press, 2011.
[10]. Odian G. G., *Principles of polymerization, 4th ed.*, Hoboken, N.J, Wiley-Interscience, 2004.
[11]. Awuzie C. I., *Conducting Polymers*, Materials Today: Proceedings, vol. 4, no. 4, p. 5721-5726, 2017.
[12]. Weitsman Y., *Fluid effects in polymers and polymeric composites*, New York, Springer, 2012.
[13]. Chikkali S., *Metal-catalyzed polymerization: fundamentals to applications*, Boca Raton: CRC Press, 2018.
[14]. ***, *Design and applications of nanostructured polymer blends and nanocomposite systems, 1st edition*, Waltham, MA, Elsevier, 2015.
[15]. Hasirci V., Huri P. Y., Tanir T. E., Eke G., Hasirci N., *1.22 Polymer Fundamentals: Polymer Synthesis*, Comprehensive Biomaterials II, Elsevier, p. 478-506, 2017.
[16]. Soroush M., Grady M. C., *Polymers, Polymerization Reactions, and Computational Quantum Chemistry*, Computational Quantum Chemistry, Elsevier, p. 1-16, 2019.
[17]. Francis R., Kumar D. S., *Biomedical applications of polymeric materials and composites*, Weinheim, Wiley-VCH Verlag GmbH & Co. KGaA, 2017.
[18]. Rezaie H. R., Shokuhfar A., Arianpour F., *Nanocomposite Materials from Theory to Application*, New Frontiers of Nanoparticles and Nanocomposite Materials, vol. 4, A. Öchsner and A. Shokuhfar, Eds. Berlin, Heidelberg: Springer Berlin Heidelberg, p. 171-232, 2012.
[19]. Ebewele R. O., *Polymer science and technology*, Boca Raton, CRC Press, 2000.
[20]. Banoriya D., Purohit R., Dwivedi R. K., *Advanced Application of Polymer based Biomaterials*, Materials Today, Proceedings, vol. 4, no. 2, 2017, p. 3534-3541.
[21]. Howell B. A. and American Chemical Society, *Introduction of macromolecular science/polymeric materials into the foundational course in organic chemistry*, Washington, DC, American Chemical Soc, 2013.
[22]. Kondratenko M. S., Elmanovich I. V., Gallyamov M. O., *Polymer materials for electrochemical applications: Processing in supercritical fluids*, The Journal of Supercritical Fluids, vol. 127, p. 229-246, Sep. 2017.
[23]. Zhu Y., Yang B., Chen S., Du J., *Polymer vesicles: Mechanism, preparation, application, and responsive behavior*, Progress in Polymer Science, vol. 64, p. 1-22, Jan. 2017.
[24]. Jordan R., *Surface-initiated polymerization. I & II*, Berlin, New York: Springer, 2006.
[25]. Chen H. *et al.*, *Thermal conductivity of polymer-based composites: Fundamentals and applications*, Progress in Polymer Science, vol. 59, p. 41-85, Aug. 2016.
[26]. Huang C., Qian X., Yang R., *Thermal conductivity of polymers and polymer nanocomposites*, Materials Science and Engineering, R. Reports, vol. 132, p. 1-22, Oct. 2018.
[27]. Mehra N. *et al.*, *Thermal transport in polymeric materials and across composite interfaces*, Applied Materials Today, vol. 12, p. 92-130, Sep. 2018.
[28]. Ramakrishna S., Mayer J., Wintermantel E., Leong K. W., *Biomedical applications of polymer-composite materials: a review*, Composites Science and Technology, vol. 61, no. 9, p. 1189-1224, Jul. 2001.
[29]. Mičicová Z., Pajtášová M., Domčeková S., Ondrušová D., Raník L., Liptáková T., *Inorganic Materials and their Use in Polymeric Materials*, Procedia Engineering, vol. 136, p. 239-244, 2016.
[30]. Sharma K. R., *Polymer thermodynamics blends, copolymers and reversible polymerization*, Boca Raton, Fla: CRC Press, 2012.
[31]. Pielichowski K., Njuguna J., *Thermal degradation of polymeric materials*, Shawbury: Rapra Technology, 2005.
[32]. van Krevelen D. W., te Nijenhuis K., *Properties of polymers: their correlation with chemical structure: their numerical estimation and prediction from additive group contributions*, 4th, completely rev. ed ed. Amsterdam, Elsevier, 2009.
[33]. Chern C.-S., *Principles and applications of emulsion polymerization*, Hoboken, N.J, Wiley, 2008.
[34]. Moad G., Solomon D. H., Moad G., *The chemistry of radical polymerization*, 2nd fully rev. ed. Amsterdam, Boston, Elsevier, 2006.
[35]. Tang Z. *et al.*, *Polymeric nanostructured materials for biomedical applications*, Progress in Polymer Science, vol. 60, p. 86-128, Sep. 2016.
[36]. Ibrahim Khan, Khalid Saeed, Idrees Khan, *Nanoparticles: Properties, applications and toxicities*, Arabian Journal of Chemistry, May 2017.
[37]. Dominick Fazarro, Walt Trybula, Jitendra Tate, Craig Hanks, *Nano-Safety, What We Need to Know to Protect Workers*, ISBN 978-3-11-037375-2, 2017.
[38]. Rajendra Kumar Goyal, *Nanomaterials and Nanocomposites Synthesis, Properties, Characterization Techniques, and Applications*, ISBN 9781498761666, 2018.
[39]. Sulabha K. Kulkarni, *Nanotechnology: Principles and Practices*, Springer International Publishing, ISBN 978-3-319-09170-9, 2015.
[40]. Jyotishkumar Parameswaranpillai, Nishar Hameed, Thomas Kurian, Yingfeng Yu, *Nanocomposite materials Synthesis, Properties and Applications*, CRC Press, ISBN 13: 978-1-4822-5807-3, 2017.
[41]. Jain N. K., Pathak S., *Electrochemical Processing and Surface Finish, Comprehensive Materials Finishing*, vol. 3, p 358-379, 2017.
[42]. Ma M., Rutledge G. C., *Nanostructured Electrospun Fibers*, Polymer Science: A Comprehensive Reference, vol. 7, p. 188-210, 2012.
[43]. Mouthuy P.-A., Ye H., *Biomaterials: Electrospinning, Reference Module in Biomedical Sciences*, Comprehensive Biotechnology (Second Edition), vol. 5, p. 23-36, 2011.
[44]. Lal A., Bleuler H., Wuthrich R., *Fabrication of metallic nanoparticles by electrochemical discharges*, Electrochemistry Communications 10, p. 488-491, 2008.
[45]. Shmigel A. V., Tikhonov P. A., Yu M., Pugachev K. E., *Electrochemical Fabrication and Studies of Metal Silver Nanoparticles*, Glass Physics and Chemistry, vol. 41, p. 329-333, 2015.
[46]. Jadhav R. A., Pandharinath S., *Electrochemical Synthesis and Characterization of Transition Metal Nanoparticles. Chapter 2: Preparation Methods and Characterization Techniques*, Shodhganga: A Reservoir of Indian Theses @ INFLIBNET, http://shodhganga.inflibnet.ac.in/jspui/handle/10603/84729.
[47]. Albrecht T., Horswell S., Allerston L. K., Rees N. V., Rodriguez P., *Review Article Electrochemical processes at the nanoscale*, Current Opinion in Electrochemistry, 2018.
[48]. Zangari G., *Fundamentals of Electrodeposition*, Reference Module in Chemistry, Molecular Sciences and Chemical Engineering, Encyclopedia of Interfacial Chemistry Surface Science and Electrochemistry, p. 141-160, 2018.
[49]. Hanawa T., *Electrodeposition of Calcium Phosphates, Oxides, and Molecules to Achieve Biocompatibility of Metals*, Reference Module in Chemistry, Molecular Sciences and Chemical Engineering, Encyclopedia of Interfacial Chemistry Surface Science and Electrochemistry, p. 129-140, 2018.
[50]. Chang Jiang Yang, Su-Moon Park, *Electrochemical behavior of PbO_2 nanowires array anodes in a zinc electrowinning solution*, Electrochimica Acta, p. 86-94, 2013.
[51]. Costello M., *Electrowinning, Gold Ore Processing*, (Second Edition) Project Development and Operations, p. 585-594, 2016.
[52]. Pyry-Mikko Hannula, Muhammad Kamran Khalid, Dawid Janas, Kirsi Yliniemi, Mari Lundstrom, *Energy efficient copper electrowinning and direct deposition on carbon nanotube film from industrial wastewaters*, Journal of Cleaner Production, p. 1033-1039, doi.org/10.1016/j.jclepro.2018.10.097, 2019.
[53]. Dong Hee Kang, Hyun Wook Kang, *Advanced electrospinning using circle electrodes for freestanding PVDF*

nanofiber film fabrication, Applied Surface Science, p. 251-257, doi.org/10.1016/j.apsusc.2018.05.211, 2018.

[54]. Elena Ewaldz, Riddhi Patel, Manali Banerjee, Blair K. Brettmann, *Material selection in electrospinning microparticles*, *Polymer*, p. 529-537, doi.org/10.1016/j.polymer.2018.08.015, 2018.

[55]. Mehran Shahhosseininia, Saeed Bazgir, Morteza Daliri Joupari, *Fabrication and investigation of silica nanofibers via electrospinning*, Materials Science & Engineering C, p. 502-511, doi.org/10.1016/j.msec.2018.05.068, 2018.

[56]. Santhosh S. Nair, Aji P. Mathew, *Porous composite membranes based on cellulose acetate and cellulose nanocrystals via electrospinning and electrospraying*, Carbohydrate Polymers, p. 149-157, dx.doi.org/10.1016/j.carbpol.2017.07.048, 2017.

[57]. Rolf Wüthrich, Jana D., Abou Ziki, *Chapter 2 Historical Overview of Electrochemical Discharges, Micromachining Using Electrochemical Discharge Phenomenon*, (Second Edition), Fundamentals and Application of Spark Assisted Chemical Engraving, p. 13-33 doi.org/10.1016/B978-0-444-53178-0.00003-1, 2015.

[58]. Rolf Wüthrich, Philippe Mandin, *Electrochemical discharges-Discovery and early applications*, Electrochimica Acta 54, p. 4031-4035, doi:10.1016/j.electacta.2009.02.029, 2009.

[59]. Jens Muff, *Chapter 3 - Electrochemical Oxidation – A Versatile Technique for Aqueous Organic Contaminant Degradation*, Chemistry of Advanced Environmental Purification Processes of Water, Fundamentals and Applications, p. 75-134, doi.org/10.1016/B978-0-444-53178-0.00003-1, 2014.

[60]. Kuravappullam V., Radha Karunamoorthy Sirisha, *Chapter 11 - Electrochemical Oxidation Processes, Advanced Oxidation Processes for Waste Water Treatment*, Emerging Green Chemical Technology, p. 359-373, doi.org/10.1016/B978-0-12-810499-6.00011-5, 2018.

[61]. Kobayashi S., Müllen K., *Encyclopedia of polymeric nanomaterials*, Berlin, Springer, 2015.

[62]. Muralisrinivasan Subramanian, *Basics of polymers: fabrication and processing technology*, New York, Momentum Press., 2015.

[63]. Das R., *Polymeric materials for clean water*, 2019.

[64]. Babapoor A., Karimi G., Khorram M., *Fabrication and characterization of nanofiber-nanoparticle-composites with phase change materials by electrospinning*, Applied Thermal Engineering, vol. 99, p. 1225-1235, 2016.

[65]. Jasim S. E., Jusoh M. A., Hafiz M., Jose R., *Fabrication of Superconducting YBCO Nanoparticles by Electrospinning*, Procedia Engineering, vol. 148, p. 243-248, 2016.

[66]. Wei Y. *et al.*, *Fabrication of TiN/Carbon nanofibers by electrospinning and their electromagnetic wave absorption properties*, Journal of Alloys and Compounds, vol. 735, p. 1488-1493, 2018.

[67]. Lu X., Li L., Zhang W., Wang C., *Preparation and characterization of Ag 2 S nanoparticles embedded in polymer fibre matrices by electrospinning*, Nanotechnology, vol. 16, no. 10, p. 2233-2237, 2005.

[68]. Rodaev V. V., Zhigachev A. O., Golovin Y. I., *Fabrication and characterization of electrospun ZrO_2/Al_2O_3 nanofibers*, Ceramics International, vol. 43, no. 17, p. 16023-16026, 2017.

[69]. Sun G.-X., Liu F.-T., Bi J.-Q., Wang C.-A., *Electrospun zirconia nanofibers and corresponding formation mechanism study*, Journal of Alloys and Compounds, vol. 649, p. 788-792, 2015.

THE ANNALS OF "DUNAREA DE JOS" UNIVERSITY OF GALATI
FASCICLE IX. METALLURGY AND MATERIALS SCIENCE
N°. 4 - 2018, ISSN 2668-4748; e-ISSN 2668-4756
Article DOI: https://doi.org/10.35219/mms.2018.4.04

CONSIDERATIONS ON APPLYING PRACTICAL CONTROL METHODS IN THE BIOLOGICAL TREATMENT OF WASTEWATERS FROM PAPER MANUFACTURING

Petronela NECHITA[1], Carmen Mariana BURTEA[1], Vasilica BARBU[2]

[1]Department of Environmental, Applied Engineering and Agriculture,
"Dunarea de Jos" University of Galati, Romania
[2]Department of Food Science and Engineering and Applied Biotechnology,
"Dunarea de Jos" University of Galati, Romania
e-mail: Petronela.Nechita@ugal.ro

ABSTRACT

Due to high efficiency, in terms of effluent quality, the activated sludge treatment is the most common method for removing the biodegradable impurities from industrial and urban wastewaters. Although these engineering systems of biological wastewater treatments increase the rate of biodegradable substances removing, in most cases, these are rarely able to achieve the maximum performances due to the lack of some fast methods to monitor and control the living biomass. In this context, in present paper are described some methods for evaluation of viability and biological activity of activated sludge, as essential parameters for ensuring the performance of biological treatment process. The proposed methods are based on the determination of metabolically active bacteria in activated sludge, using the activity of dehydrogenase enzymes (Triphenyl tetrazolium chloride TTC method) in the biological treatment of wastewaters generated from the paper manufacturing process.

KEYWORDS: activated sludge, bacterial respiration, biomass living, triphenyl-formazan, wastewater treatments, recovered papers

1. Introduction

The pulp and paper industry are ranked as large consumers of water and are consequently producing high amounts of wastewaters [1]. The environmental impact of pulp and paper industry is a particular concern since it generates large quantities of effluent with a high pollution loading, being considered a sixth largest polluter in the world (after oil, cement, leather, textile, and steel industries), eliminating a variety of gaseous, liquid, and solid wastes to the surroundings [2, 3].

Generally, pulp and paper industrial effluent is rich in recalcitrant compounds that cause severe pollution. For the treatment of such compounds, activated sludge process is frequently used to reduce the biodegradable organic pollutants from these wastewaters [4]. Practically, the process consists in treating of wastewater loaded with high content of organic impurities with a mass of microorganisms (activated sludge) in the presence of oxygen and controlled temperature, pH or the inhibitors content. The wastewater pollutants are mineralised to CO_2 and H_2O.

$$\mathbf{C_xH_y + O_2 + \textit{m/n} = H_2O + CO_2 + biomass}$$

(m – microorganisms, n – nutrients)

The activated sludge consists of a complex biological community including viruses, bacteria, protozoa fungi and metazoa that achieve the degradation of organics in waste water [5, 6]. Quantitatively, bacteria represent around 95% (approx. 108 – 1010 microorganisms/l) of the total microbial population and are essential for biological removal of organic carbon, ammonium and phosphate in the aeration tank.

The activated sludge technology is based on the ability of microorganisms to form flocs when wastewater is aerated. Within flocs, living and dead cells, organic and inorganic particles, fibres are held together by a slime matrix produced by bacteria.

THE ANNALS OF "DUNAREA DE JOS" UNIVERSITY OF GALATI
FASCICLE IX. METALLURGY AND MATERIALS SCIENCE
No. 4 - 2018, ISSN 2668-4748; e-ISSN 2668-4756
Article DOI: https://doi.org/10.35219/mms.2018.4.04

Optimal formation of flocs is essential for sludge quality and clean water leaving the final clarifier.

1.1. Methods for control of activated sludge viability and activity

Determination of microbial activity is of high importance for process analysis in biological wastewater because the degradation of organic matter, system productivity, and biomass turnover all depend on metabolically active microorganisms [7]. Control tests for monitoring the wastewater treatment plants are performed aiming to respect the regulation regarding wastewater effluents. The activity of bacteria in activated sludge is usually evaluated by measuring general parameters such as rate of oxygen uptake, adenosine triphosphate (ATP) content, biomass, or substrate utilisation. Other physical-chemical parameters are Mixed Liquor Suspended Solids (MLSS) that is a measure of total solids contained in the bioreactor, and the Mixed Liquor Volatile Suspended Solids (MLVSS), measuring the total microorganisms' compound, regardless to the fact if it is dead or alive. These parameters do not provide any information about the distribution of microbial activity or viability in sludge populations [7].

As of yet it is not known which bacteria in activated sludge are metabolically active and what constitutes their impact on system performance. However, only living and active biomass is important for degrading organic pollution and there is a lack today of operational tools allowing direct measurement of active biomass in the bioreactors [8].

Bacterial counts (aerobic mesophilic bacteria-AMB) can be determined using various techniques such as plate counting turbidity measurement, microscope enumeration and dehydrogenase activity measurement, but the procedure is time consuming and considerably underestimates the number of viable bacteria cells in activated sludge.

The standard parameter of the biomass that forms the activated sludge is the volatile part of the suspended matter called volatile suspensions. The active volatile biomass fraction depends on the organic fraction of the raw wastewater and the activated sludge age (as the sludge is the older the higher quantity of intra- and extracellular, inert and hardly degradable polymers is presented). The biodegradable fraction (about 77%) can be a parameter of the biological activity of the activated sludge. It represents the difference between initial volatile suspensions of an activated sludge taken from the WWTP and volatile slurries of the same sludge after an extended aeration period (about 30 days when the degradation no longer occurs) related to the initial volatile feedstock.

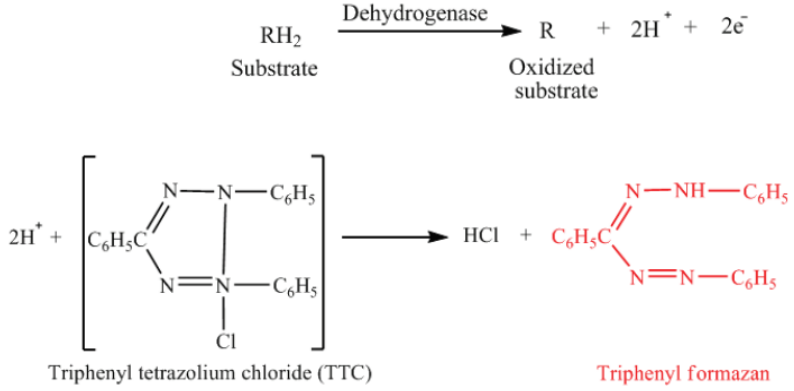

Fig. 1. *Mechanism showing the role of dehydrogenase in the reduction of triphenyl tetrazolium chloride (TTC) to triphenyl formazan (TF)* [10]

The dehydrogenase activity measurement technique has the advantage over other methods in being able to quantify the number of live cells that are present in the medium and it can be used in a relatively short time as well as at a low cost [9]. The dehydrogenase activity test is based on the principle that dehydrogenase enzymes are produced by all living cells and the extent to which this enzyme group oxidizes organic matter can be related to the number of live cells present. This group of enzymes transports electrons and hydrogen through a chain of intermediate electron carriers to a final electron acceptor (oxygen), resulting in the formation of water. The activity of the co-enzymes Nicotinamide Adenine Dinucleotide (NAD) and Flavin Adenine Dinucleotide (FAD) which act as intermediate electron acceptors can be measured by the visible colour change of a dye such as triphenyl tetrazolium

THE ANNALS OF "DUNAREA DE JOS" UNIVERSITY OF GALATI
FASCICLE IX. METALLURGY AND MATERIALS SCIENCE
N°. 4 - 2018, ISSN 2668-4748; e-ISSN 2668-4756
Article DOI: https://doi.org/10.35219/mms.2018.4.04

chloride (TTC). The process of measuring of dehydrogenase activity involves incubating the sample in the presence of triphenyl tetrazolium chloride and an electron-donating substrate. In its oxidized form, TTC is colourless, but in the presence of dehydrogenase enzymes, TTC is reduced to triphenyl formazan (TF), a red water insoluble compound [10]. The TF is retained within microbial cells and can result in highly coloured colonies when grown on agar plates [11]. The mechanism of the process is summarized in Figure 1. Triphenyl formazan (TF) can be extracted from cells using a solvent and the concentration is determined using colorimetry method by measuring the absorbance at 450-484 nm [10]. However, the amount of TF extracted depends on number of extractions, extraction solvent, incubation time and temperature, and medium pH.

The main objective of our study was to develop and to verify a dehydrogenase activity test to quantify the live bacterial cells from the mixed liquor suspended solids of aeration reactor from recycled paper wastewater treatment plant. Some correlations between the obtained results with this method and physical-chemical parameters of activated sludge from aeration tank, have been completed.

2. Experimental

2.1. Materials

The triphenyl tetrazolium chloride (TTC), as solution with 1% concentration was used for the dehydrogenase test. The triphenyl formazan (TF) was extracted from the microorganisms' cells using ethylic alcohol (96% purity). The activated sludge was collected from aeration reactors of biological treatment plant of wastewaters generated from recycled papers processing. The study was based on instant collected samples for a period of 5 days.

2.2. Methods

Dehydrogenase activity: 4.3 mL of activated sludge (diluted with distilled water until its total solids content is about 1 g/L) was removed into test tubes and mixed with 0.5 mL TTC, solution 1%. The test tubes were gently swirled to mix the content and then incubated at 20-25 °C for 30 min – 2 hours until the red colour appears. After this, the tubes were centrifuged for 3-10 min to separate the cells from other medium components. The resulted supernatant was discarding. The water-insoluble formazan extracted with ethanol was measured with a photometer. Thus, TF extraction was carried out three times using 5 mL ethanol each time. All the filtrates were combined and the absorbance of each solution was measured using a spectrophotometer at a wavelength of 450-484 nm (Figure 2).

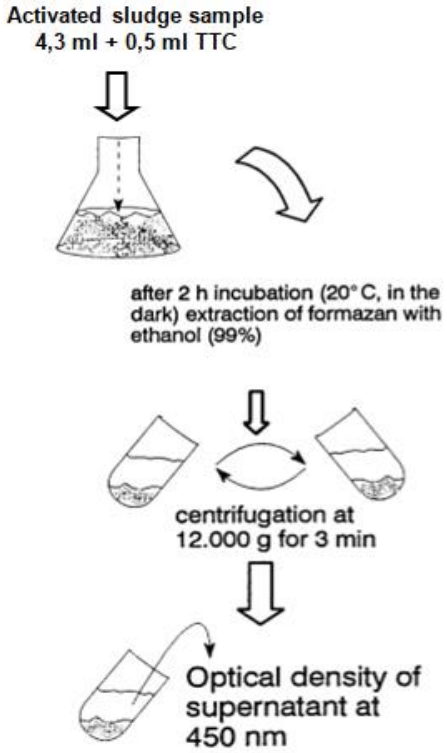

Fig. 2. *Flow diagram of the dehydrogenase activity assay in activated sludge*

The absorbance readings were used to calculate the activated sludge activity **(As)** as follow:

$$\mathbf{As = C_1/C_2} = \mu g \text{ formazan/mg sludge total solids} \quad (1)$$

where:

C1 = measurement result (concentration of formazan (μg))

C2 = concentration of activated sludge (mg):

$$\mathbf{C_2 = V \times TS} \quad (2)$$

where:

V = volume of activated sludge (mL), TS = total solids content in MLSS (g/L)

As = activity of the sludge expressed in μg formazan, represented by 1 mg sludge total solids.

Mixed Liquor Suspended Solids (MLSS) contained in the mixed liquor from aeration reactor was determined by drying at 105 °C. The test is essentially the same as the test performed for TSS in the wastewaters, except for the use of mixed liquor (activated sludge and wastewater) as sample. In

THE ANNALS OF "DUNAREA DE JOS" UNIVERSITY OF GALATI
FASCICLE IX. METALLURGY AND MATERIALS SCIENCE
N°. 4 - 2018, ISSN 2668-4748; e-ISSN 2668-4756
Article DOI: https://doi.org/10.35219/mms.2018.4.04

addition, the concentration of suspended solids found in the mixed liquor is typically much greater than that found in the wastewater.

Mixed Liquor Volatile Suspended Solids (MLVSS), is a test for volatile suspended solids (organic amount) found in a sample of mixed liquor. Volatile solids are those solids which are burnt up when a sample is heated to 550 °C. Most of the volatile solids in a sample of mixed liquor will consist of microorganisms and organic matter. As a result, the volatile solids concentration of mixed liquor is approximately equal to the amount of microorganisms in the water and can be used to determine whether there are enough microorganisms present to digest the sludge. The normal range of volatile portion in a mixed liquor sample is usually between 60-80% from total suspended solids.

Aerobic mesophilic bacteria (AMB) determined as plate (Plate Count Agar) counting of aerobic mesophilic bacteria in the suspension volume unit.

Sludge volumetric index (SVI) as ratio between the volume of sedimentary activated sludge for 30 minutes expressed in ml/l of slurry and the amount of dry matter expressed in g dry weight/L of slurry).

3. Results and discussions

The results obtained of each parameter during the study period are shown in Table 1.

Table 1. The physical-chemical parameters of activated sludge from aeration tank

Sample	**MLSS** mg/L	**MLVS,** %	**As** µg formazan/mg MLSS	**SVI**	**AMB,** ufc/g	**T, °C**	**pH**
Day 1	7866	76.96	0.326	109	3.5×10^6	27	7.85
Day 2	6147.5	82.27	0.404	120	6×10^5	28.3	8.11
Day 3	8090	80.69	0.542	123	1.4×10^6	27.2	8.09
Day 4	7935	78.91	0.612	124.5	2.5×10^6	27.1	7.95
Day 5	5307.5	68.16	0.722	123.5	4.5×10^6	27.4	8.01

There can be observed a high solid content of MLSS in aeration reactor that caused a high sludge volume index. Generally, a higher SVI (> 150) results in the growth of filamentous bacteria with negative effects on biological wastewater treatment performances. However, the number of aerobic mesophilic bacteria in aeration tank is at a certain level to enhance the degradation process of the organic impurities from wastewater. In Figure 3 is presented the evolution of activated sludge activity expressed as µg formazan/mg MLSS versus the number of live cells from aeration basin.

The results obtained emphasize a good correlation between these two parameters, as the number of viable cells is higher the viability and activity of activated sludge (dehydrogenase activity) is improved.

In this respect, the dehydrogenase activity test is able to quantify the number of live cells that are present in the aeration reactor, and it can be used in a relatively short time comparing with counting cells method.

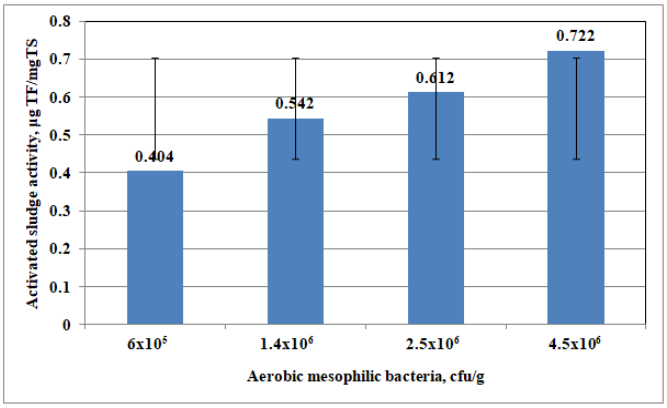

Fig. 3. *The correlation between activated sludge activity and aerobic mesophilic bacteria from aeration tank*

THE ANNALS OF "DUNAREA DE JOS" UNIVERSITY OF GALATI
FASCICLE IX. METALLURGY AND MATERIALS SCIENCE
Nº. 4 - 2018, ISSN 2668-4748; e-ISSN 2668-4756
Article DOI: https://doi.org/10.35219/mms.2018.4.04

During the study period, the volatile suspended solids were between 68.16% and 82.27% that involve a good activity of microorganisms in aeration tank. As is presented in Figure 4, between the volatile suspended solids and sludge activity expressed as extracted tryphenil formazan there is no linear correlation. This can be explained by the fact that the active fraction from volatile suspended solids is influenced by the sludge age (as the age of activated sludge is higher the fraction of inert and no biodegradable intra and extra cellular polymers is higher). In this case the high content of TSS of mixed liquor from aeration reactor confirm the high activated sludge age.

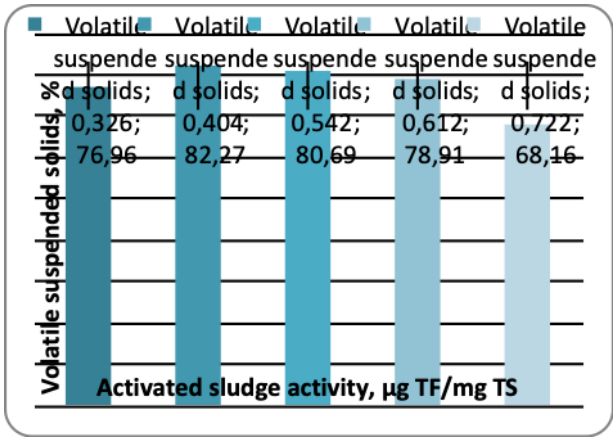

Fig. 4. *The correlation between sludge activity and volatile suspended solids*

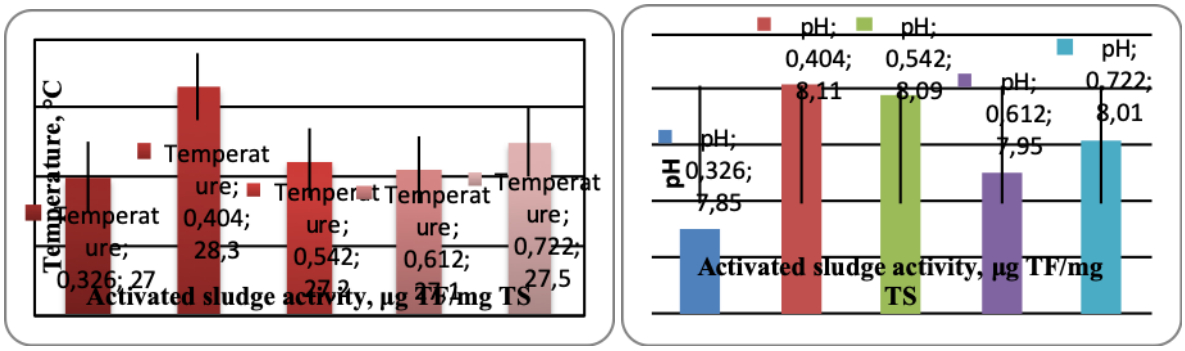

a) b)

Fig. 5. *The influence of temperature (a) and pH (b) on the activated sludge activity*

For most bacteria, the optimal pH range for growth is 6.5-7.5. The pH of mixed liquor from aeration tank was between 7.85 and 8.11 as is presented in Table 1. Based on the results presented in Table 1 and Figure 5(b) the activated sludge activity is not influenced by the medium pH as well as its temperature. The temperature in aeration tank had a lower variation (27 °C and 28.3 °C) and no influenced the activated sludge activity (Figure 5(a)).

5. Conclusions

A dehydrogenase activity measurement test using triphenyl tetrazolium chloride (TTC) was successfully developed and tested to evaluate the activity and viability of microorganisms involved in the biological treatment of wastewaters generated from paper manufacturing process. The obtained results using this method were compared with physical-chemical parameters of biological treatment process. The results showed that TTC method is well suited for measurements of microbial activity in activated sludge.

The analysis of the activated sludge activity based on cells counting or measuring of volatile suspended solids are good indicators and gives useful information regarding the live cell viability, but are time-consuming. Based on the obtained results and good correlation between the activated sludge activity measured using in situ method based on the tetrazolium salt TTC, for the routine measurements this test can be used with good results, giving the information about the live cells after 30 min (by red colour appearance after the activated sludge is mixed

with TTC). Furthermore, the TTC method constitutes a convenient and rapid approach for quantification and monitoring of inhibitory effects in activated sludge treatment processes.

Acknowledgement

This work was supported by a grant of the Romanian National Authority for Scientific Research and Innovation, CNCS/CCCDI-UEFISCDI, project number PN-III-P2-2.1-BG-2016-0040, contract no. 86BG/2016.

References

[1]. Sevimli M. F., *Post-treatment of pulp and paper industry wastewater by advanced oxidation processes*, Ozone: Science and Engineering 27, p. 37-43, 2005.
[2]. Ali M., Sreekrishnan T. R., *Aquatic toxicity from pulp and paper mill effluents: a review*, Adv Environ Res 5, p. 175-196, 2001.
[3]. Mathur R. M., Panwar S., Gupta M. K., Endlay N., Kukarni A. G., *Agro-based pulp and paper mills: environmental status, issues and challenges and the role of Central Pulp and Paper Research Institute*, Tewari PK (eds) Liquid asset, proceedings of the Indo-EU workshop on promoting Efficient Water Use in Agro Based Industries. TERI Press, New Delhi, India, p. 99-114, 2004.
[4]. Kumar V., Dhall P., Naithani S., Kumar A., Kumar R., *Biological Approach for the Treatment of Pulp and Paper Industry Effluent in Sequence Batch Reactor*, J Bioremed Biodeg, 5(3), http://dx.doi.org/10.4172/2155-6199.1000218, 2014.
[5]. Al-Shahwani S. M., Horan N. J., *The use of protozoa to indicate changes in the performance of activated sludge plants*, WaterRes., 25, p. 633-638, 1991.
[6]. Madoni P., *Role of protozoans and their indicator value in the activated sludge process*, Madoni P, (ed.) Biological Approach to Sewage Treatment Process: Current Status and Perspectives. Centro Bazzucchi, Perugia, Italy, p. 21-27, 1991.
[7]. Griebe T., Schaule G., Wuertz S., *Determination of microbial respiratory and redox activity in activated sludge*, Journal of Industrial Microbiology & Biotechnology, 19, p. 118-122, 1997.
[8]. Madoni P., *A sludge biotic index (SBI) for the evaluation of the biological performance of activated sludge plants based on the microfauna analysis*, Water Research, 28, p. 67-75,1994.
[9]. Backor M., Fahselt D., *Tetrazolium reduction as an indicator of environmental stress in lichens and isolated bionts*, Environ Exper Bot, 53, p. 125-133, 2005.
[10]. Burdock T. J., Brooks M. S., Ghaly A. E., *A dehydrogenase activity test for monitoring the growth of streptomyces venezuelae in a nutrient rich medium*, J Bioproces Biotechniq, 1(1), p. 1-10, http://dx.doi.org/10.4172/2155-9821.1000101, 2011.
[11]. Zhao X., Li H., Wu Q., Li Y., Zhao C., *et al.*, *Analysis of dehydrogenase activity in phytoremediation of composite pollution sediment*, 2nd Conference on Environmental Science and Information Application Technology, 2010.

THE ANNALS OF "DUNAREA DE JOS" UNIVERSITY OF GALATI
FASCICLE IX. METALLURGY AND MATERIALS SCIENCE
N°. 4 - 2018, ISSN 2668-4748; e-ISSN 2668-4756
Article DOI: https://doi.org/10.35219/mms.2018.4.05

CLIMATE CHANGE POLICIES IN THE EUROPEAN UNION

Bianca Georgiana OLARU, Cristian Silviu BĂNACU
The Bucharest University of Economic Studies, 6 Piata Romana, 1st District, Bucharest, 010374, Romania
e-mail: biancageorgiana.olaru@gmail.com

ABSTRACT

This article aims to highlight European policies on climate change taking into account the objectives of the Paris Agreement which aim to keep the global temperature below 2 °C and reduce carbon emissions. Therefore, Member States shall take measures to reduce greenhouse gas emissions in order to achieve the objectives set. Presently, a particular emphasis is placed on mitigating climate change that is related to the reduction of greenhouse gas emissions, and therefore EU Member States have adopted national programs to reduce emissions. The EU Energy-Climate Framework of 2030 was presented by the Commission on 22 January 2014, it is an effective way of communication which establishes a framework for EU policies on climate and energy in 2020-2030. In addition to mitigation climate change, adaptation is also needed to identify appropriate solutions to the effects of climate change and taking the best possible measures to prevent or reduce the damage that they may cause, as well as to identify the appropriate measures to achieve the objectives. EU strategy on adaptation to climate change has the role of supporting funding and research for the development of national strategies in the Member States, but also other actions related to EU policies.

KEYWORDS: reducing emissions, climate change mitigation, EU-level policies, adaptation to climate change, strategies

1. Introduction

Further, this article will highlight European, national and local policies and strategies to support stakeholders of climate change. At European level, climate action has the role of maintaining and reducing the negative effects of climate change.

Thus, the EU has the role of reducing greenhouse gas emissions, this being a major action at global level. Also, it is desirable to implement and implement the necessary actions and measures in response to changes and environmental effects due to climate change. At European level, these actions are classified by subdomains for better problem management: reducing greenhouse gas emissions, emissions trading, adaptation to climate change, low-carbon technologies, fluorinated greenhouse gases, etc.

1.1. Policies and strategies at EU level on climate change

One of the greatest challenges is climate change which refers to setting ambitious targets for short, medium and long-term emission reductions. According to researchers in the field, `in urban environments, great emphasis is put on mitigation and adaptation efforts to the effects of climate change` (Rosenzweig *et al.*, 2010). The involvement of decision-makers is necessary for the development of urban communities through instruments or policies that take account of environmental, in particular adaptation to climate change. At the same time, the involvement of decision-makers needs to be developed and awareness and information measures on the importance of this area have been taken. In this regard, `support efforts to implement measures and policies are recognized by scientists` (Leck and Simon, 2013). However, we should consider that these policies, strategies and other tools must be implemented at national / regional / local level and "the existence of international or even national climate policies is not a guarantee for local plans and actions" (Villarroel Walker *et al.*, 2014).

According to brief presentations on the European Commission website, in 2013, the European Union Strategy for Adaptation to Climate Change, which has been agreed by all EU Member

THE ANNALS OF "DUNAREA DE JOS" UNIVERSITY OF GALATI
FASCICLE IX. METALLURGY AND MATERIALS SCIENCE
N°. 4 - 2018, ISSN 2668-4748; e-ISSN 2668-4756
Article DOI: https://doi.org/10.35219/mms.2018.4.05

States, has been adopted. This strategy wants an Europeqn continent that adapts to climate change and resists over time in order to make the other generations benefit of optimal environmental conditions. These approaches and tools that can ensure better organization and coordination in climate action will lead to improved preparation and implementation by all Member State governments.

The EU Adaptation Strategy focuses on the following main objectives:

(i) Promoting climate action by Member States, through which the European Commission wishes to encourage Member States to implement and implement adaptation strategies and plans. Thus, to achieve this goal are needed European or national funds to support the development and improvement of adaptation to climate change impacts through key measures and specific instruments. At European level, it is intended to support actions and adaptation measures through a beneficial initiative called `the Covenant of Mayors for Climate and Energy`.

(ii) The implement of "climate proofing" action at European level by encouraging and promoting adaptation in vulnerable areas, such as agriculture, fisheries and cohesion policy, ensuring greater resistance in terms of European infrastructure and promoting the use of insurance against extreme weather phenomena or natural anthropogenic disasters.

(iii) Better informing decision makers on understanding gaps and inconsistencies to raise awareness of the adaptation and development of the European adaptation platform to the effects of climate change (Climate-ADAPT), which represents a unique way to inform in the field of adaptation to the effects of climate change.

According to the European Commission, the EU wants to achieve its greenhouse gas reduction targets by 2050 and taking into account the 2020 Climate and Energy Strategy and the Energy Climate Framework 2030. At European level, a low-carbon economy is needed and these set goals are the basis for achieving these goals. At EU level, with certain steps, we are on track to achieve the 20% target by 2020 to reduce carbon emissions and is following the application of legislation to reach the next target set by 2030. The 2020 target does not include emissions from the arable sector, land or forestry, but includes emissions from aviation.

However, target 2030 requires the EU to implement legislation to reduce emissions by at least 40% by 2030 as part of the EU's climate and energy framework 2030 and contribution to the Paris Agreement. This target 2030 targets the following issues: (i) Revision of the EU Emission Trading Scheme, (ii) national emission targets for non-ETS sectors; (iii) Integration of land use, land use change and forestry (LULUCF) in the efforts to reduce emissions; (iv) Renewable Energy Legislation, Energy Efficiency and Governance of the Energy Union. The European Commission wants to implement some more effective ways for a greener and less energy-efficient economy. The EU should reduce its greenhouse gas emissions by up to 80% compared to 1990 levels by 2050, and this process takes place gradually, so by 2030 emissions have to be reduced by 40% and by 60% by 2040 by 1990 levels. As regards adaptation to climate change, the European Commission has adopted an adaptation strategy by all Member States, as well as national plans to deal with the unavoidable effects of climate change. These plans and strategies refer to decreasing water consumption, adjusting regulations, building flood protection systems and developing crops that are resistant to drought.

Also, it is desired to keep global warming below 2 °C, because it is necessary to limit this threshold of 2 °C to the average temperature in the pre-industrial period in order to avoid the occurrence of extreme meteorological phenomena. In general, a large proportion of the world's states have joined this objective in 1992 on the occasion of the United Nations Framework Convention on Climate Change (UNFCCC). However, the specialists have shown that if no action is taken to reduce global emissions or if the measures are insufficient by the end of the century, global warming could exceed the 2 °C threshold and could even reach 5 °C. However, besides the EU climate change strategy, is also taken into account and the White Paper on Adaptation to Climate Change which refers to a framework for action at European level which establishes a framework which aims at reducing vulnerability at EU level to the impact of climate change.

1.2. National policies and strategies on climate change

Nationally, it is taken into account the national strategy on climate change and economic growth based on low carbon, as well as the National Action Plan on Climate Change.

a. National strategy on climate change and low carbon growth

The main objective of the national strategy on climate change and low-carbon growth is to mobilize and to allow private and public actors to reduce greenhouse gas (GHG) emissions from economic activities according with the proposed targets. The EU wants to adapt to the impacts of climate change, both current and future. As regards the process of reducing GHG emissions, this strategy adopts quantifiable targets in line with EU 2030 aspirations.

THE ANNALS OF "DUNAREA DE JOS" UNIVERSITY OF GALATI
FASCICLE IX. METALLURGY AND MATERIALS SCIENCE
Nº. 4 - 2018, ISSN 2668-4748; e-ISSN 2668-4756
Article DOI: https://doi.org/10.35219/mms.2018.4.05

As regards adaptation to climate change, the aim is to support and promote environmental protection, human communities and economic activities against the effects of climate change, especially to extreme events. The strategy will guide Romania's actions on climate change and low-carbon development by 2030 representing an update and extension of the National Strategy on Climate Change 2013-2020 are made in the light of recent developments.

b. National Action Plan on Climate Change

The National Action Plan 2016-2020 is being carried out in the framework of the Technical Assistance Service Agreement for "Romania: Climate Change and Low-carbon Economic Growth Program", signed between the Ministry of Environment, Water and Forests and the International Bank for Reconstruction and Development and financed by the European Regional Development Fund, through the Operational Program Technical Assistance 2007-2013. The major objective of the National Action Plan on Climate Change is to develop concrete measures for the implementation of the national strategy on climate change and low carbon growth and starts from the priorities mentioned in these documents. For this purpose, it is necessary to specify with more precision the necessary activities to address priorities for mitigating the effects of climate change and adaptation to them and set milestones for development and their implementation.

1.3. Policies and strategies at the local level on climate change

Locally, the projects funded by European or national funds play an important role because climate change is punctual and a "micro" vision acts strictly in that area of study. Mitigation measures are less costly and more effective than adaptation, that is why mitigation is done before reaching the adaptation measures.

However, it can be specified that the mitigation measures can be closely with policies in other sectors of activity (transport, waste management or even master plans in urban areas). Adaptation becomes a challenge of this century because climate change acts in different ways depending on various factors. Locally, as stated by the European Commission, clear strategies are not established, but the EU Adaptation Strategy reflects the need for new EU initiatives including reference to local adaptation. However, adaptation to climate change needs to be ensured by local authorities, because the types of impact and interdependencies are different and the proposed objectives can be achieved in a timely, concrete and shorter time.

The subject of adaptation to climate change presents of particular importance at the local level because of the following aspects:

a. The impact of climate change is higher at the local level even if the average temperature increase is global resulting in climatic changes that may have a greater influence at regional or local level, such as: very high temperatures, high intensity storms, insufficient precipitation, and the change of seasons / crop growing seasons. Also, climate change can lead to changes in professional activities, changing the role of institutions / enterprises, as well as the decrease of the national economy, as well as the health of the population. However, climate change works closely with local geomorphology and geology, economic and socio-political indicators.

b. Locally, the degree of vulnerability and adaptability are in direct correlation because together they can represent interactions between different socio-ecological factors and processes, such as income levels, infrastructure, ecosystem and human health, gender, political participation and individual behaviour, etc. The actors involved have the ability to determine ways to reduce or eliminate the negative impacts of climate change. Vulnerability indicators established at regional or national level have the role of determining climatic variations at the local level.

c. At local level, measures to adapt to climate change can be more effectively identified. The adaptation decision making and the implementation of climate action is reflected in the experience of previous studies and researchers in this field.

2. The correlation between the implementation of strategies and projects at national and local level

The government, institutional and legal institutions have the role of implementing urban plans that could be treated differently, depending on the influence of climate change. In Romania, projects are being carried out at national level, but also locally to provide support for adaptation to climate change.

Locally, the impact of climate change can be identified and evaluated in a more concrete and easy way in order to prevent the occurrence of risks what can happen. In the decision-making process on adaptation, there must be clear differentiations at local level, national and regional levels. Adaptation to the effects of climate change also needs to be differentiated between urban and rural areas.

In order to achieve success on adaptation to climate change short, medium and long-term plans, strategies and investments are required to address the risks with which we are confronted, but also to act in a timely manner to reduce vulnerability. Locally, the

THE ANNALS OF "DUNAREA DE JOS" UNIVERSITY OF GALATI
FASCICLE IX. METALLURGY AND MATERIALS SCIENCE
Nº. 4 - 2018, ISSN 2668-4748; e-ISSN 2668-4756
Article DOI: https://doi.org/10.35219/mms.2018.4.05

communities need support and to have full decision-making capacity for adaptation in order to implement successful climatic actions.

3. The influence of climate change on agriculture

Nowadays, the particular emphasis is placed on identifying and implementing actions in agricultural systems that can contribute to mitigation and adaptation to climate change through the CAP instruments, but especially of rural development programs. The Common Agricultural Policy (CAP) has recently been revised by the European Union and one of the key changes was aimed at complete elimination of milk production quotas. In the context of farmers facing with issues related to climate change, any changes made may have important consequences land use, water supply and fertilizer application, as well as achieving economic performance in rural areas.

In general, the agricultural sector and climate change are closely linked, having a relationship cause-effect. Agriculture is a source of greenhouse gas emissions. The changes of temperature and growth seasons could, also, affect the proliferation and spread of certain species, such as insects, invasive weeds or diseases, all of which have the effect of affecting crop yields. However, in order to achieve the yield of crops, agricultural practices are necessary, such as rotation of crops, modification of sowing data according to temperature and precipitation amounts, as well as the use of certain crop varieties more resistant to the new conditions.

3.1. The influence of climate change on agriculture at European level

While some anticipated effects may be beneficial for agriculture in certain European regions, especially in the northern areas (e.g. prolonging vegetation season and improving crop yields due to warmer climate), most of them will most likely be adverse, leading to economic losses, they are emerging in regions already under pressure due to socio-economic and environmental factors. Regional variations anticipated in climatic conditions are significant, however, throughout the 21st century, the anticipated effects can be summed up in mild and humid winters, hotter and drier summers and increasingly intense weather events. The worst consequences of changing weather conditions may not be feeling until 2050, but earlier adverse effects from extreme weather events are anticipated, such as frequent and prolonged heat waves, droughts and floods.

In order to sustain the investments, EU funds are implemented, including the European Agricultural Fund for Rural Development, Common Agricultural Policy (CAP) and loans from the European Investment Bank which are available for agriculture and fish farming to adapt to climate change. Apart from the above-mentioned funds, there are other funds which refers to the reduction of greenhouse gas emissions resulting from agricultural activities. Farmers cannot cope alone with the burden of climate change. Public policy must provide the right support so that agricultural producers adapt their agricultural structures and production methods and continue to provide rural services. The CAP already contains constituents which should facilitate adaptation to climate change. Facilitating farmers' access to risk management tools, such as insurance programs, which can help them cope with the losses from weather-related disasters, due to climate change. Rural development policies provide chances to offset adverse effects which climate change can cause to agricultural producers and rural economies, for example, to provide investment aid for more efficient irrigation equipment. Agricultural and environmental programs to encourage better soil management and water resources by agricultural producers are, also, important for adaptation. At European level, the use of irrigated systems in agricultural crops is desirable for a good approach to water conservation and reuse, especially in southern Europe. In Europe, adapting to the effects of climate change will happen in a differentiated way depending on the geographic region.

3.2. The influence of climate change on agriculture at national level

Agriculture requires a dual approach, one to reduce GHG emissions and one to adapt to the anticipated effects of climate change. The agricultural sector issues greenhouse gases into the atmosphere, although on a smaller scale than other economic sectors. At the same time, this sector can provide solutions for climate change issues. Climate change affects many economic sectors and agriculture is one of the most exposed because agricultural activities depend directly on climatic factors. This is important for the European area because 90% of this area is composed of agricultural land and forests. Adaptation is a critical challenge for agriculture and rural areas. Negative effects on agricultural production will be influenced by extreme weather events. Subsistence agriculture will be particularly affected, because it has less capacity to adapt. This will cause the growth risk of famine.

THE ANNALS OF "DUNAREA DE JOS" UNIVERSITY OF GALATI
FASCICLE IX. METALLURGY AND MATERIALS SCIENCE
N°. 4 - 2018, ISSN 2668-4748; e-ISSN 2668-4756
Article DOI: https://doi.org/10.35219/mms.2018.4.05

Climate change is, also, a real concern for EU agriculture. Agriculture will face many challenges in the coming decades, such as: (i) increasing international competition; (ii) liberalization of trade policy; (iii) continued decline in population from rural areas in many regions.

4. The role of adaptation to climate change

Nowadays, climate change is a twofold challenge: reducing the emissions of gases that cause heating (known as attenuation) and adaptation to future climate change to reduce adverse effects.

These are the major challenges for agriculture in the European Union (EU) and for the development of agricultural policies.

There is a wide range of adaptation measures, from technological options to improving farm management practices, but also of political instruments (e.g. action plans for adaptation). To deal with anticipated changes of climatic conditions, farmers can change crop rotation for best use of available water, can adapt sowing data according to temperature and rain patterns, can use crop varieties more suited to new weather conditions (e.g. more resistant to heat and drought) or can plant shrubs or small pines areas on arable land to reduce water leakage and to act as a parapet. It is, also, important to better inform agricultural producers on climate risks and achievable adaptation solutions. Member States have already taken action to adapt. Much of the work done so far have focused on preventing the effects of meteorological extremes, perceived as imminent risk (such as, floods).

5. International climate change negotiations

United Nations Framework Convention on Climate Change (UNFCCC) was signed in Rio de Janeiro in 1992. The main objective of the Convention is to stabilize greenhouse gas (GHG) concentrations in the atmosphere to a level that prevents the dangerous anthropic disturbance of the climate system. The Kyoto Protocol is a subsidiary legal instrument of the UNFCCC and the negotiations were initiated at the 3rd Conference of the Parties, in Berlin in 1995, as the measures provided for in the Convention were not effective. The main feature of the Protocol is represented by the fact that sets firm commitments to reduce emissions over the base year (1990) in the first commitment period, respectively 2008-2012, for industrialized countries. Individual targets were assumed by each country on the basis of the "shared responsibility, but differentiated" and which take into account: the historical responsibility of emissions, the need for economic development and development. The Kyoto Protocol has entered into force internationally on 16 February 2005 and was ratified by 182 States Parties. Under the first commitment period under the Kyoto Protocol (KP1) and 2008-2012 respectively, developed countries have, on average, assumed a 5% reduction in greenhouse gas emissions compared to 1990 levels. Also, under the first commitment period under the Kyoto Protocol, most Member States, including Romania, have individually assumed a greenhouse gas reduction target of 8% compared to the base year of 1989. All 28 EU Member States with commitments to reduce greenhouse gas emissions have exceeded their targets for reducing greenhouse gas emissions.

The Paris Climate Change Agreement was adopted following a vast and intense negotiation process, imposes legal obligations on all Parties to achieve the long-term global objective of maintaining global warming below 2 °C above pre-industrial levels depending on the capabilities and responsibilities and powers they have. The unprecedented element of the Agreement is the 1.5 °C target for limiting global warming, namely, the possibility of achieving a global target of maintaining global temperature increase below 1.5 °C, given that this would significantly reduce the risks and negative impacts of climate change.

Under the provisions of the Paris Agreement, it will enter into force on the thirtieth day after the deposit of instruments of ratification by at least 55 of the Parties to the United Nations Framework Convention on Climate Change which bring together at least 55% of greenhouse gas emissions globally.

From a political point of view, given the leadership role played by the EU in the adoption of the Paris Agreement and in the fight against climate change in general through the joint announcement of the two major states, the pressure of the entry into force of the agreement has been transferred to the EU, which, on October 4, 2016, has adopted the Decision on ratification, by the EU, of the Paris Agreement. Independent from the action of global partners, through the Energy Package - Climate Change 2020, the EU has set itself a target of a 20% reduction in greenhouse gas emissions by 2020 compared to the level reached in 1990, and in the case of similar actions from the other developed countries, this target will increase to 30%. By 2030, the EU has set itself a target of 40% reduction in greenhouse gas emissions compared to 1990 levels.

6. Conclusions

The subject of "climate change" will be a global challenge which implies a responsible approach,

THE ANNALS OF "DUNAREA DE JOS" UNIVERSITY OF GALATI
FASCICLE IX. METALLURGY AND MATERIALS SCIENCE
Nº. 4 - 2018, ISSN 2668-4748; e-ISSN 2668-4756
Article DOI: https://doi.org/10.35219/mms.2018.4.05

undertaking concrete actions at international, regional, national and local level. A realistic approach to this phenomenon requires the cooperation of all international actors in order to identify the best ways of action, the tools needed to stop the global temperature increase.

The issue of climate change is maintained on the European Union's agenda of priorities, the subject being brought to the attention of Heads of State and Government at the European Council meeting in March 2016. European Council Conclusions of March 2016 stresses the need to ratify the agreement by the EU and its Member States as soon as possible.

The measures to address climate change and reduce greenhouse gas emissions are, thus, a priority for the EU. In particular, EU leaders have committed themselves to transforming Europe into a highly energy-efficient economy, with low carbon dioxide emissions. Also, the EU has set itself the objective of reducing greenhouse gas emissions by 80% to 95% by 2050 compared to 1990 levels.

The international agreements play an important role in terms of cooperation and action at international level resulting from the global nature of climate change. In this regard, the EU wants to advance international negotiations on climate change. EU Member States support the development of the United Nations Framework Convention on Climate Change (UNFCCC), the Kyoto Protocol and the Paris Climate Change Agreement.

References

[1]. Leck H., Simon D., *Fostering Multiscalar collaboration and co-operation for effective Governance of climate change adaptation*, Urban Stud. 50, p. 1221-1238, 2013.
[2]. Rosenzweig C., Solecki W., Hammer S. A., Mehrotra S., *Cities lead the way in climate change action*, Nature 467, p. 909-911, 2010.
[3]. Villarroel Walker, R., Beck M. B., Hall J. W., Dawson R. J., Heidrich O., *The energy water-food nexus: strategic analysis of technologies for transforming the urban metabolism*, J. Environ. Manag., 141, p. 104-105, 2014.
[4]. ***, https://ec.europa.eu/clima/policies/adaptation/what_en.
[5]. ***, *Climate- Adapt – Sharing adaptation information across Europe*, European Climate Adaptation Platform https://climate.
[6]. ***, adapt.eea.europa.eu/https://www.eea.europa.eu.

THE ANNALS OF "DUNAREA DE JOS" UNIVERSITY OF GALATI
FASCICLE IX. METALLURGY AND MATERIALS SCIENCE
N°. 4 - 2018, ISSN 2668-4748; e-ISSN 2668-4756
Article DOI: https://doi.org/10.35219/mms.2018.4.06

EFFECT OF SURFACE ROUGHNESS Ti6Al4V MODIFIED BY HYDROXYAPATITE COATING

Mohammed Alqasim ALSABTI[1], Ion CIUCA[2], Bogdan ŞTEFAN VASILE[3], Roxana TRUSCA[4], Alaa ABOU HARB[5]

[1]PhD Student, Doctoral School Faculty Material Science and Engineering, Polytechnic University of Bucharest, Romania,
[2]Prof. univ. dr. ing. Faculty Material Science and Engineering, Polytechnic University of Bucharest, Romania
[3]Ph.D. Faculty of Applied Chemistry and Materials Science, Polytechnic University of Bucharest, Romania.
[4]PhD Student, Doctoral School Engineering and Management of Technological Systems, Industrial Engineering Department, Polytechnic University of Bucharest, Romania,
[5]PhD Student, Doctoral School Faculty Material Science and Engineering, Polytechnic University of Bucharest, Romania,
e-mail: mohammedalkasim_faik@yahoo.com; ion.ciuca@medu.edu.ro; bogdan.vasile@upb.ro; roxana_gheta@yahoo.com

ABSTRACT

Several studies have described the use of HAp layers on titanium alloys in the recent years. Among the methods of strengthening the adherence of such layers, which call the researchers' attention, there is the development of coating by sol-gel type techniques. Coatings of HAp on the alloy of Ti6Al4V allow the formation of uniform layers, with controlled porosity and better adhesion and with properties required for its use as orthopaedic implants.

In this paper, samples of Ti6Al4V alloy were used as substrates with different surface roughness, coated with HAp layers that were deposited by a spin-coating technique, using a solution obtained by the sol-gel method. The layers have good homogeneity and good adhesion to the substrate, where stability and uniformity observes for Hap_250 and Hap_110 compared with Hap_29 and Hap_45, that indicate to the importance of surface roughness. Therefore, the biological characterization was investigated, including the film stability in the Simulated Body Fluid (SBF) and the antimicrobial activity of Ti6Al4V alloys coated with hydroxyapatite. Also, the biofilm formation by P. aeruginosa species was evaluated. The morphology and structure of the films were performed by scanning electron microscopy (SEM) and X-ray diffraction (XRD).

KEYWORDS: Hydroxyapatite, thin film, Ti6Al4V alloy, XRD, SEM

1. Introduction

The mineral phase of the bone similar to hydroxyapatite HA synthetic, of chemical formula $[Ca_{10}(PO_4)_6(OH)_2]$, has been widely studied and used in the field of medicine as a biomaterial because its excellent biocompatibility characteristics promote its acceptance and adequate osseointegration in the biological environment [1].

Calcium phosphates are the most important mineral phase in the hard tissues of vertebrates, and since the beginning of the 20th century, different studies have demonstrated the similarity between bone minerals and calcium phosphate minerals with an apatite structure.

As a consequence, these calcium phosphates of natural or synthetic origin are one of the most used routes in bone or dental surgery today, when a supply of material is necessary [2].

There are, according to their physical chemistry, three families of calcium phosphates (metaphosphates, pyrophosphates, and orthophosphates), and within this last family, different subfamilies, according to their Ca/P ratio (TTCP-tetracalcium phosphate-, Hap - hydroxyapatite-, TCP)- tricalcium phosphates-, OCP-octacalcium phosphate-, etc.), but of all of them, the

THE ANNALS OF "DUNAREA DE JOS" UNIVERSITY OF GALATI
FASCICLE IX. METALLURGY AND MATERIALS SCIENCE
N°. 4 - 2018, ISSN 2668-4748; e-ISSN 2668-4756
Article DOI: https://doi.org/10.35219/mms.2018.4.06

material used in prosthesis coatings, par excellence, is hydroxyapatite [3].

Apatites are a family of ionic compounds described by the chemical formula $M_{10}(RO_4)_6$ X_2 (where M = Ca2+, Pb2+, Na+, etc., X = OH-, F-, Cl=, etc.; RO4 = PO43- , AsO43-,VO43-, etc.). The X will be the one that gives the name to the apatite. In hard tissues, the apatite present is hydroxyapatite; that is, an apatite where the X is an OH-. Thus, the formula of the stoichiometric hydroxyapatite (calcium), with a hexagonal crystalline structure, would be $Ca_{10}(PO_4)_6(OH)_2$ [4, 5].

The recent years have witnessed the use of HAp layers on titanium alloys. Among the methods of strengthening the adherence of such layers, which draw the attention of researchers, there is the development of coating by sol-gel type techniques. Coatings of HAp on the alloy of Ti6Al4V allow the formation of uniform layers with controlled porosity, better adhesion and protective effect to the phenomenon of corrosion, having properties that recommend its use as orthopaedic implants [6].

2. Materials and methods

2.1. Selection of Materials and the Coating Process

This section of the article covers the materials selected for synthesis and deposition. Titanium alloy (Ti6Al4V) is in the form of plates of about 5x5 mm with a thickness of 2 and 0.5 mm respectively. These plates were further processed by using particles of Al_2O_3 blasting process with differently sized particles (29, 45, 110 and 250 µm respectively) to produce different surface roughness for each sample.

The preparation of hydroxyapatite is made as follows: a high concentration of Triethylphosphate 98% $P(OCH_2CH_3)_3$ (Sigma-Aldrich Inc., St. Louis, MO), Ethanol (CH_3CH_2OH), deionized water and Calcium nitrate hydrate 99% ($Ca(NO_3)_2{\cdot}4H_2O$)(Sigma-Aldrich Inc., St. Louis, MO), and Ammonia solution were used to obtain the solution for sol-gel method, coupled with the spin coating technique. The equipment used to obtain the coated samples is A Spin Coater from Laurell model WS-650.

The obtained samples of Ti6Al4V, coated with hydroxyapatite samples investigated via SEM (coupled with EDX), XRD. In addition, stability tests were made in SBF. All samples were subjected to microbiological characterization and cell culture testing for biocompatibility issues.

Figure 1 shows the technological flow of synthesis of Ti6Al4V coated alloys with hydroxyapatite (HAp) and their characterization.

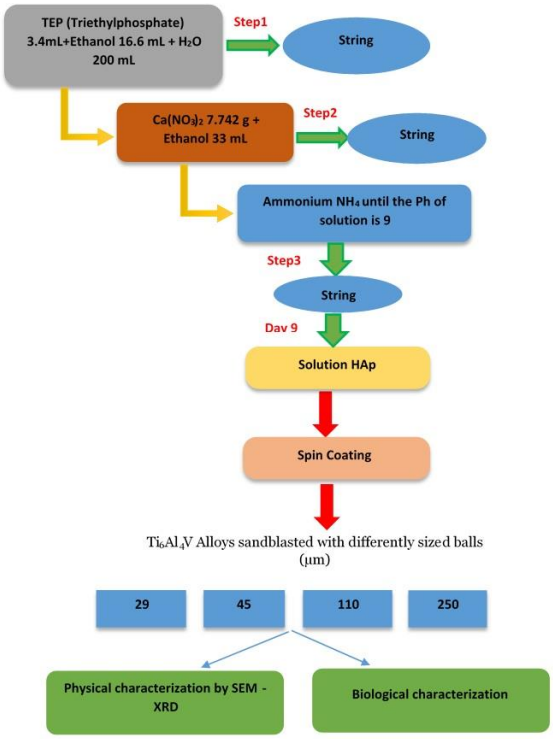

***Fig. 1.** shows the technological workflow*

2.2. Preparation of materials to coated process

For the first step in the synthesis of HAp, the solution was prepared as follows: i) distilled water was added to 1M solution of Triethylphosphate (TEP) in ethanol and allowed for 24 hours to be homogenized under continuous stirring; ii) after 24 hours, the TEP solution was added to 1M of calcium nitrate solution in ethanol, maintaining a Ca/P ratio of 1.67, and homogenized for 24 hours. In this step, the pH was maintained at a value of 9 by ammonia solution addition and finally, iii) the obtained solution was left to homogenize for 7 days.

After the solution was obtained, Ti6Al4V alloys were coated using a spin coater machine. The samples were coated with 20 thin layers of Hap solution at a speed of 2000 rpm for 5 seconds. After every deposited layer, the films were dried at 80 °C for 10 min on a heating plate. The sample code obtained is shown in Table 1 below:

***Table 1.** Code of Ti6Al4V coated with HAp*

Code	Alloy	Blasting particles size (µm)
HAp_29	Ti6Al4V	29
HAp_45	Ti6Al4V	45
HAp_110	Ti6Al4V	110
HAp_250	Ti6Al4V	250

THE ANNALS OF "DUNAREA DE JOS" UNIVERSITY OF GALATI
FASCICLE IX. METALLURGY AND MATERIALS SCIENCE
Nº. 4 - 2018, ISSN 2668-4748; e-ISSN 2668-4756
Article DOI: https://doi.org/10.35219/mms.2018.4.06

The morphology and microstructure of the films were observed with an electronic scanning microscope (SEM) Quanta Inspect F, which had been purchased from the FEI, the resulting images being made by recording the resultant secondary electron beam with 30 keV energy. The crystal structure of the coated films was identified using a PANalytical Empyrean model diffractometer equipped with a hybrid monochromator (2xGe 220) on the side and a parallel plate collimator mounted on the PIXcel 3D detector on the diffracted side. Grazing Incidence X-ray Diffraction (GIXRD) measurements were performed at room temperature with an incidence angle of ω = 0.5° for Bragg angle values of 20 between 10° and 80°, using Cu Kα radiation with λ = 1.5406 Å (40 mA and 45 kV). The elemental composition of the coating was identified using Energy Dispersive Spectroscopy (EDS).

3. Results and Discussion

3.1. X-ray characterization (XRD)

In Figure 2, the X-ray diffraction spectra of the uncoated Titanium alloy (Ti6Al4V) can be observed. By analysing the spectra for the uncoated sample, we can see that it has the peaks which are all attributed to α phase titanium, and there is no β phase diffraction peak in the alloy.

Thus, the X-ray diffraction spectra of the coated Titanium alloy (Ti6Al4V) can be observed. The X-ray diffraction spectra of Hap_29 and Hap_45, with roughness obtained by using particles of 29 μm and 45 μm respectively, have a phosphatic ceramic film with a rhombohedral structure, composed of β-tricalcium phosphate $Ca_3(PO_4)_2$ in the hexagonal form, according to ASTM sheets 04-010-0295.

It should be noted that the samples are well crystallized in both cases but also that the intensity of diffraction lines for $Ca_3(PO_4)_2$ decreases with increased roughness, which is induced by the particle with 45 μm. This can be attributed to the fact that Tricalcium diphosphate (TCP) $Ca_3(PO_4)_2$ was formed in holes due to the larger size of the particles.

In the case of diffraction spectra obtained for HAp_110 and HAp_250, one can see that the samples exhibit lower crystallinity compared to HAp_29 and HAp_45, which is demonstrated by the intensity of smaller high diffraction lines. Both XRD Spectra reveal that the layer obtained and analysed for the surface of titanium alloys is $Ca_5(PO_4)_3(OH)$ and is formed according to ASTM datasheets 00-009-0432 with Hexagonal structure, indicating that deposition has been successful.

In all samples Ti is identified from the substrate ASTM 04-010-0295. In addition, Figure 2 a, b, c, d, and e shows a compression between Ti6Al4V alloy uncoated and Ti6Al4V alloy coated with HAp, where different structures of $Ca_5(PO_4)_3(OH)$ (HAp) and $Ca_3(PO_4)_2$ (TCP) are formed after coating as a result of the roughness obtained by using particles [7, 8].

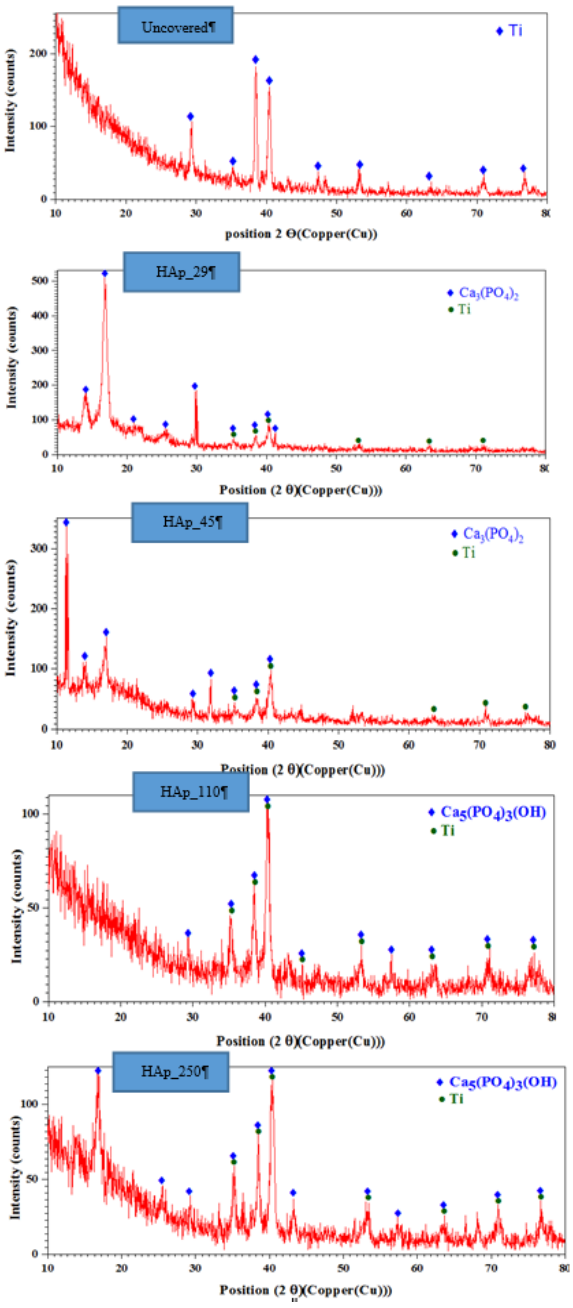

Fig. 2. *shows the compared XRD Spectra for all samples of Ti6Al4V uncovered and covered HAp with different roughness*

The importance of the HAp stability (HAp_250 and HAp_100) layer is higher than that of the TCP (HAp_45 and HAp_29) layer, although the TCP is more soluble than the HA in physiological pH and

THE ANNALS OF "DUNAREA DE JOS" UNIVERSITY OF GALATI
FASCICLE IX. METALLURGY AND MATERIALS SCIENCE
Nº. 4 - 2018, ISSN 2668-4748; e-ISSN 2668-4756
Article DOI: https://doi.org/10.35219/mms.2018.4.06

therefore more susceptible to biological radiation. But high solubility leads to early failure of TCP coating, due to high solubility, which is unpredictable. Moreover, HA has a strong inhibition of growth, better than TCP.

3.2. Electronic Scanning (SEM)

Electronic Scanning Microscopy (SEM) is an investigative method that can provide relevant information about the structure and state of the material surfaces. This analysis was used to investigate the morphological characteristics of the hydroxyapatite, hydroxyapatite with silver, respectively the film deposited Ti6Al4V surfaces

3.2.1. SEM of uncoated Ti6Al4V

Increased surface roughness was observed as the size of particles increased through the surface morphology of titanium samples, with different surface roughness as shown in Figure 3, which presents the SEM data obtained.

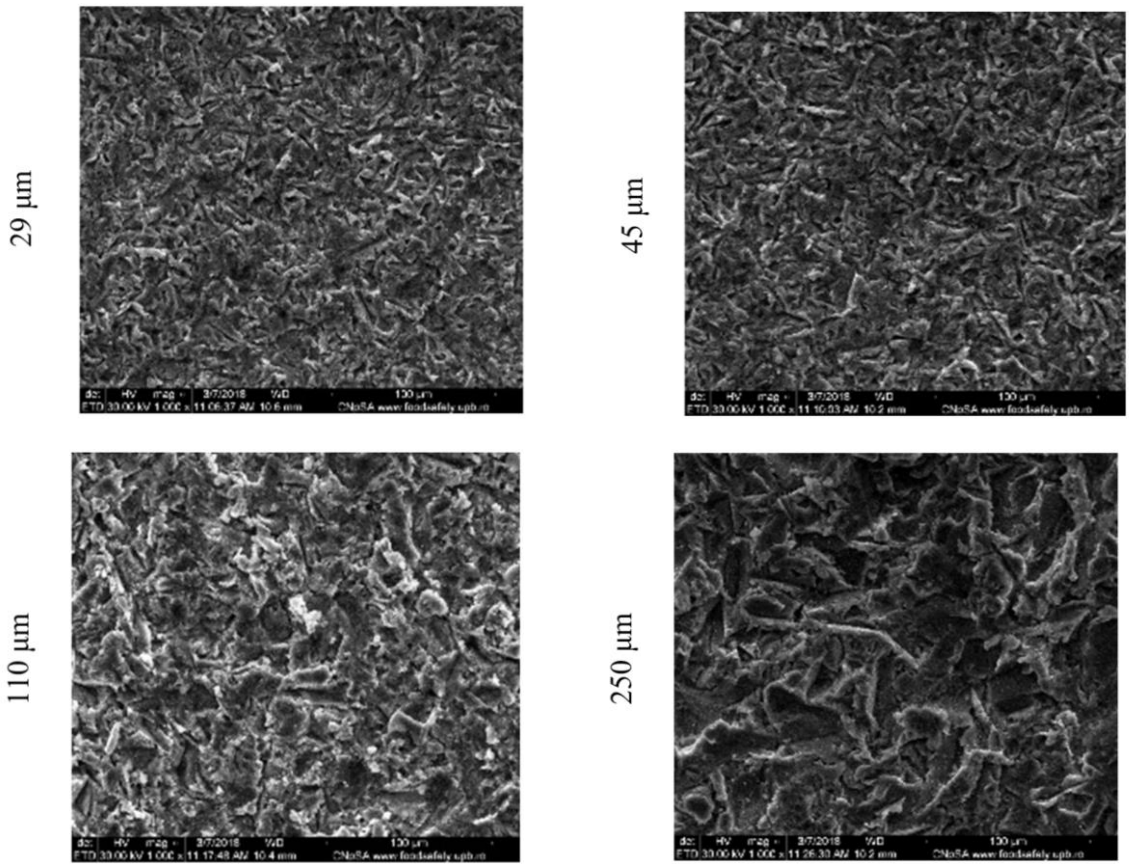

Fig. 3. *shows SEM micrographs of Ti6Al4V with different roughness*

3.2.2. SEM analysis of undoped samples HAp_29, HAp_45, HAp_110, HAp_250

The micrographs obtained of the samples HAp_29, HAp_45, HAp_110, HAp_250 show that the deposited layer on the surface of titanium support is uniform and distributed in all the recesses formed by particle halls of different sizes (29, 45, 110, 250 µm).

The HAp_110 and HAp_250 samples have a deposition of HAP layer morphology present in polyhedral forms because in this case HAp is formed not of $Ca(PO_4)_2OH$.

The EDXS analysis, performed on the titanium alloy samples with HAp layers, which have been deposited using the spin coating method simultaneously, confirms the uniform distribution of the specific species found, such as calcium, phosphorus, and oxygen, characteristic of the solution submitted, as illustrated in Figure 4.

THE ANNALS OF "DUNAREA DE JOS" UNIVERSITY OF GALATI
FASCICLE IX. METALLURGY AND MATERIALS SCIENCE
Nº. 4 - 2018, ISSN 2668-4748; e-ISSN 2668-4756
Article DOI: https://doi.org/10.35219/mms.2018.4.06

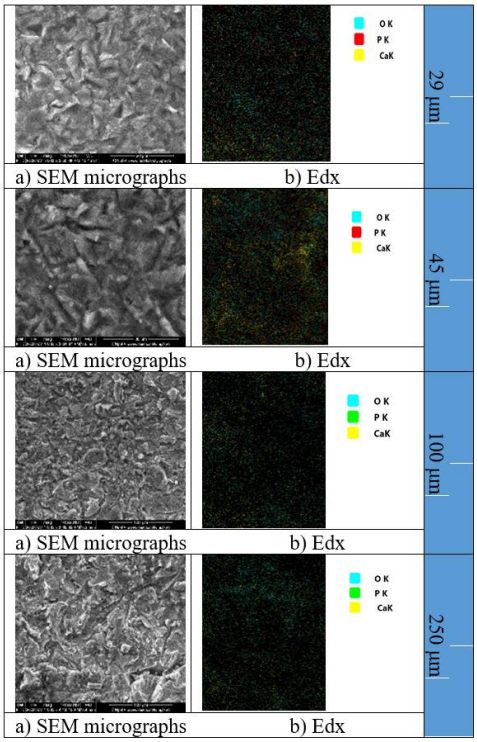

Fig. 4. *shows the SEM micrograph and EDX for HAp with different roughness*

3.3. Stabilization of thin films in SBF

The method of coating with HAp can be based on practical bio-mimicry by immersing implants in the simulated body fluid (SBF), which is an equal inorganic composition with the pH and temperature of the human blood plasma.

The surface morphology of the spinning coated specimens was observed by a field scanning electron microscope and X-ray spectra (XRD) analysis was performed.

3.3.1. X-ray Diffraction Analysis of samples HAp_29, HAp_45, HAp_110, HAp_250 after 7, 14, 28 days of immersion in SBF

In Figure 5, the X-ray diffraction spectra of HAp 29 and HAp 45, with roughness obtained by using particles of 29 µm and 45 µm respectively, have had a phosphorus ceramic film with Monoclinic crystal of Calcium Phosphate Hydrate ($Ca_2(P_4O_{12}).4H_2O$ and Calcium Phosphate ($Ca(PO_3)_2$).

With HAp_29, it crystallized with Calcium Phosphate Hydroxide $Ca_5(PO_4)_3(OH)$, While the intensity of diffraction lines for ($Ca_2(P_4O_{12}).4H_2O$ of HAp_45 indicates to the decrease of crystallization compared with Hap_29.

In the case of HAp_110 and HAp_250, it can be seen that the samples exhibit lower crystallinity compared to HAp_29 and HAp_45, which is demonstrated by the intensity of smaller high diffraction lines.

The hexagonal structure of Apatite $Ca_5(PO_4)_3(OH)$ afford the stability of hydroxyapatite as an excellent biomaterial used for bone repair or implants.

With immersion in SBF solution, HAp_29, HAp_45, HAp_110, and HAp_250 were converted into a more stable HAp. By increasing of immersion time to 28 days, HAp peaks have risen, which confirms the growth of HAp.

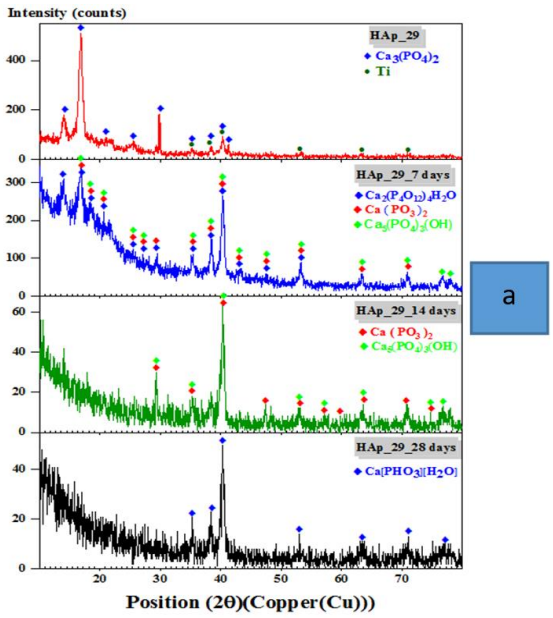

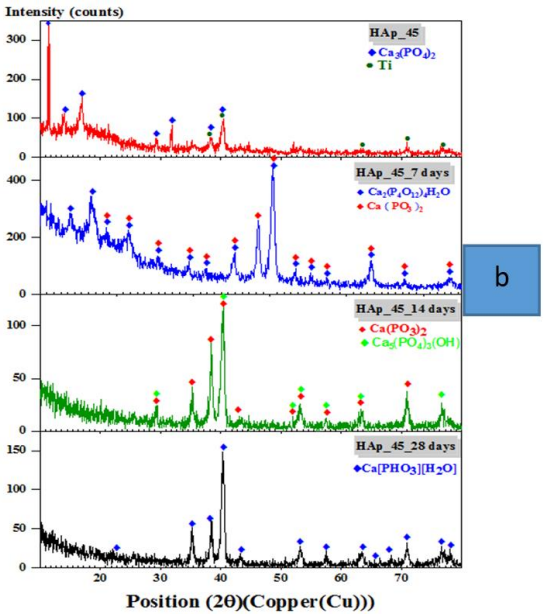

THE ANNALS OF "DUNAREA DE JOS" UNIVERSITY OF GALATI
FASCICLE IX. METALLURGY AND MATERIALS SCIENCE
N°. 4 - 2018, ISSN 2668-4748; e-ISSN 2668-4756
Article DOI: https://doi.org/10.35219/mms.2018.4.06

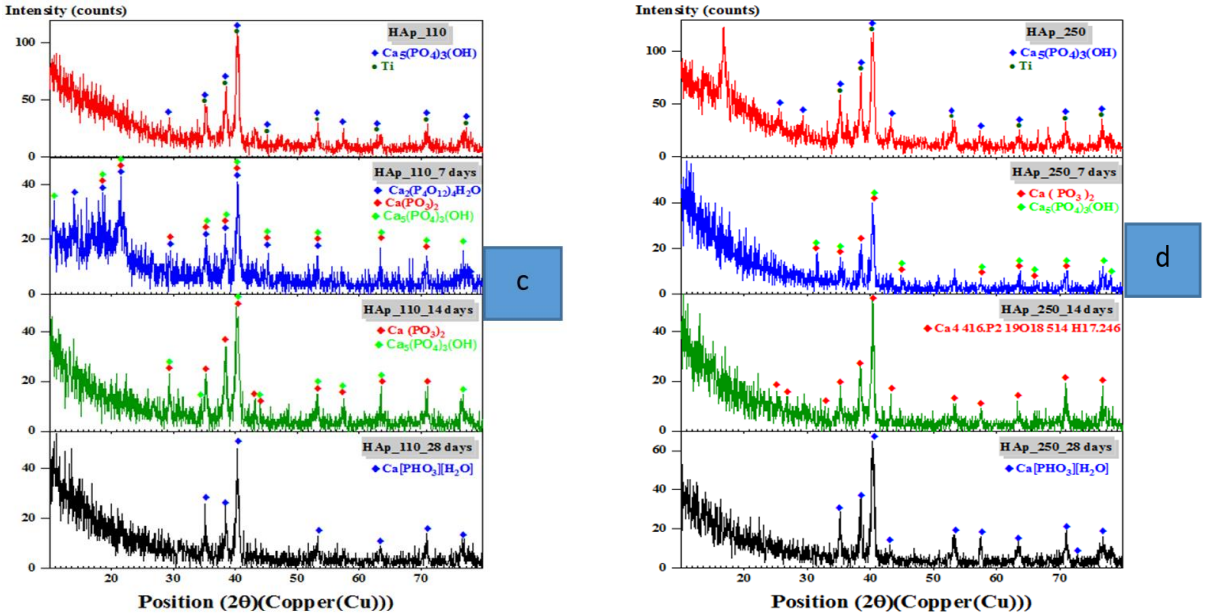

Fig. 5. *shows the X-ray Diffraction, registered for samples a) HAp_29, b) HAp_45, c) HAp_110, d) HAp_250, after immersion in SBF for 0, 7, 14 and 28 days respectively*

3.3.2. Scanning Electron Microscopy (SEM)

In Figure 6, according to SEM micrographs which were performed at 7 days after immersion in SBF, it can be seen that the HAp film has developed quantitatively, presenting, at the same time, a homogeneous arrangement on the surface of the titanium alloys, which is an indication of high activity of the hydroxyapatite in contact with the physiological fluid in the human body.

According to the SEM micrographs obtained after 14 days of immersion in SBF, the HAp film has a more significant development on the surface of the titanium alloy substrate than the micrographs obtained at 7 days after immersion.

Via the analysis of samples after 28 days immersion in SBF, emphasized the success of hydroxyapatite deposition as homogeneous and agglomeration.

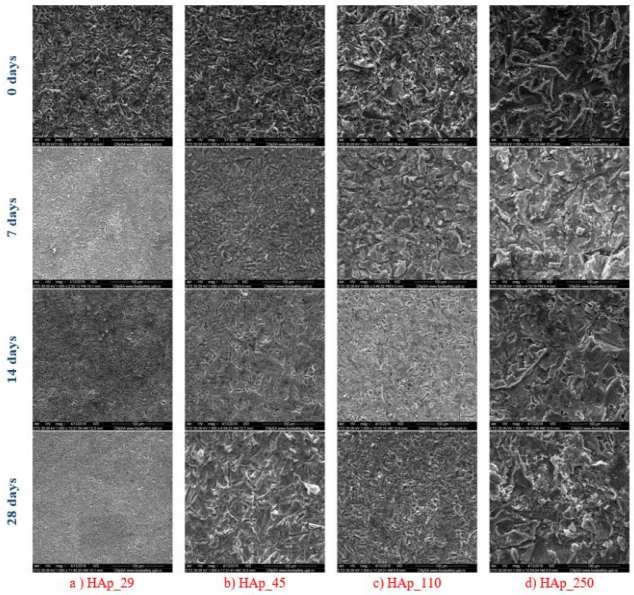

Fig. 6. *shows the SEM micrographs, registered for samples HAp_29 a), HAp_45 b), HAp_110 c), HAp_250 d) after 0, 7, 14 and 28 days respectively*

THE ANNALS OF "DUNAREA DE JOS" UNIVERSITY OF GALATI
FASCICLE IX. METALLURGY AND MATERIALS SCIENCE
Nº. 4 - 2018, ISSN 2668-4748; e-ISSN 2668-4756
Article DOI: https://doi.org/10.35219/mms.2018.4.06

3.4 Biological characterization

The effect of the materials obtained on the growth of microorganisms in liquid media (planktonic cultures), and the effect of the surfaces obtained on the production of biofilms were tested in order to establish the antimicrobial activity of titanium alloys coated with hydroxyapatite. the numbering of the sample CODs, shown on the images taken during the biological analysis, as shown in Figure 7:

HAP 29, 6. HAP 45, 7. HAP 110, 8. HAP 250, 9. CONTROL TI, 10. P. aeruginosa ctrl.

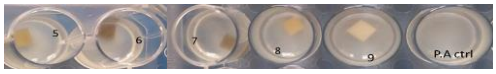

Fig. 7. *shows the CODS samples used with Planktonic cultivation*

3.4.1. Growth of planktonic microorganisms in the presence of materials

To test the effect of the materials obtained on the growth of microorganisms in liquid media (planktonic cultures), the materials obtained were sterilized by exposure to UV radiation for 20 minutes on each side. The material (sterile fragment) was individually put into a well with 6 sterile plate. Over the deposited materials, were added 2 mL of liquid medium (simple broth) and then 50 µL of McFarland microbial suspension (Bacteria) with density = 0.5. The 6 plates prepared were incubated at 37 °C for 24 hours. After the expired of incubation time, 200 µL of the obtained microbial suspensions were transferred to 96 sterile plates and the turbidity of the microbial cultures was measured spectrophotometrically (UV) at 600 nm.

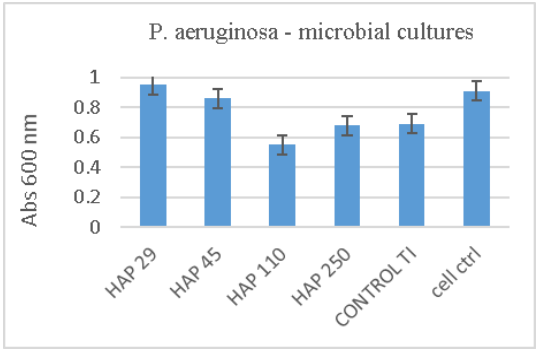

Fig. 8. *shows the Abs values at 600 nm suggesting the growth of planktonic microorganisms in the presence of Ti-based materials*

For samples 3 and 4 no microbial growth was detected visually or spectrophotometrically, which demonstrates the high antimicrobial effect of the obtained materials.

When the spectrophotometric investigation completed, it can be seen from the graph that the samples have an inhibitory effect on bacterial action on the P. aeruginosa strain as seen in Figure 8. HAp110 and HAp250. That means the roughness of the materials obtained by using particles of dimensions 110 and 250 µm, have positive influences on the antibacterial activity for the samples on the P. aeruginosa strain.

3.4.2. Biofilm product

To test the effect of the surfaces obtained on the production of biofilms, the materials obtained were sterilized by exposure to UV radiation for 20 minutes. After one by one sterile material fragment was individually deposited in a well of a 6 sterile plate. Over the deposited materials, 2 mL of liquid medium (plain bullion) and subsequently 50 µL of McFarland (density 0.5) microbial suspension were added to the plates. The 6 plates still prepared were incubated at 37 °C for 24 h, 48 h or 72 h. After incubation, the materials were washed with AFS (physiological saline water). After the expiration of each incubation period, the sample on which the biofilm was developed was washed with AFS and deposited in a sterile tube in 1 mL of AFS. The tube was vortexed vigorously for 30 seconds to detach the cells from the biofilm. The cell suspension obtained was diluted and various dilutions were seeded on solid culture media plates to obtain and quantitate the number of colonies forming units (UFC / mL). Sow plates were grown for 24 h and the number of UFC / mL was calculated based on the number of viable colonies and the dilution taken into account.

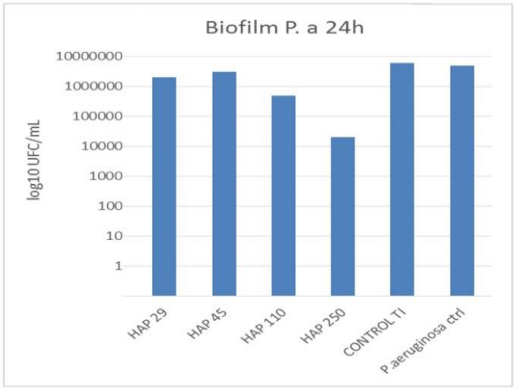

Fig. 9. *Graphical representation of UFC / mL values, representing the development of biofilms on the tested surfaces*

THE ANNALS OF "DUNAREA DE JOS" UNIVERSITY OF GALATI
FASCICLE IX. METALLURGY AND MATERIALS SCIENCE
Nº. 4 - 2018, ISSN 2668-4748; e-ISSN 2668-4756
Article DOI: https://doi.org/10.35219/mms.2018.4.06

It can be seen from the Figure 9 some inhibitory effect being observed in samples 3 and 4 on the formation of monospecific biofilms by P. aeruginosa species, indicated to most significant effects of the high roughness of surface on hydroxyapatite coating which inhibitory of their development.

4. Conclusions

The samples HAp_29 and HAp_45 are well crystallized in both cases, however, the intensity of diffraction lines for $Ca_3(PO_4)_2$ also decreases with increased roughness, which induced by the particles with 45 μm. This can be attributed to the fact that Tricalcium diphosphate (TCP)$Ca_3(PO_4)_2$ was formed in holes due to the larger size of the particles.

HA_110 and HAp_250 can be seen to exhibit lower crystallinity compared to HAp_29 and HAp_45, which is demonstrated by the intensity of smaller high diffraction lines.

The hexagonal structure of Apatite $Ca_5(PO_4)_3(OH)$ afford the stability of hydroxyapatite as an excellent biomaterial used for bone repair or implants.

The deposited layer formed on the surface of titanium support is uniform and distributed in all the recesses.

EDX analysis, performed on titanium alloy samples, the samples with phosphate ceramic layers, which have been deposited by using the spin coating method simultaneously, confirm the uniform distribution of the specific species found, such as calcium, phosphorus, and oxygen.

The roughness of the materials obtained by using particles of dimensions 110 and 250 μm have a positively influences of the antibacterial activity and biofilms activity for the samples on the P. aeruginosa strain.

References

[1]. Yilmaz B., Alshemary A. Z., Evis Z., *Co-doped hydroxyapatites as potential materials for biomedical applications*, Microchem. J., vol. 144, no. July 2018, p. 443-453, https://doi.org/10.1016/j.microc.2018.10.007, 2019.

[2]. Combes C., Cazalbou S., Rey C., *Apatite Biominerals*, Minerals, vol. 6, no. 2, p. 34, 2016.

[3]. Canillas M., Pena P., De Aza A. H., Rodríguez M. A., *Calcium phosphates for biomedical applications*, Bol. la Soc. Esp. Ceram. y Vidr., vol. 56, no. 3, p. 91-112, 2017.

[4]. Deng T., Xia Z., Ding H., *Effect of [PO4]3−/[VO4]3−substitution on the structure and luminescence properties of Ca5[(P,V)O4)]3F:Eu3+ phosphors*, Chem. Phys. Lett., vol. 637, p. 67-70, 2015.

[5]. Gallo J., Langova K., Havranek V., Cechova I., *Poor survival of ABG I hip prosthesis in younger patients*, Biomed. Pap. Med. Fac. Univ. Palacky. Olomouc. Czech. Repub., vol. 152, no. 1, p. 163-168, 2008.

[6]. Liu F., Song Y., Wang F., Shimizu T., Igarashi K., Zhao L., *Formation characterization of hydroxyapatite on titanium by microarc oxidation and hydrothermal treatment*, J. Biosci. Bioeng., vol. 100, no. 1, p. 100-104, 2005.

[7]. Al-Sanabani J. S., Madfa A. A., Al-Sanabani F. A., *Application of calcium phosphate materials in dentistry*, Int. J. Biomater., vol. 2013, no. May 2013.

[8]. Santos E. A., Farina M., Soares G. A., Anselme K., *Chemical and topographical influence of hydroxyapatite and b - tricalcium phosphate surfaces on human osteoblastic cell behavior*, 2008.

THE ANNALS OF "DUNAREA DE JOS" UNIVERSITY OF GALATI
FASCICLE IX. METALLURGY AND MATERIALS SCIENCE
No. 4 - 2018, ISSN 2668-4748; e-ISSN 2668-4756
Article DOI: https://doi.org/10.35219/mms.2018.4.07

NON-DESTRUCTIVE TESTING OF DUPLEX WELDING JOINTS

Roxana-Alexandra GHEȚA, Maria-Cristina DIJMĂRESCU, Laurenția BICHIR, Gabriel Marius DUMITRU
Politehnica University of Bucharest, No. 313, Splaiul Independenței, sector 6, Bucharest, Romania
e-mail: roxana_gheta@yahoo.com, cristina_dijmarescu@yahoo.com, laura_bichir@yahoo.com, gmdumitru@yahoo.com

ABSTRACT

This paper presents results of non-destructive examination of welding belt and the heat affected zone. The samples were made using sheets of duplex stainless steel, welded through the method of manual welding with coated electrode, by utilizing 4 types of electrodes. The specimens were subjected to different non-destructive examination methods in order to identify the defects, to establish new efficient procedures and to achieve high productivity in detection of defects appeared.

KEYWORDS: non-destructive testing, duplex stainless steel, welding joints

1. Introduction

Nowadays the non-destructive examination is used to verify the integrity of the products starting from the early stages of the manufacturing processes to the last stages of the product exploitation process. So, to know which method to use for each type of material it is essential to reduce the non-destructive testing related costs [1-3].

Developed over 70 years ago, duplex type stainless steels initially appeared to combat corrosion problems caused by aggressive chemical process fluids or seawater used for cooling. The name is due to the mixed microstructure formed of equal proportions of ferrite and austenite. Chemical composition based on high Cr, Ni and Mo content, improves resistance to intergranular and pitting corrosion. As a result of the development of offshore oil and gas exploitations, the next generation of duplex steels was developed by the deliberate addition of nitrogen as an alloying element, which improves both the tenacity of the thermally influenced area of the joint and the corrosion resistance in ion-containing environments of chlorine [1, 4, 5].

This paper presents the application of different non-destructive methods in order to identify the imperfections in duplex stainless-steel welded joints with four different types of electrodes. Obtaining different structures in the welded seams can be a problem for the non-destructive examination. So, the main focus of the paper is to establish which method provides more information about the welded seam.

2. Experimental data

2.1. Samples description

Steel sheet of duplex stainless steel X2CrNiMoN22-5-3 of 15 mm thickness were used in the study presented in this paper. The chemical composition and the mechanical proprieties of the base material are presented in Table 1 and Table 2.

Table 1. *Chemical composition of the base material X2CrNiMoN22-5-3*

Chemical Composition	C %	Cr %	Mn %	Mo %	N %	Ni %	P %	S %	Si %
UNS S32205	0.30 max	22.0-23.0	2.00 max	3.00-3.50	0.14-0.20	4.50-6.50	0.030 max	0.020 max	1.00 max

THE ANNALS OF "DUNAREA DE JOS" UNIVERSITY OF GALATI
FASCICLE IX. METALLURGY AND MATERIALS SCIENCE
No. 4 - 2018, ISSN 2668-4748; e-ISSN 2668-4756
Article DOI: https://doi.org/10.35219/mms.2018.4.07

Table 2. *Mechanical proprieties of the base material X2CrNiMoN22-5-3*

Properties	Value
Drip limit (R_{p02})	min. 480 N/mm^2
Tensile strength (R_m)	min. 680 N/mm^2
Elongation (A_5)	min. 25%
Hardness (HB)	max. 290
Resilience (KCV)	min. 100 J/cm^2

2.2. Welding process

Samples of 200 mm x 50 mm x 15 mm were welded using the SMAW process. For the experiment were used four types of electrodes as following ASP308MN, OK68.81, Duplex 25/16/3 and E309Mo17. The chemical composition of the filling materials is presented in Table 3 and the mechanical properties in Table 4. The welding parameters used are presented in Table 5.

The configuration of the chosen groove and the number of layers deposited are presented in Figure 1.

The samples were welded in horizontal position on each sample were used 2 types of electrodes as it can be seen in Figure 2.

The resulted welded samples are presented in Figure 3.

Table 3. *Chemical composition of the filling materials*

Filler material	C [%]	Si [%]	Mn [%]	P [%]	S [%]	Cr [%]	Ni [%]	Mo [%]	Cu [%]	N [%]
ASP308Mn	0.10	0.50	6.00	-	-	18.00	9.00	-	-	-
OK68.81	min. 0.08 - max. 0.15	min.0.50 - max. 1.00	min.0.50 - max. 1.00	max. 0.030	max. 0.020	min.28.00 - max. 30.00	min. 9.00 - max. 10.50	max. 0.50	max. 0.30	max. 0.15
INOX 25/16/3	≤0.04	0.80	0.60	-	-	23.00	13.00	3.00	-	-
E309Mo17	≤0.12	≤1.00	min. 0.50 - max. 2.50	≤0.04	≤0.03	min. 22.00 - max. 25.00	min. 12.00 - max. 14.00	min. 2.00 - max. 3.00	≤0.75	-

Table 4. *The mechanical properties of the filler materials*

Properties	ASP308Mn	OK68.81	INOX 25/16/3	E309Mo17
Yield Strength [N/mm^2]	420	610	≥ 490	-
Tensile Strength [N/mm^2]	640	790	≥ 670 to 810	550
Elongation [%]	35	25	≥ 25	30
Impact Strength [J] at 20 ºC	100	30	47	-

THE ANNALS OF "DUNAREA DE JOS" UNIVERSITY OF GALATI
FASCICLE IX. METALLURGY AND MATERIALS SCIENCE
No. 4 - 2018, ISSN 2668-4748; e-ISSN 2668-4756
Article DOI: https://doi.org/10.35219/mms.2018.4.07

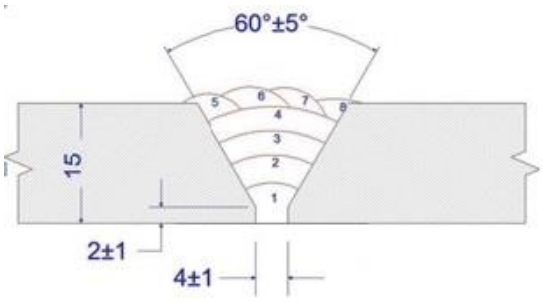

Fig. 1. *The groove configuration and the layer layout 1÷8 - number of layers*

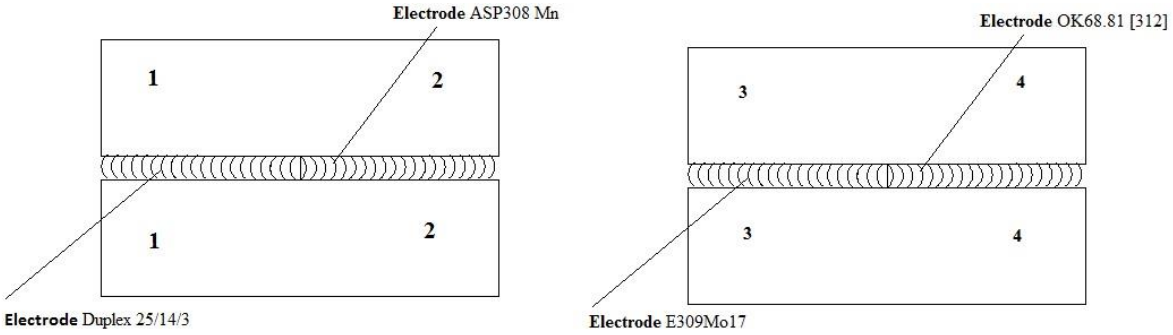

Fig. 2. *Position of the electrodes used 1 - Duplex 25/14/3 electrode, 2 - ASP308 Mn electrode, 3 - E309Mo17electrode, 4 - OK68.81 electrode*

Table 5. *Welding parameters*

Type of electrode	Number of layers	Welding current [A]	Voltage, U_a [V]
Duplex 25/14/3	8	120 ± 10	20 ± 5
ASP308 Mn	8	115 ± 10	20 ± 5
E309Mo17	8	110 ± 10	20 ± 5
OK68.81	8	110 ± 10	20 ± 5

Fig. 3. *Welded sample 1 - sample 1, a) - E309Mo17 electrode, b) - OK68.81electrode 2 - sample 2, c) - ASP308 Mn electrode, d) - Duplex 25/14/3 electrode*

THE ANNALS OF "DUNAREA DE JOS" UNIVERSITY OF GALATI
FASCICLE IX. METALLURGY AND MATERIALS SCIENCE
Nº. 4 - 2018, ISSN 2668-4748; e-ISSN 2668-4756
Article DOI: https://doi.org/10.35219/mms.2018.4.07

2.3. Non-destructive examination of the samples

To analyse the integrity the welding joints and to see which method shows a better result, the samples were subjected to non-destructive examinations. The samples were pre-cleaned before starting the non-destructive examination. For the examination, 4 methods were used: Visual Testing, Penetrant Testing and Ultrasonic Testing. The non-destructive examination was applied to see if there are any macroscopic flows in the welded seam and in the basic materials.

Visual Testing

The examination was made using the direct visual testing. On the samples there could be identified slag inclusions, spatter and scratches made by the tools used.

Dry Penetrant Testing

The examination with dry penetrant testing was conducted at the ambient temperature of 20 ºC.

For the examination with penetrant testing, the following steps were undertaken:

- Preparation and pre-cleaning of the surface – the samples were chemically cleaned by degreasing using the METAFLUX 70-9801 cleaner;
- Surface drying - it was forced by a hot air jet;
- Penetrant application and dwell time - see Figure 4.
  - penetrant - METAFLUX 70-9802;
  - the penetrant was applied on the surface by spraying:
  - Dwell time – 10 min.
- Excess penetrant removal – it was made by washing;
- Surface drying - it was forced by a hot air jet;
- Developer application – see Figure 5:
  - developer - METAFLUX 70-9803;
  - the developer was applied in a uniform and thin layer, on the entire surface to be examined, only after having been well shaken beforehand;
  - after application of the developer, the examined surface was left to dry at room temperature;
  - the development time starts immediately after the surface has dried, the development time being 30 min;
- Inspection - interpretation of the results was made at the end of the development time;
- Cleaning the surface.

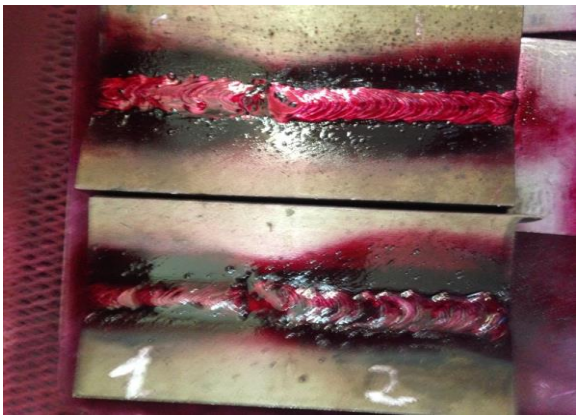

Fig. 4. *Penetrant Application*

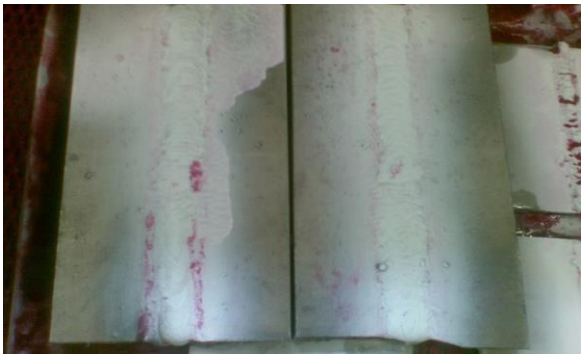

Fig. 5. *Developer Application*

The imperfections identified with the dry penetrant testing were:

- Surface imperfections (cavities, spatter, surface pore),
- Slag inclusions.

Magnetic Testing

In order to conduct the magnetic testing, the following steps were undertaken:

- Preparation of the test specimen - the samples were chemically cleaned by degreasing;
- Magnetization of the test specimen - it was conducted using electromagnets, as it can be seen in Figure 6. In the samples was created a longitudinal magnetic field composed by magnetic lines of force that run parallel to the long axis of the welded seam;
- Application of the magnetic powder – it was conducted using a suspension of fluorescent magnetic particles in low-viscos carrier oil with special additives PFINDER 150. With PFINDER 150 surface defects of materials can be indicated under UV-light. The suspension was applied on the surface by spraying;
- Viewing and recording of indications - The magnetic field was oriented so that its line of force was perpendicular to the maximum size of the imperfection, see Figure 7;

THE ANNALS OF "DUNAREA DE JOS" UNIVERSITY OF GALATI
FASCICLE IX. METALLURGY AND MATERIALS SCIENCE
Nº. 4 - 2018, ISSN 2668-4748; e-ISSN 2668-4756
Article DOI: https://doi.org/10.35219/mms.2018.4.07

- Demagnetization - to demagnetize the samples, AC current was used gradually to reduce the applied current to zero;
- Cleaning the surface - after the examination the samples was chemically cleaned by degreasing.

After examining the samples with this method no imperfections were identified on the welded seam and the adjacent areas.

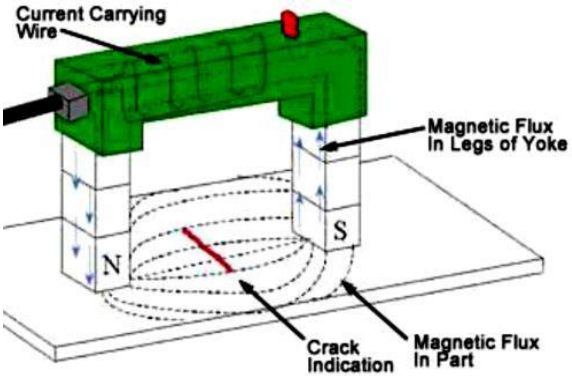

Fig. 6. *The electromagnets - method principle*

Fig. 7. *Magnetization of the samples*

Ultrasound Testing

To conduct the examination, a Krautkramer USM-35 device was used, along with an angle beam transducer.

The following equipment was used:

- Krautkramer USM-35 – see Figure 8;
- Angle beam transducer: 70º - AM4R-8x9-70;
- Calibration block used – A1;
- Couplant medium – grease;
- Frequency – 4 MHz.

The ultrasound testing conducted on the samples is presented in Figure 9.

Using the ultrasound testing in sample 2, it was identified a lack of fusion between the root layer and second layer.

Fig. 8. *Krautkramer USM-35 device*

Fig. 9. *Ultrasound examination*

3. Conclusions

The following conclusions have been drawn from the experiments conducted:

- In the case of the Visual Testing and the Penetrant Testing, surface imperfections could be highlighted, as well as the ones in the immediate vicinity of the surface that communicates with the outside surface. Both methods were easy to apply and provided conclusive results.
- In the case of the Magnetic Testing, the results obtained were inconclusive. An impediment can be the low magnetic permeability of stainless steels.
- The result obtained by Ultrasound Testing of the welded samples was inconclusive, obtaining only the identification of some big imperfections in the case of sample 2. Ultrasonic Testing of stainless steels is difficult due to the grain size of those steels.

References

[1]. Paul Kah, Belinga Mvola, Jukka Martikainen, Raimo Suoranta, *Real Time Non-Destructive Testing Methods of Welding*, Advanced Materials Research, vol. 933, p. 109-116, 2014.

THE ANNALS OF "DUNAREA DE JOS" UNIVERSITY OF GALATI
FASCICLE IX. METALLURGY AND MATERIALS SCIENCE
Nº. 4 - 2018, ISSN 2668-4748; e-ISSN 2668-4756
Article DOI: https://doi.org/10.35219/mms.2018.4.07

[2]. Bisgrove P., Hayward P., Hirasawa H., Holstein R., Khan A. A., Ooka N., Thiam Siong S., Yzelman W., *Guidebook for the Fabrication of Non-Destructive Testing (NDT) Test Specimens*, International Atomic Energy Agency (IAEA), Vienna, 2001.

[3]. Oral Büyüköztürk, Mehmet Ali Taşdemir, *Nondestructive Testing of Materials and Structures*, Springer Science & Business Media, 2012.

[4]. Jing W., Min-Xu L., Lei Z., Wei C., Ningxu L., Li-Hua H., *Effect of welding process on the microstructure and properties of dissimilar weld joints between low alloy steel and duplex stainless steel*, vol. 19, no. 6, p. 518-524, 2012.

[5]. Mvola B., Kah P., Martikainen J., *Dissimilar ferrous metal welding using advanced gas metal arc welding processes*, Rev. Adv. Mater. Sci., 38, p. 125-137, 2014.

[6]. ***, *EN ISO 5817 - Arc-welded joints in steels – Guidance on quality levels for imperfections. Welding – Fusion welded joints in steel, nickel, titanium and their alloys (beam welding excluded) – Quality levels for imperfections*.

[7]. ***, *EN ISO 6520-1 - Welding and allied processes – Classification of geometric imperfections in metallic materials – Part 1: Fusion welding*.

THE ANNALS OF "DUNAREA DE JOS" UNIVERSITY OF GALATI
FASCICLE IX. METALLURGY AND MATERIALS SCIENCE
N°. 4 - 2018, ISSN 2668-4748; e-ISSN 2668-4756
Article DOI: https://doi.org/10.35219/mms.2018.4.08

RESEARCH ON THE CORROSION BEHAVIOR OF THE STAINLESS-STEEL THIN FILMS COATED BY PVD METHOD, MAGNETRON ASSISTED

Simona BOICIUC
"Dunarea de Jos" University of Galati, Romania
e-mail: simonaboiciuc@yahoo.com

ABSTRACT

The paper follows the corrosion behaviour of X10CrNi 18-8 stainless steel thin films coated by PVD method, magnetron assisted, on glass and copper substrates. It was found that with the increase of the coating time increases of the thickness of the coated layer which leads to the decrease of the corrosion rate. The surface condition can influence the corrosion behaviour through the existing defects and the size of the roughness. Coating uniformity, respectively corrosion, changes with the distance from the axis of symmetry of the magnetron.

KEYWORDS: d.c. magnetron, stainless steel deposition

1. Introduction

PVD coatings have multiple applications that can be used as biocompatible materials, for protection against corrosion, erosion having, on the one hand, good properties of wear resistance, mechanical resistance, hardness, good adhesion, resistance to oxidation and temperature and, on the other hand, good optical, electrical, magnetic properties. Due to these properties, PVD coatings can be an alternative to conventional surface treatments, presenting a low-cost price, under the conditions of using non-polluting installations, respectively technologies [1].

Depending on the coating parameters used, the microstructure of the films obtained by the PVD method can vary from a porous columnar shape to a compact columnar one, and can also reach shapes with equiaxial grains with a high degree of compactness (the increase of the temperature favours the phenomena of recrystallization leading to the obtaining polyhedral grains) [2, 3]. In the case of films that require good corrosion and wear behaviour, it is necessary to obtain a structure as compact as possible (aspect favoured by low pressure coatings) [3].

The surface may contain pores or cracks which may affect corrosion resistance. However, this does not only depend on the degree of porosity resulted and the existing structural defects, but also depends on other factors such as chemistry of coating-substrate interface, coating adhesion, structure, surface/substrate defect density, film/substrate roughness, film uniformity and residual stresses.

One of the factors that influence the structure, adhesion, film roughness and residual stresses is the substrate temperature. It is well known that low temperature coatings impede the mobility of atoms to migrate on the surface of the substrate, leading to the formation of high residual stresses. The roughness of the film decreases with increasing substrate temperature [3].

The problems that arise in the case of thin film corrosion are due to the penetration of the corrosive agents by these defects and their reaching the substrate.

Thus, it becomes important to determine the origin of these defects and how they develop on the surface. A number of defects specific to PVD coatings are: shallow conical structures (droplets), acicular holes with dimensions of the order of micrometres and large but not deep craters, with dimensions between 10-40 μm [4]. The defects of conical shape have a quite high incidence and develop in the layer during its growth. Their appearance is due either to the presence of foreign particles with which the layer comes in contact (dust) or to the metal droplets in the target (from the vacuum chamber). Usually the region under the cone is not completely filled with material [4].

The needle holes defects extend throughout the entire coating and originate from surface defects (a small hole in the substrate) or can be caused by corrosion products (wet cleaning) or dust particles

THE ANNALS OF "DUNAREA DE JOS" UNIVERSITY OF GALATI
FASCICLE IX. METALLURGY AND MATERIALS SCIENCE
N°. 4 - 2018, ISSN 2668-4748; e-ISSN 2668-4756
Article DOI: https://doi.org/10.35219/mms.2018.4.08

that have not been removed from the surface of the substrate during the coating process. The high roughness of the substrates used could have the same effect. The PVD method has a poor ability to cover these defects (due to the shadow effect) [4].

The origin of large but not deep craters could be explained by the presence of particles that appeared immediately after the coating began (corrosion products resulting from wet cleaning, dust particles) [4].

Regarding the methods of processing the surface of the substrate, they must take into account its cleaning and activation, respectively the creation of a clean surface from a chemical point of view (by removing the impurities and gases adsorbed on the surface) and making stable and strong physical-chemical connections between the substrate and the coated material.

The applications of thin films with anticorrosive properties are: in the aerospace industry, in the automotive industry, to reduce their weight and implicitly to reduce the fuel consumption, in the electronic industry, to the coating of thin films anticorrosive on the objects of art and architecture obtained from brass or bronzes.

In recent years, many efforts have been made to develop new anticorrosive coatings through PVD methods. Thus, the stainless-steel coating has become more and more interesting and studied.

The austenitic stainless steels were initially designed to make the necessary equipment for home use and interior decoration, and then to expand their use in fields such as the food industry, chemical, petrochemical, energy and medical industries when developing medical prostheses, orthopaedic implants, endodontic instruments and dental implants. The means of land, naval, air, space transport also include component parts made of materials coated with stainless steel that have good mechanical strength as well as resistance to aggressive environments and atmospheres.

The content of more than 12% Cr gives the steel the property to cover with a passive layer in most environments (air, water, acids, industrial atmosphere etc.), making them resistant to oxidation and corrosion, in relation to other metallic materials. As a rule, corrosion resistance increases with increasing of chromium content. The passive layer is mainly composed of chromium oxides (formed in the presence of oxygen), is adherent, dense, impermeable and slightly soluble, which makes it resistant to the action of a large number of aggressive environments. It has been observed the erosion resistance, practically unlimited, of austenitic stainless steels compared to the low corrosion resistance of copper in which the corrosion products are fragile and easy to shear [5].

The use of stainless steels in the medical industry is due to both good mechanical resistance properties, physical, chemical properties, and good biocompatibility, respectively, good corrosion resistance to biological fluids.

However, stainless steels are liable to corrosion (in saline environment) compared to titanium alloys, releasing metal ions (Ni^{2+}, Cr^{3+}, Cr^{6+}) into the body that can cause allergic, inflammatory reactions (Speide and Uggowitzer, 1998). For this reason, stainless steels are used only for temporary medical implants such as fixing screws and orthopaedic rods for fracture fixation [6].

The purpose of the paper is to study the corrosion behaviour in salt mist of thin films of X10CrNi 18-8 stainless steel and their micro-structural characterization.

2. Experimental conditions

To obtain the films, a circular austenitic stainless-steel plate X10CrNi 18-8 with a diameter of 46.5 mm and a thickness of 1 mm was used as target.

The substrate material consisted of glass plates with dimensions 76x25x1 mm and copper plates with dimensions of 80x20x1 mm.

The films were obtained using a PVD spray coating machine, consisting of a vacuum chamber with a capacity of 2 litters, a planar magnetron with ferrite magnets (ϕ40x22x9) neodymium (ϕ15x8), a vacuum pump with sliding blades, a variable source of DC voltage from 100 to 600 volts.

The machine allows the variation of the magnetron substrate spacing between 25 and 90 mm, and the substrate temperature can be monitored with a chromel-alumel thermocouple.

The atmosphere used to maintain the plasma during coating process was the rarefied argon in a pressure range between $3 \cdot 10^{-2}$ - $8 \cdot 10^{-3}$ mbar. The argon flow used was 100 cm^3/min.

The stages of obtaining the coatings were the following:

a. Preparation of the substrate surface

b. Coating films by PVD method, magnetron assisted

a. Preparation of the substrate surface

This step consisted of: washing the plates with a special detergent, washing them with water, then with distilled water, ultrasonic cleaning with ethanol and then drying with compressed air.

b. Coating films by PVD method, magnetron assisted

The regimes used for coating stainless steel films are presented in Table 1. The samples P1 and P2 were obtained by coating stainless steel films on the glass substrate and P3 and P4 on the copper substrate.

THE ANNALS OF "DUNAREA DE JOS" UNIVERSITY OF GALATI
FASCICLE IX. METALLURGY AND MATERIALS SCIENCE
Nº. 4 - 2018, ISSN 2668-4748; e-ISSN 2668-4756
Article DOI: https://doi.org/10.35219/mms.2018.4.08

Table 1. *Regimes for obtaining X10CrNi 18-8 steel films*

Sample code	Voltage [V]	Current [mA]	Pressure [mbar]	Substrate temperature [°C]	Target - substrate distance [mm]	Deposition time [min]
P1	545	55	2.5×10^{-2}	34	66	20
P2	545	55	2.5×10^{-2}	34	66	40
P3	550	55	2.5×10^{-2}	34	66	20
P4	550	55	2.5×10^{-2}	34	66	40

2.1. Microscopic characterization of the obtained films

Microscopic analysis of the obtained films was performed using a Neophot 2 optical microscope with computerized data acquisition.

2.2. Corrosion behaviour of the obtained films

The corrosion behaviour of thin films in saline mist was studied using a corrosion chamber, provided with an automatic system for measuring and regulating the temperature, exhaust system of the used solution or of the condensation, obtained during the tests.

The samples were placed on plastic bars.

Accelerated corrosion test in saline mist was performed according to SRISO 9227.

To perform the test, the necessary solution was prepared, by dissolving in distilled water, with a conductivity less than or equal to 20 µS/cm^2 la 35 ± 2 ºC, of a quantity of sodium chloride, to obtain a concentration of 50 ± 5 g/L. The relative density of a solution with this concentration ranges from 1.00255 to 1.0400.

The pH of the salt solution was adjusted so that the pH of the solution collected in the spray chamber to range between 6.5 and 7.2. It was measured with a pH meter HI 991001, produced by "Hanna Instruments", provided with a temperature indicator.

The corrosion test was performed for a period of 120 hours at 35 ºC. Initially the samples were degreased with alcohol, weighed on the analytical balance with an accuracy of 0.01 mg.

At an interval of 24 hours, the samples were removed from the chamber, the corrosion products were removed by washing with water and dried. Subsequently, the weighing on the analytical balance was carried out with an accuracy of 0.01 mg.

3. Experimental results

3.1. Microscopic characterization of the obtained films

Following microscopic analysis, it was observed that the obtained films of X10CrNi 18-8 stainless steel show no cracks, are relatively homogeneous and adherent as can be seen in Fig. 1. The samples deposited on glass substrate have a mirror surface and show a series of imperfections from the vacuum chamber and those deposited on a copper substrate are matte and have a surface whose roughness is consistent with that of the substrate.

The roughness of the copper substrate was Ra = 0.21 µm and after the film coating it reached Ra = 0.24 µm. To determine this parameter a NAMICON TR 100 device was used.

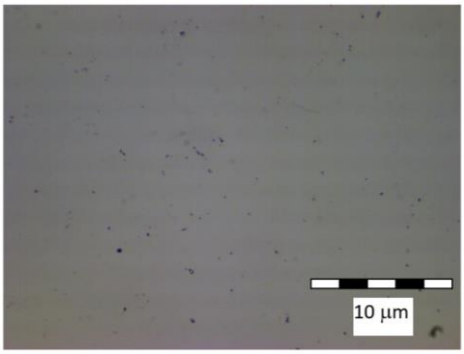

P1

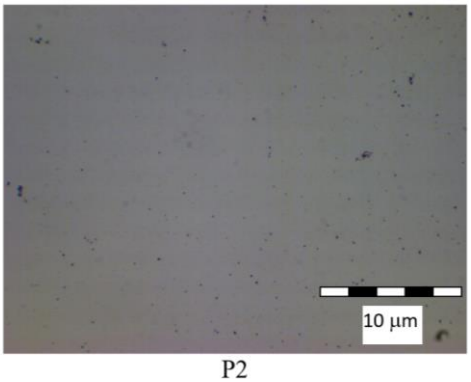

P2

THE ANNALS OF "DUNAREA DE JOS" UNIVERSITY OF GALATI
FASCICLE IX. METALLURGY AND MATERIALS SCIENCE
Nº. 4 - 2018, ISSN 2668-4748; e-ISSN 2668-4756
Article DOI: https://doi.org/10.35219/mms.2018.4.08

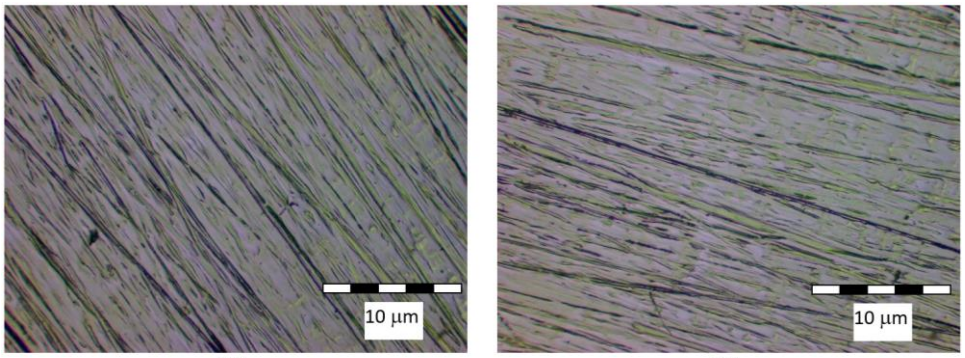

P3 P4

Fig. 1. *Image of films with different coating regimes*

3.2. Corrosion behaviour of the obtained films

Following the corrosion test in saline mist, it was found that the films coated on glass substrate did not change after 120 hours. In the case of films coated on copper substrate, it was found that the best corrosion behaviour was noticed on sample P4 (with longer coating duration), aspects highlighted in Fig. 2 and Fig. 3. It can be observed that the roughness of the substrate influences the geometry of the surface of the coated film, respectively the appearance, concentration, corrosion on certain areas.

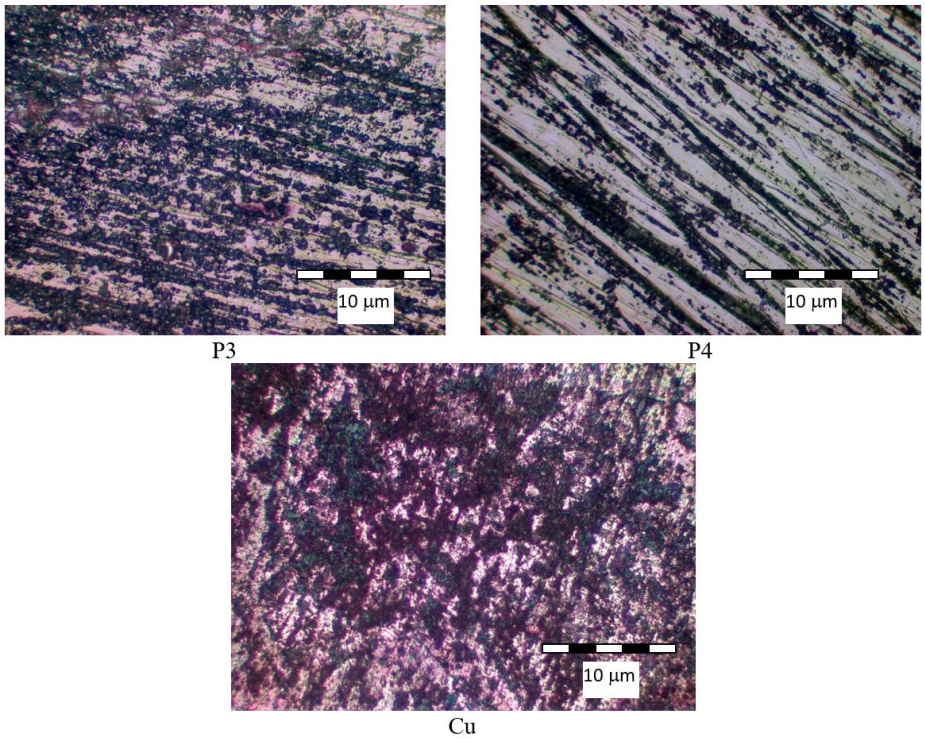

P3 P4

Cu

Fig. 2. *Image of films with different coating regimes, after corrosion*

When analysing Fig. 2, it can be seen that the stainless-steel films coated on copper substrate are affected by corrosion in saline mist, a point corrosion (concentrated on surfaces of several mm^2) quite deep. This is caused by the presence of chlorine ions which lead to the passage of the passive film from place to place.

The corrosion behaviour is increasingly better with the increase of the coated film thickness. Also, with increasing the coating time, the film thickness and grain size increase which leads to its roughness.

Another factor influencing the corrosion behaviour is the uniformity of the coated film. This decreases with increasing distance from the axis of

THE ANNALS OF "DUNAREA DE JOS" UNIVERSITY OF GALATI
FASCICLE IX. METALLURGY AND MATERIALS SCIENCE
N°. 4 - 2018, ISSN 2668-4748; e-ISSN 2668-4756
Article DOI: https://doi.org/10.35219/mms.2018.4.08

symmetry of the magnetron, which makes the corrosion velocity different (the areas further away from the axis have more pronounced corrosion).

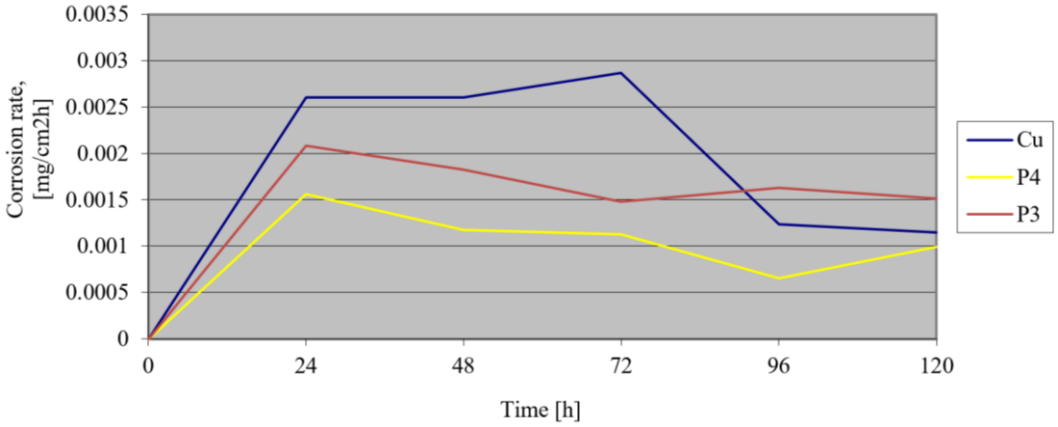

Fig. 3. *Corrosion behaviour of the coated films*

4. Conclusions

The corrosion behaviour of thin films is influenced by the state of the surface, respectively by the surface defects and roughness. The defects can be due to either a poor preparation of the substrate during its cleaning and activation or due to the impurification of the film in the vacuum chamber (droplets of target metal, dust). Corrosion occurs by penetrating corrosion solutions through these defects and attacking the substrate material.

The roughness of the coated film is influenced by the roughness of the substrate material and the coating conditions. The roughness of the substrate material depends on the preparation method. This should ensure a reduced surface roughness.

As the coating time increases, the film thickness and grain size increase which leads to its roughness.

The corrosion behaviour of stainless-steel films in saline mist revealed that the corrosion decreases with the increase of the coated film thickness.

On the other hand, the behaviour is influenced by the uniformity of the coated film. This decreases with increasing distance from the axis of symmetry of the magnetron, which causes a relatively uneven corrosion of the film.

The method represents an efficient alternative to the classic technologies for surface protection against corrosion, realized with a reduced consumption of materials and with a minor impact on the environment.

References

[1]. Viorica Muşat, *Filme subţiri multifuncţionale*, Editura CERMI Iaşi, 20, p. 33-59, 2005.
[2]. Thornton J. A., *The microstructure of sputter-deposited coatings*, Journal of Vacuum Science & Technology A: Vacuum, Surfaces, and Films, vol. 4, p. 3059-3065, 1986.
[3]. Robert-A. Pato, *Straturi subtiri multifunctionale de nitrura de titan*, Teza de doctorat, Universitatea Tehnica Cluj Napoca, 2011.
[4]. Darja Kek Merl, Ingrid Milosev, Peter Panjan, Franc Zupanic, *Morphology and corrosion properties PVD Cr – N coatings deposited on aluminium alloys*, MTAEC9, 45(6), 593, Materiali in technologije, ISSN 1580-2949, 2011.
[5]. Levcovici M. S., Vasilescu E., Gheorghieş L. ş.a., *Ingineria suprafeţelor*, EDP Bucureşti, 2003.
[6]. Vasilescu V., Vasilescu E., *Physical–Mechanical and Technological Characteristics of Ti10Zr Alloy for Dental Applications*, The Annals of "Dunarea de Jos" University of Galati, Fascicle IX, Faculty of Metalurgy and Materials Science, no. 3, ISSN 1453-083X, 2016.

THE ANNALS OF "DUNAREA DE JOS" UNIVERSITY OF GALATI
FASCICLE IX. METALLURGY AND MATERIALS SCIENCE
Nº. 4 - 2018, ISSN 2668-4748; e-ISSN 2668-4756
Article DOI: https://doi.org/10.35219/mms.2018.4.09

RESEARCH ON THE COVERAGE OF COLD-ROLLED FLAT PRODUCTS WITH FILM-FORMING MATERIALS

Simona BOICIUC
"Dunarea de Jos" University of Galati, Romania
e-mail: simonaboiciuc@yahoo.com

ABSTRACT

The paper aims to characterize film-forming materials from the micro-structural, mechanical point of view for the assessment of the elasticity and flexibility of films, and from the chemical point of view, to determine their resistance to various chemicals, distilled water, 3% hydrochloric acid and 3% sodium hydroxide and their behaviour at corrosion in saline mist. It aims to develop a coating technology with film-forming materials for protection against corrosion.

KEYWORDS: film-forming materials, anti-corrosion protection

1. Introduction

The film-forming materials, capable of forming films, are used in various industrial sectors, besides providing anti-corrosion protection and abrasion resistance, non-stick and anti-lubricant qualities, thermal or electrical insulation, high or low friction coefficient, decorative appearance [1].

In the case of use as protective materials, they are used in the form of solutions, emulsions or dispersions in different solvents, on the basis of which varnishes, paints, enamels, primers and grouts, plastisols, organosols are produced [1].

Varnishes are solutions of cellulose derivatives, natural or synthetic resins in volatile organic solvents (chlorinated hydrocarbons, benzene, lower alcohols, ethyl acetate or amyl) with or without the addition of vegetable oils or corrosion inhibitors. They are colourless or weakly coloured by the used resins or dyes. After drying they give transparent and glossy films. The dissolution of the film-forming material is carried out at a much lower temperature than the boiling temperature of the solvent [1].

Paints consist of a film-forming substance (natural or synthetic resins, cellulose and rubber derivatives, flax oil, bitumen), a suitable solvent, specific to the resin used (benzene, toluene, xylene alcohols, acetone) and a pigment (metal oxides, Pb_3O_4, ZnO, TiO_2, iron oxides, metals in finely dispersed state Zn, Al) in order to accelerate the polymerization of the film-forming substance or to provide film gloss [2].

To ensure corrosion protection the film must be sufficiently thick, chemically and mechanically resistant and stable against water soaking (electrolyte). The structure, porosity, permeability of the film depends on the nature of the resin, its concentration and the adhesion to the substrate.

The purpose of the paper is to establish a technology for coating flat products with film-forming materials (varnishes and paints). In this respect, a number of film-forming materials will be structurally, mechanically and chemically characterized.

2. Experimental conditions

2.1. Sampling and coating with film-forming materials

In the experimental researches, it was used a steel sheet, C10E type, with a thickness of 1 mm.

The following technological flow was used to obtain the samples needed to coat with film-forming materials: mechanical pre-cleaning, alkaline chemical degreasing, hot washing, degreasing (tricolorethylene), washing, oxalic acid pickling, washing, phosphating, coating with film-forming materials (with brush or rolls), drying (polymerization).

The quality of the coating and its durability depend on the correct preparation of the surface before painting. In this case, surface cleaning was done mechanically with abrasive materials (fine abrasive polishing). The resulting roughness was 0.4 - 0.6 µm.

The next step is the alkaline chemical degreasing which aims to remove fats (especially

THE ANNALS OF "DUNAREA DE JOS" UNIVERSITY OF GALATI
FASCICLE IX. METALLURGY AND MATERIALS SCIENCE
N°. 4 - 2018, ISSN 2668-4748; e-ISSN 2668-4756
Article DOI: https://doi.org/10.35219/mms.2018.4.09

unsoapable fats). The solution used consists of 20 g/L sodium hydroxide, 45 g/L sodium carbonate, 20 g/L trisodium phosphate, 3 g/L surfactant (detergent). The working temperature was 70-75 °C, duration of 20-30 seconds. After degreasing the samples were washed with demineralized water at a temperature of 60-65 °C.

The next step consists of degreasing in tricolorethylene followed by washing and pickling in 20 g/L oxalic acid at a temperature of 18-25 °C. After degreasing the samples were washed with demineralized water at room temperature.

Phosphating aims to form on the metal surface a layer of fine crystals of insoluble secondary and tertiary metal phosphates (iron, magnesium or zinc phosphates) from aqueous solutions containing primary metal phosphates. The solution heated to temperatures ranging from 40-100 °C, upon immersion of the sample, attacks its surface due to the acid present, and a small amount of metal passes into the solution together with the formation of a phosphate deposit. In this process, the surface of the metal (sample) is presented as a polyelectrode which implies the existence of micropiles composed of anodic areas (where the metal dissolves) and cathodic areas (where hydrogen is released) in the acid solution [3].

The phosphate film provides anti-corrosion protection in combination with other film-forming materials (service life 5 to 10 years). Their deposition is favoured by the intercrystalline porosity (0.1-5%), the resulting roughness (0.7-0.9 µm) of the phosphate layer and their absorbing properties. The layer obtained has good stability, is hard, and withstands temperatures up to approx. 200 °C. It can also be useful for increasing wear resistance, as a solid lubricant and a lubricant in the cold deformation process (cleavage planes appear that facilitate the movement of crystalline particles during cold plastic deformation) [3].

The phosphating solution used in the experimental research has the following composition: phosphoric acid 418 g/L, nitric acid 130 g/L, Zn 162 g/L, Ni 0.65 g/L. The samples were immersed in the solution at a temperature of 80-90 °C where they were kept approx. 3-4 minutes (until the beginning of the hydrogen release).

After the operations presented above, the samples were subjected to coating (with a brush) with film-forming materials in a number of 4 layers. The number of layers is determined according to the thickness of the film and the nature of the materials used (the thickness of an individual layer is about 20-30 µm). After coating and drying the samples were placed in the oven at temperatures of approx. 100-160 °C (depending on the type of coating) for further polymerization (increasing the mechanical strength of the film).

The coatings were made with the following types of film-forming materials.

1. Alorex (P1) - black colour, is a paint composed of two components: the epoxy component and the hardener (mix in a ratio of 5:1). The cross-linking time of the polymer is 24 hours. They are thermoreactive products obtained by condensing dioxifenylpropane with epichlorohydrin. They have a greater flexibility (greater than the phenolic ones) and a better chemical resistance than the alkyd resins. They are resistant to most inorganic salts, their solutions, to oxidizing ones, to the action of bases and of aliphatic alcohols as well as of hydrocarbons.

These resins can form films only as a result of the reaction of polyaddition with polyaminoamides, anhydrides, polyisocyanates, by oven drying in combination with resins containing hydroxyl groups.

2. Email epoxidic seria 3100 (P2) – red colour, is made from high molecular weight epoxy resins that form films by cross-linking with polyamide adducts. The film is formed by chemical conversion in combination with 3304 epoxy-polyamide hardeners at room temperature or in the oven. Drying is carried out at temperatures between 80-120 °C. It provides colorful, smooth, glossy, hard films, with high coverage power, resistant to industrial atmosphere.

3. Rodin (P3) – transparent film, is a product made of nestrapol and a hardener (based on epoxy resins). For the preparation, mix 100 g nestrapol with 35 g of hardener and stir for 15 minutes. The mixture obtained lasts 30 to 50 minutes depending on the ambient temperature (this duration decreases with increasing temperature). The applied layer dries at temperatures of 80-100 °C. Nestrapol (450) is an unsaturated, orthophthalic polyester resin. It is delivered as a solution 66% in styrene. Cobalt naphthenate entering the preparation of nestrapol is a product obtained by saponification of organic acids and precipitation with cobalt nitrate solution. The product is flammable (temperature 28 °C) and toxic. Esterified epoxy paints have good weather resistance, are easy to apply but lose their shine over time, are expensive and dry slowly.

The samples thus obtained were characterized from micro-structural, mechanical point of view for the assessment of the elasticity and flexibility of the films and chemically, for determining their resistance to different chemicals as well as the corrosion behaviour in saline mist.

THE ANNALS OF "DUNAREA DE JOS" UNIVERSITY OF GALATI
FASCICLE IX. METALLURGY AND MATERIALS SCIENCE
Nº. 4 - 2018, ISSN 2668-4748; e-ISSN 2668-4756
Article DOI: https://doi.org/10.35219/mms.2018.4.09

2.2. Characterization of the films obtained

2.2.1. Microscopic characterization of films

The microstructure of the obtained film-forming materials was revealed by optical microscopy using a Neophot 2 microscope.

2.2.2. Determining the elasticity of films

The elasticity of the film was determined by stamping the metal support on which the film material is applied. After the test the film must not show cracks or exfoliation. The test was performed using a spherical punch with a diameter of 20 mm, F = 10 kN. The samples had the dimensions of 210x70 mm.

2.2.3. Determining the flexibility of films

The flexibility of the film was determined by bending at 180º of the substrate on which it is applied, on cylindrical spindles with dimensions of ϕ32 mm and ϕ0.3 mm under certain conditions and observing its behaviour. After the test the film must not show cracks or exfoliation.

2.2.4. Determining the resistance of films to liquids

The resistance of films to the action of some liquids is their ability not to modify their initial properties under the action of the respective liquid. To determine this, the samples (100x500 mm) coated with the film-forming materials were immersed in distilled water, 3% hydrochloric acid and 3% sodium hydroxide, at a temperature of 23±2 ºC for 24 hours. After the test the film must not show cracks, exfoliation or swelling.

2.2.5. Corrosion behaviour of films

The corrosion behaviour in saline mist of the film-forming materials was studied using a corrosion chamber, provided with an automatic system for measuring and regulating the temperature, exhaust system of the used solution or of the condensation, resulted during the tests.

The samples were placed on plastic bars.

The accelerated corrosion test in saline mist was performed according to SRISO 9227.

To perform the test, the necessary solution was prepared, by dissolving in distilled water, with a conductivity less than or equal to 20 µS/cm^2 at 35 ± 2 ºC, of a quantity of sodium chloride, to obtain a concentration of 50 ± 5 g/L. The relative density of a solution with this concentration ranges from 1.00255 to 1.0400.

The pH of the salt solution was adjusted so that the pH of the solution collected in the spray chamber is between 6.5 and 7.2. It was measured with a pH meter HI 991001, produced by "Hanna Instruments", provided with a temperature indicator.

The corrosion test was performed for a period of 120 hours at 35 ºC. Initially the samples were degreased with alcohol, weighed on the analytical balance with an accuracy of 0.01 mg.

At an interval of 24 hours, the samples were removed from the chamber, the corrosion products were removed by washing with water and then dried. Subsequently, the weighing on the analytical balance was carried out with an accuracy of 0.01 mg.

3. Experimental results

3.1. Microscopic characterization of the obtained films

Following the microscopic analysis, it was observed that the obtained films, show no cracks, are homogeneous and adherent as can be seen in Figure 1.

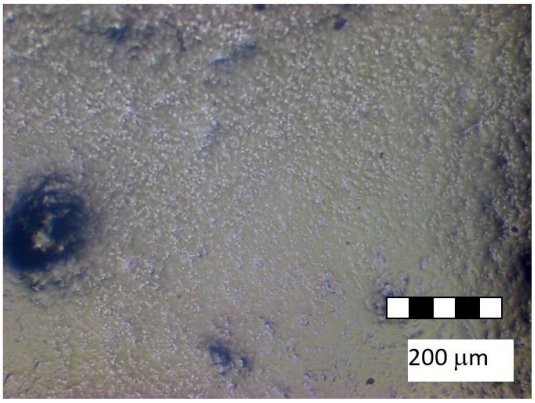

P1

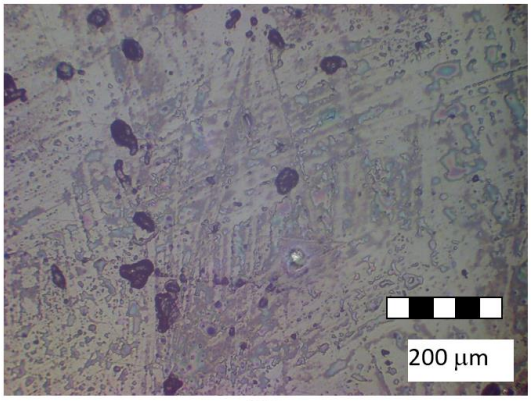

P2

THE ANNALS OF "DUNAREA DE JOS" UNIVERSITY OF GALATI
FASCICLE IX. METALLURGY AND MATERIALS SCIENCE
Nº. 4 - 2018, ISSN 2668-4748; e-ISSN 2668-4756
Article DOI: https://doi.org/10.35219/mms.2018.4.09

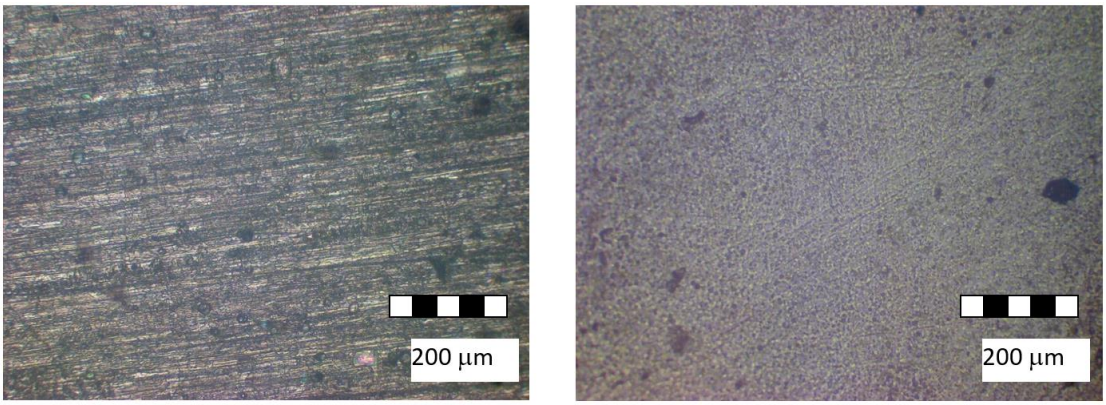

P3 Substrate

Fig. 1. *The metallographic aspect of the film-forming materials*

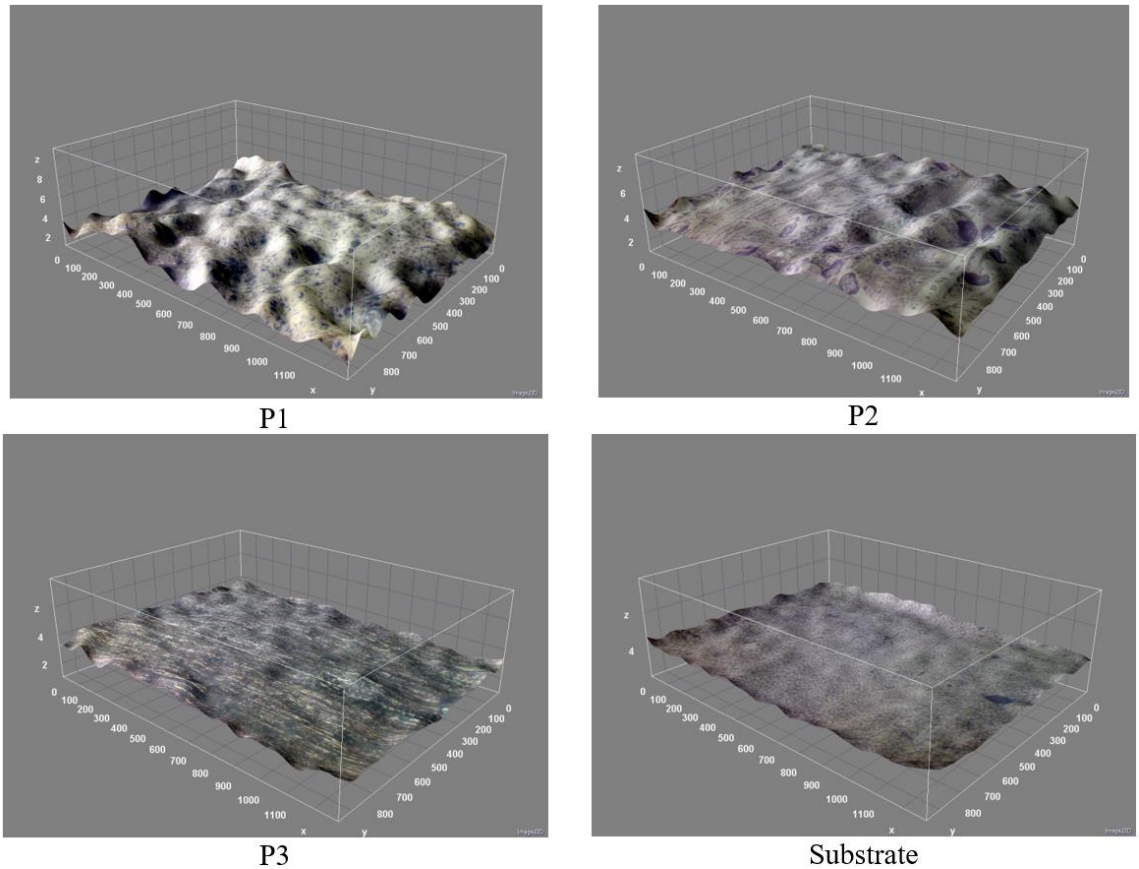

P1 P2

P3 Substrate

Fig. 2. *3D images of film-forming materials*

Fig. 2 shows the qualitative, 3D aspect, of the surface profile for the obtained film-forming materials. It can be seen that the film P3 - Rodin shows a higher uniformity (lower roughness) compared to the films P1 - Alorex and P2 - Epoxy enamel 3100 series.

3.2. Determining the elasticity of films

Analysing Table 1 it can be observed that after stamping the substrate on which the film-forming material is applied, it was found that the best elasticity is noticed to sample P3 - Rodin and the lowest to sample P1 - Alorex.

THE ANNALS OF "DUNAREA DE JOS" UNIVERSITY OF GALATI
FASCICLE IX. METALLURGY AND MATERIALS SCIENCE
No. 4 - 2018, ISSN 2668-4748; e-ISSN 2668-4756
Article DOI: https://doi.org/10.35219/mms.2018.4.09

Table 1. *Determining the elasticity of films*

Erichsen index I_E[mm]	Sample code			
	P1 - Alorex	P2 - Epoxy enamel 3100 series	P3 - Rodin	Substrate
	1.4	1.6	8.8	11

3.3. Determining the flexibility of films

After bending the samples at 180° on cylindrical spindles with dimensions of ϕ32 mm and ϕ0.3 mm it was noticed that the best flexibility was found to the P3 - Rodin sample. The other films showed cracks and exfoliation even when bent on the large spindle.

3.4. Determining the resistance of films to liquids

After immersion of the samples, 24 hours, in distilled water, 3% hydrochloric acid and 3% sodium hydroxide, it was found that they withstood well in distilled water and 3% sodium hydroxide, and of those immersed in 3% hydrochloric acid only those covered with Epoxy enamel 3100 series showed swelling and exfoliation.

The anticorrosive protection of film-forming materials is a complex phenomenon because they have pores and capillaries which makes them permeable to liquids. Thus, their most important role is to reduce the speed of the electrochemical reactions of the corrosion process, by making it difficult for the film to access the metal surface of the depolarized elements and ions [1, 2].

When the paint film is in a certain environment, it is subjected to absorption phenomena and diffusion forces that allow it to penetrate to the surface of the substrate. The film thus becomes the site of osmotic phenomena due to its porous structure. The electrolyte absorption can usually be achieved by electroosmosis (due to potential differences) or by osmosis (due to differences in ion concentration) [1, 2].

Thus, it is necessary for the paint film (usually negatively charged) to have a capillary system that has a negative charge of the walls against the electrolyte solutions because in this way the electroosmotic dehydration of the anodic zones takes place, not allowing the substrate to dissolve. The electroosmotic flow of water or electrolytes occurs from anodic to cathodic areas (formed on the surface of the substrate) [1, 2].

On the other hand, the capillary system must be sufficiently permeable to facilitate the removal of liquid from the cathodic areas and release of the discharged hydrogen into these areas. Otherwise, swelling occurs in these areas [1, 2].

In these conditions, it is important to achieve the passivation the substrate favoured by the phosphating performed prior to the deposition of the film-forming material.

3.5. Corrosion behaviour of films

Analysing Fig. 3 it can be seen that the best corrosion behaviour in saline mist is noticed on sample P1 - Alorex and the lowest on sample P3 - Rodin with a maximum at 24 hours. This behaviour is due to the lower absorption capacity of the electrolyte solution by sample P1.

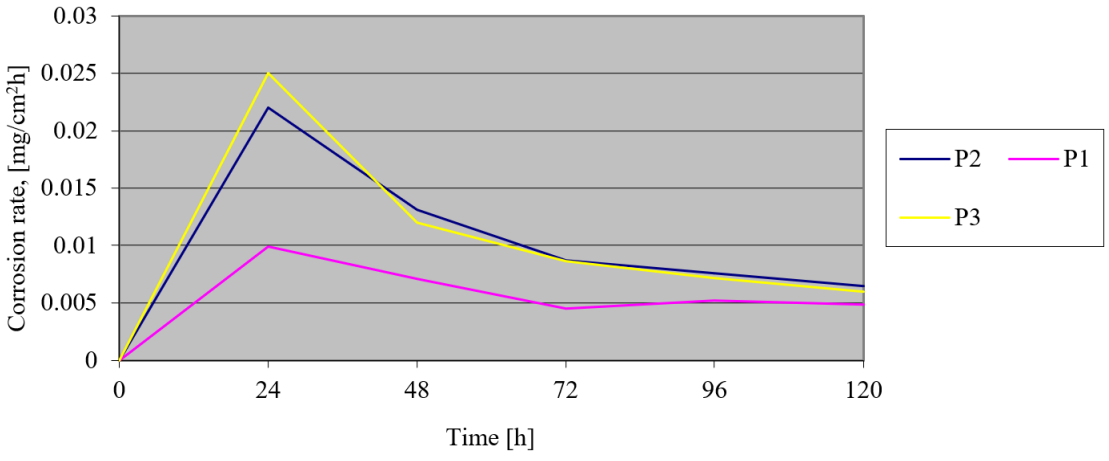

Fig. 3. *Corrosion behaviour in saline mist of film-forming materials*

THE ANNALS OF "DUNAREA DE JOS" UNIVERSITY OF GALATI
FASCICLE IX. METALLURGY AND MATERIALS SCIENCE
Nº. 4 - 2018, ISSN 2668-4748; e-ISSN 2668-4756
Article DOI: https://doi.org/10.35219/mms.2018.4.09

4. Conclusions

Following the testing of the film-forming materials applied on steel substrate results in the following conclusions:

- the films obtained have no cracks, are homogeneous and adherent;
- the film elasticity test performed by stamping the metallic substrate showed that the Rodin film is the most elastic one IE = 8.8 mm and the most rigid one is the Alorex film IE = 1.4 mm (IE substrate = 11 mm);
- the best flexibility was noticed on Rodin film, the other films showing cracks and exfoliation after bending the substrate to 180 on cylindrical spindles with different diameters; this behaviour is due to the presence in the composition of nestrapol;
- following the test to determine the resistance of films to liquids it was found that the samples have a good resistance in distilled water and 3% NaOH and of those immersed in 3% HCl only those with Email 3100 showed swelling and exfoliation on the surface of the substrate;
- the corrosion test performed in saline mist showed that the best behaviour was noticed on sample P1 - Alorex and the lowest on sample P3 - Rodin with a maximum at 24 hours;
- to ensure anticorrosive protection, the film-forming material should be soaked with water, electrolyte solutions, have a negative charge against them, have a reduced capillary system to oppose a higher ohmic resistance, thus ensuring a low corrosion rate; on the other hand, it must be sufficiently loose to allow the electroosmotic water to flow outwards.

References

[1]. Maria Constantinescu, *Protecţia anticorozivă a metalelor*, Editura Tehnică, Bucureşti, 1979.
[2]. Ioan Rădoi, *Introducere în coroziunea şi protecţia metalelor şi aliajelor*, Editura Facla, 1982.
[3]. Marinescu A., Andonianţ Gh., Bay E., *Tehnologii electrochimice şi chimice de protectie a materialelor metalice*, Editura Tehnica Bucureşti, 1984.
[4]. Alexandru Constantinescu, *Detectarea şi măsurarea coroziunii*, Editura Tehnică, Bucureşti, 1976.

THE ANNALS OF "DUNAREA DE JOS" UNIVERSITY OF GALATI
FASCICLE IX. METALLURGY AND MATERIALS SCIENCE
Nº. 4 - 2018, ISSN 2668-4748; e-ISSN 2668-4756
Article DOI: https://doi.org/10.35219/mms.2018.4.10

ESSENCE, CONTENT AND IMPORTANCE OF STRATEGIC MANAGEMENT

Marioara TULPAN, Cristina SUCIU
Industrial Engineering, University of Petrosani, Romania
e-mail: maryat1977@yahoo.com; cristina_suciu27@yahoo.com

ABSTRACT

From a historical point of view, it can be said that at the level of the enterprises, especially the profitable ones, there has always been a strategic thinking even if it was a strategy lacking in formalism that did not rely on the methods of analysis and did not have a wide communication. The growing business development, the high absorption capacity of the market, the low cost of energy and the labour force, the accelerated pace of technical progress represented all the phenomena that made the need for strategies to be less prominent.

KEYWORDS: strategic, management, enterprises, economic

1. Introduction

Even though the strategic management statement has made its official entrance to theoretical language since 1973, at The First International Conference of Strategic Management, organized by I.H. Ansoff at Vanderbilt University. The idea given to this concept by authors are generally quite different, the strategic management being considered as:

- the process that aims to facilitate the leadership of an organization and uses the strategy to guide its actions, integrates the commissioning of strategic actions related to structural and cultural factors;
- the form of leadership that seeks to ensure the best possible relationship between the demands of the environment, the internal and external partners and the objectives of the leaders, in time to be interested both in the interior and the outside of the enterprise, in the economic, organizational dimension;
- a set of decisions and actions that lead to the development of an effective strategy to help meet corporate goals;
- the process through which the company's management establishes the organization's long-term directions and results, ensuring a slow formulation, proper implementation and ongoing evaluation of the strategy.

The diversity of conceptual definitions used by authors sometimes means not only differences in language but also in substance, depending on the different perception of the phenomena and the scope of each of them to the strategic management, the changes that took place in the plan of strategic thinking and conceptions about the organization.

Strategic management is a complex process of prefiguring its future, its long-term evolution, process in which its strategy formulation, implementation, evaluation and permanent control are combined and complement each other in a continuous, dynamic flow. So strategic management is not a process of formulating the strategy that overlaps the enterprise management system, but a new form of strategy-based management.

2. Strategic management features

Table. 1. *The three dimensions of strategic management*

The rational and analytical process (economic dimension)	The socio-political process (human dimension)	The bureaucratic process (organizational dimension)
What does he wants? - defining strategic areas of activity - mission statement - fix the targets -choosing the portfolio of activities	Who are the "actors"? - identifying " actors " - dynamic analysis of the link between the enterprise and " actors" - looking for a political base and assessing the opposition	What kind of organization is it? - choosing the degree of decentralization - determining the size of operational units - division of labour - choosing the means of coordination

THE ANNALS OF "DUNAREA DE JOS" UNIVERSITY OF GALATI
FASCICLE IX. METALLURGY AND MATERIALS SCIENCE
Nº. 4 - 2018, ISSN 2668-4748; e-ISSN 2668-4756
Article DOI: https://doi.org/10.35219/mms.2018.4.10

		- developing the international system
Who are we? What is the situation? - environmental analysis - evaluation of resources - determining the planning	What can 'actors' do? - analysis of internal and external political influences - evaluating the 'actors' political system - anticipating the reaction of "actors"	Which decision-making process? - choosing the type of plan - determining the incremental steps - choosing the horizon - explaining the content of the plans - developing the decision-making process
What does he want to do? - formulation of strategies and policies - evaluating strategies and policies	What can be done with or against "actors"? - searching for 'actors' independence - select alliances and correlations	What animation style? - determining the level of participation - developing an evaluation and reward system - choosing the degree of freedom of operations - setting the intensity of each person's tracking and tracking
What will he do? - choice of strategy - setting up programs, action plan and budget - looking for an adapted management system	What does he decide to do? - formulation of political strategy - anticipating the reactions of the opponents	Which control procedures? - choosing the concentration of control - determining the frequency and level of control - selecting the detail of the control - search for control orientation

3. Similarities and differences between strategic management and strategic planning

Although similar, the terms of strategic planning and strategic management are not synonyms, and their scope is different.

- while strategic planning describes the periodic activities undertaken by the enterprise to cope with changes in its environment and has a sequential nature, an unforeseen event occurring outside a phase of strategic reflection being taken into account only in the next phase, strategic management is a continuous process, dynamic updating and permanent adaptation of strategic decisions according to the various important elements that appear along the way;

- if strategic planning is limited to business relationships with the environment, strategic management has in its internal structure and decisions, the development of skills and competencies capable of giving the enterprise the flexibility necessary to new situations, to ensure its efficient operation and optimal integration into the environment from which is part of it;

- unlike strategic planning, which involves formulating and evaluating strategic alternatives, choosing the strategy and drawing up detailed plans for its implementation, strategic management includes strategic control, which is to ensure that the chosen strategy is properly implemented and brings the desired results, respectively in analysing differences and making the necessary changes when they occur;

- if the strategic planning process is a plan that can leave unchanged the culture of the enterprise, the organization, the behaviour, the strategic management consists of a series of decisions, strategies and actions, in a new strategic behaviour that involves the transformation of the organization itself in view of its depreciation the external environment.

From the perspective of what has been said, it is clear that the strategic management has a richer content and a broader scope than the strategic planning which, in fact, includes it as a tool of realization. It consists of a set of decisions and actions that result in the formulation, implementation and control of the adopted strategies, in order to achieve the organization's objectives and its profitable adaptation to the changes of the environment.

4. Strategic typologies in the competitive economy

The analysis of the theory and practice of the contemporary market economy highlights an appreciable typological variety of strategies that actually outlines the way companies can deliver their mission and adapt to change. Of course, in terms of enterprise strategy, it is hard to appreciate and we do not believe it can be guaranteed that the application of one or the other will automatically lead to the success of a company, given the multitude of influence factors, ranging from the specifics of the enterprises to the particular characteristics of the environment in which each operates.

THE ANNALS OF "DUNAREA DE JOS" UNIVERSITY OF GALATI
FASCICLE IX. METALLURGY AND MATERIALS SCIENCE
Nº. 4 - 2018, ISSN 2668-4748; e-ISSN 2668-4756
Article DOI: https://doi.org/10.35219/mms.2018.4.10

Table 2. *Types of strategies*

Level of goal hierarchy	Overall (of the corporation)	More general. It focuses on the business portfolio and the allocation of resources between different businesses
	Business	focuses on how to compete in a business, highlighting the competitive advantage that the company has in relation to competitors. Targets average horizons of 1-3 years.
	Functional	are more specific than business strategies. Target short time horizons 1 year or less.
Time horizon	Long-term	refers to the evolution of firms for periods of 10, 15 or 20 years.
	In the medium term	target small periods of time
	Short term	typically, small firms focused on immediate results
The degree of participation of the firm in the development of the strategy	full	the characteristics of the state-owned enterprises are elaborated by their management together with the menus of the supersystem they belong to.
	independent	defining for private companies. focus on maximizing profits, strengthening market position and ensuring survival
The dynamics of the main objectives	offensive (growth or development)	aim to increase the volume of sales, revenues and profits, increase the activity of the company by achieving a large quantity of goods or services
	setting, maintaining	maintaining the current business situation is considered satisfactory. The increase is possible but slow and unpromising
	defensive	the main purpose: survival, cost reduction, elimination of losses

5. Conclusions

Beyond other factors, effective implementation of the strategy and performance of an enterprise depends to a large extent on the quality of the personnel and its identification with the purpose and objectives of the organization. As managerial and human relations representatives say (McGregor's Y theory, for example), people assume their responsibilities and participate in the work process to the extent that they are motivated and stimulated in their actions. Taking into account the complexity of human nature, motivation is an essential concept in psychology, expressing the fact that the basis of the human condition is always a set of needs, tendencies, intentions, ideals that support the realization of certain actions, deeds and attitudes.

Assuming the permanent adaptation of the enterprise to the environment in which it operates, strategic management involves the transformation of the enterprise in time. This means that any transformation produced in one of the components of the strategic management model may require changes in any or all of the other components, the strategic management representing a permanent process of updates and re-evaluations, within which the strategy formulation, implementation and evaluation are merged and complement each other in a continuous flow. The strategy must therefore be approached not as a rigid projection of the future of the enterprise but as a flexible process of adaptation and re-adaptation to changes in dimensional parameters or of the enterprise and its environment so as to permanently reflect the mutations in the competition perimeter but also the broader (economic, social, cultural) national and international environment.

The printing of this behavioural trait, specific to the market economy, consists of a scientific adaptation of the strategy, which implies both a thorough knowledge and mastery of the concepts and techniques of strategic management, as well as the amplification of the foreseeable, prospective dimension of the management, without which cannot be achieved a strategic projection able to provide an adequate response to the major challenges of transition and the world economy.

THE ANNALS OF "DUNAREA DE JOS" UNIVERSITY OF GALATI
FASCICLE IX. METALLURGY AND MATERIALS SCIENCE
Nº. 4 - 2018, ISSN 2668-4748; e-ISSN 2668-4756
Article DOI: https://doi.org/10.35219/mms.2018.4.10

References

[1]. Abrudan I., *Premises and landmarks of Romanian managerial culture*, Dacia Publishing House, Cluj-Napoca, 1999.
[2]. Abrudan I., *et al.*, *Economic Engineering Manual. Production Systems Engineering*, Dacia Publishing House, Cluj-Napoca, 2002.
[3]. Abrudan I., *et al.*, *SMEs and their specific management, Dacia Publishing House*, Cluj-Napoca,
[4]. Abrudan I., *At the gates of Europe. A vision on the European integration of Romania*, Management and Economic Engineering Magazine, vol. 5, no. 4(20), p. 5, Cluj-Napoca, 2006.
[5]. Abrudan I., *Time Factor Management*, Management and Economic Engineering Magazine, vol. 5, no. 3, Cluj-Napoca, 2006.
[6]. Abrudan I., *Leibnitz's triumph of Leibnitz's "sufficient reasoning principle" or 10 years since the founding of the Consortium of Economic Engineering in Romania*, Management and Economic Engineering Magazine, vol. 5, no. 2(18), p. 5, Cluj-Napoca, 2006.
[7]. Baron T., *Statistical methods for analysis and quality control of production*, Didactic and Educational Publishing House, Bucharest, 1979.
[8]. Baron T., *et al.*, *Quality and Reliability*, Technical Publishing House, Bucharest, 1988.
[9]. Baron T., *Theoretical and Economic Statistics*, Didactic and Educational Publishing House, Bucharest, 1996.
[10]. Bălan G., Țîțu M., Bucur V., *The Management of Change and The Competition Advantage*, 10th International Research / Expert Conference "Trends in the Development of Machinery and Associated Technology", TMT 2006, p. 497-500, Barcelo-Lioret de Mar, Spain, 11-15 September, 2006.
[11]. Cănănău N., Dima O., Gură Gh., Barajas Gonzales Ana, *Quality Assurance Systems*, Junimea Publishing House, Iași, 1998.
[12]. Cicală E., *Methods of Statistical Processing of Experimental Data*, Polytechnic Publishing House, Timișoara, 1999.
[13]. Ciobanu I., *Strategic Management*, Polirom Publishing House, Iași, 1998.

MANUSCRISELE, CĂRŢILE ŞI REVISTELE PENTRU SCHIMB, PRECUM ŞI ORICE CORESPONDENŢE SE VOR TRIMITE PE ADRESA:

MANUSCRIPTS, REVIEWS AND BOOKS FOR EXCHANGE COOPERATION, AS WELL AS ANY CORRESPONDANCE WILL BE MAILED TO:

LES MANUSCRIPTS, LES REVUES ET LES LIVRES POUR L'ECHANGE, TOUT AUSSI QUE LA CORRESPONDANCE SERONT ENVOYES A L'ADRESSE:

MANUSCKRIPTEN, ZIETSCHRITFTEN UND BUCHER FUR AUSTAUCH SOWIE DIE KORRESPONDENZ SID AN FOLGENDE ANSCHRIFT ZU SEDEN:

After the latest evaluation of the journals by the National Center for Science Policy and Scientometrics (**CENAPOSS**), in recognition of its quality and impact at national level, the journal will be included in the B^+ category, 215 code (http://cncsis.gov.ro/userfiles/file/CENAPOSS/Bplus_2011.pdf).

The journal is already indexed in:

SCIPIO-RO: http://www.scipio.ro/web/182206

EBSCO: http://www.ebscohost.com/titleLists/a9h-journals.pdf

Google Academic: https://scholar.google.ro

Index Copernicus: https://journals.indexcopernicus.com

The papers published in this journal can be viewed on the website of "Dunarea de Jos" University of Galati, the Faculty of Engineering, pages: http://www.sim.ugal.ro, http://www.imsi.ugal.ro/Annals.html.

Name and Address of Publisher:
Contact person: Elena MEREUȚĂ
Galati University Press - GUP
47 Domneasca St., 800008 - Galati, Romania
Phone: +40 336 130139
Fax: +40 236 461353
Email: gup@ugal.ro

Name and Address of Editor:
Prof. Dr. Eng. Marian BORDEI
"Dunarea de Jos" University of Galati, Faculty of Engineering
111 Domneasca St., 800201 - Galati, Romania
Phone: +40 336 130208
Phone/Fax: +40 336 130283
Email: mbordei@ugal.ro

AFFILIATED WITH:

- THE ROMANIAN SOCIETY FOR METALLURGY
- THE ROMANIAN SOCIETY FOR CHEMISTRY
- THE ROMANIAN SOCIETY FOR BIOMATERIALS
- THE ROMANIAN TECHNICAL FOUNDRY SOCIETY
- THE MATERIALS INFORMATION SOCIETY (ASM INTERNATIONAL)

Edited under the care of the FACULTY OF ENGINEERING

Annual subscription (4 issues per year)

Editing date: 15.12.2018
Number of issues: 200
Printed by Galati University Press (accredited by CNCSIS)
47 Domneasca Street, 800008, Galati, Romania